



THE HONG KONG
POLYTECHNIC UNIVERSITY

香港理工大學

Pao Yue-kong Library

包玉剛圖書館

Copyright Undertaking

This thesis is protected by copyright, with all rights reserved.

By reading and using the thesis, the reader understands and agrees to the following terms:

1. The reader will abide by the rules and legal ordinances governing copyright regarding the use of the thesis.
2. The reader will use the thesis for the purpose of research or private study only and not for distribution or further reproduction or any other purpose.
3. The reader agrees to indemnify and hold the University harmless from and against any loss, damage, cost, liability or expenses arising from copyright infringement or unauthorized usage.

IMPORTANT

If you have reasons to believe that any materials in this thesis are deemed not suitable to be distributed in this form, or a copyright owner having difficulty with the material being included in our database, please contact lbsys@polyu.edu.hk providing details. The Library will look into your claim and consider taking remedial action upon receipt of the written requests.

**MODEL-BASED FAILURE DIAGNOSTICS
AND RELIABILITY PROGNOSTICS FOR
HIGH POWER WHITE LIGHT-EMITTING
DIODES LIGHTING**

JIAJIE FAN

Ph.D

The Hong Kong Polytechnic University

2014



THE HONG KONG
POLYTECHNIC UNIVERSITY
香港理工大學

The Hong Kong Polytechnic University
Department of Industrial and Systems Engineering

**Model-based Failure Diagnostics and Reliability Prognostics
for High Power White Light-emitting Diodes Lighting**

Jiajie FAN

A thesis submitted in partial fulfillment of the requirements for the
degree of Doctor of Philosophy

September, 2013

Certificate of Originality

I hereby declare that this thesis is my own work and that, to the best of my knowledge and belief, it reproduces no material previously published or written, nor material which has been accepted for the award of any other degree or diploma, except where due acknowledgment has been made in the text.

_____ (Signed)

Jiajie FAN _____ (Name of student)

To My Lovely Parents and My Dear Wife

Abstract

Nowadays, with increasing concern on environmental protection, energy crisis, and quality of life, in the context of the lighting industry, Solid-state Lighting (SSL) is considered as the next generation green lighting source, following the conventional lighting sources (like incandescent bulbs and fluorescent lamps). As a type of SSL, High Power White Light-emitting diodes (HPWLEDs) lighting, which exhibits higher luminous efficacy, longer lifetime and environmental friendliness, has begun to be used in a broad range of applications, such as general lighting, TV backlighting, traffic signals and so on. However, the mass application of LED lighting in our daily lives still faces several difficulties in areas such as cost control, failure prediction and maintenance. This can be attributed to the limitations of traditional reliability assessment and prediction methods in the new electronics-rich systems. Hence, developing a fast, accurate and effective reliability testing and prediction method to determine the service life for LED lighting is becoming a key issue in popularizing this novel electronic device in the lighting market.

This research developed failure diagnosis and reliability prediction methods for HPWLEDs lighting within the Prognostics and Health Management (PHM) methodology framework. The originality of this work mainly relates to the establishment of failure criteria and data analysis methods for HPWLEDs lighting.

Firstly, the Physics-of-Failure (PoF) based PHM approach is used to diagnose the failure modes and failure mechanisms for HPWLEDs lighting, from the chip level to the system level, and then to build damage models to estimate the reliability. Three failure modes: (i) Catastrophic failure; (ii) Lumen degradation; (iii) Chromaticity state shift are firstly categorized for HPWLEDs lighting systems. The data-driven prognostic methods with both statistical and learning approaches are then applied to predict the lumen lifetime, lumen maintenance and the chromaticity state of HPWLEDs lighting. The results show that the proposed Degradation Data Driven Method (DDDM) can predict more reliability messages (e.g. Mean Time To Failure, Confidence Interval and Reliability Function) compared to the IES TM-21-11 standard projecting method, which only can estimate L_{70} . The recursive Unscented Kalman Filter (UKF) method, replacing the ordinary least squares (OLS) implementation recommended in the IES TM-21-11 standard, can improve the prediction accuracy for both lumen maintenance and chromaticity state applications. Finally, a new reliability estimation method is developed to predict the reliability of HPWLEDs lighting by integrating the proposed statistical and filter based data-driven PHM methods. With the proposed new reliability estimation method, the traditional reliability testing procedures can be optimized with a Six Sigma DMAIC step-wise framework by considering both time- and cost- reductions.

Publications arising from the thesis

The undertaken research project in this thesis has been summarized and documented in the following papers:

[Journal Papers]

- [1] Jiajie Fan*, K.C. Yung, Michael Pecht, “*Physics-of-Failure-Based Prognostics and Health Management for High-Power White Light-Emitting Diode Lighting*”, IEEE Transactions on Device and Materials Reliability, Vol. 11, Issue 3, pp. 407–416, Sept.2011; **(Grade A)** in ENGINEERING, ELECTRICAL & ELECTRONIC (rank 45 out of 246, 18.3%)
- [2] Jiajie Fan*, K.C. Yung, Michael Pecht, “*Lifetime Estimation of High Power White LED using Degradation Data Driven Method*”, IEEE Transactions on Device and Materials Reliability, Vol. 12, Issue 2, pp. 470–477, Sept.2012; **(Grade A)** in ENGINEERING, ELECTRICAL & ELECTRONIC (rank 45 out of 246, 18.3%)
- [3] Jiajie Fan*, K.C. Yung, Michael Pecht, “*Prognostics of Chromaticity State for Phosphor-converted White Light Emitting Diodes Using an Unscented Kalman Filter Approach*”, IEEE Transactions on Device and Materials Reliability, Vol. 14, Issue 1, pp. 564–573, Mar.2014; **(Grade A)** in ENGINEERING, ELECTRICAL & ELECTRONIC (rank 45 out of 246, 18.3%)
- [4] Jiajie Fan*, K.C. Yung, Michael Pecht, “*Prognostics of Lumen Maintenance for High Power White Light Emitting Diodes Using a Nonlinear Filter-based Approach*”, Reliability Engineering & System Safety, Vol.123, March 2014, pages 63-72; **(Grade A)**
- [5] Jiajie Fan*, K.C. Yung, Moon-hwan Chang, Michael Pecht, “*Optimal Design of Life Testing for High Brightness White LEDs Using Six Sigma DMAIC Approach*”, Reliability Engineering & System Safety (Under Review); **(Grade A)**

- [6] Jiajie Fan*, K.C. Yung, Michael Pecht, “*Predicting Long-term Lumen Maintenance Life of LED Light Sources Using a Particle Filter-based Prognostic Approach*”, Expert Systems with Applications (Submitted); **(Grade A)**
- [7] Jiajie Fan*, K.C. Yung, Michael Pecht, “*Online Prediction of Remaining Useful Performances for High Brightness White LEDs Using a Fusion Prognostic Approach*” (In Preparation);

[Conference Papers]

- [8] Jiajie Fan*, K.C. Yung, Michael Pecht, “*Failure Modes, Mechanisms, and Effects Analysis for LED Backlight Systems used in LCD TVs*”, Proceeding of 2011 Prognostics & System Health Management Conference(PHM2011 Shenzhen), IEEE Xplore, 23-25 May 2011;
- [9] Jiajie Fan*, K.C. Yung, Michael Pecht, “*Comparison of Statistical Models for the Lumen Lifetime Distribution of High Power White LEDs*”, Proceeding of 2012 Prognostics & System Health Management Conference(PHM May-2012, Beijing), IEEE Xplore, 23-25 May 2012;
- [10] Jiajie Fan*, K.C. Yung, Michael Pecht, “*Anomaly Detection for Chromaticity shift of High Power White LED with Mahalanobis Distance Approach*”, Proceeding of the 14th International Conference on Electronics Materials And Packaging (EMAP2012, Hong Kong), IEEE Xplore, 13-26 December 2012;

Acknowledgements

My deepest gratitude goes first and foremost to my chief supervisor, Dr *Winco K.C. Yung*, for the guidance and encouragement he gave me in every stage of my Ph.D research study. Thanks to his continual supports and advice, I can complete this thesis on time. I also would like to thank my Co-supervisor, Prof. *Michael Pecht* from University of Maryland, College Park, for his great support on my exchange program to the US. This is a great experience in my Ph.D study.

Secondly, I would like to express my sincere thanks to the staff and students from The PCB Technology Center of The Hong Kong Polytechnic University, The Center for Advanced Life Cycle Engineering of University of Maryland, College Park, and The Center for Prognostics and System Health Management of City University of Hong Kong. They are Dr *H.M. Liem*, Dr *Henry Choy*, Miss *Joanne Wong*, Dr *Diganta Das*, Dr *Chaochao Chen*, Mr *Moon-Hwan Chang*, Dr *Eden Ma*. Thanks for their generous help in providing me with various kinds of supports to my research.

Last but not least, my biggest thanks must go to my family for their love and support throughout these years.

Table of Contents

Abstract		i
Publications arising from the thesis		iii
Acknowledgements		v
Table of Contents		vi
List of Figures		x
List of Tables		xiii
List of Abbreviations		xv
Chapter 1	Introduction	1
	1.1 Research Background	1
	1.2 Problem Statement	2
	1.3 Research Objectives	6
	1.4 Research Contributions	8
	1.5 Organization of the Thesis	10
Chapter 2	Literature Review	12
	2.1 Framework of The Literature Review	12
	2.2 Brief Overview of LED Lighting	12
	2.2.1 LED Chips	14
	2.2.2 LED Packages	17
	2.2.3 LED Systems	21
	2.2.4 High Power White LEDs Lighting	24
	2.3 Review of Traditional Reliability Prediction Methods for Electronics	28
	2.3.1 MIL-HDBK-217	30
	2.3.2 RiAC-HDBK-217PLUS	32
	2.3.3 Telcordia SR-332 (Bellcore)	35
	2.3.4 FIDES Guides	36
	2.4 Review of Failure Analysis and Reliability Prediction Methods for LEDs	41
	2.5 Concluding Remarks	50
Chapter 3	Research Methodology and Experimental Setup	51
	3.1 Research Methodology	51
	3.1.1 Prognostics and Health Management	51
	3.1.1.1 Physics-of- Failure (PoF) Method	52

	3.1.1.2 <i>Data-driven Method</i>	58
	3.1.2 <i>Six Sigma DMAIC Methodology</i>	72
3.2	Experimental Setup	76
	3.2.1 <i>Performance Data Collection based on IES-LM-80-08 Standard</i>	76
	3.2.2 <i>High Temperature Reliability Test</i>	78
Chapter 4	Physics-of-Failure Modeling for High Power White LED Lighting	81
4.1	Introductory Remarks	81
4.2	Physics-of-Failure based PHM	82
	4.2.1 <i>Materials and Geometries Analysis</i>	83
	4.2.2 <i>Failure Modes, Mechanisms and Effects Analysis</i>	86
	4.2.2.1 <i>Chip level degradation</i>	88
	4.2.2.2 <i>Package level degradation</i>	91
	4.2.2.3 <i>System level degradation</i>	95
	4.2.2.4 <i>Rank Priority for Potential Failure Mechanisms</i>	99
	4.2.3 <i>Physics-of-Failure based Damage Modeling</i>	100
	4.2.3.1 <i>Thermal-induced luminous degradation modeling</i>	100
	4.2.3.2 <i>Thermal cycle-induced solder interconnects fatigue modeling</i>	107
4.3	Concluding Remarks	108
Chapter 5	Lumen Lifetime Estimation Using a Statistical Data-driven Method	110
5.1	Introductory Remarks	110
5.2	Device under Test Description	111
5.3	Theory and Methodology	114
	5.3.1 <i>IES TM-21-11 Method</i>	114
	5.3.2 <i>Statistical Data-driven Method</i>	116
	5.3.2.1 <i>Approximation method</i>	118
	5.3.2.2 <i>Analytical method</i>	119
	5.3.2.3 <i>Two-stage method</i>	120
5.4	Results and Discussion	122
	5.4.1 <i>Lumen Maintenance Data</i>	122
	5.4.2 <i>Lumen Lifetime Estimation with the IES TM-21-11 Method</i>	123
	5.4.3 <i>Lumen Lifetime Estimation with the Approximation Method</i>	125
	5.4.4 <i>Lumen Lifetime Estimation with the Analytical Method</i>	130
	5.4.5 <i>Lumen Lifetime Estimation with the Two-stage Method</i>	132
5.5	Concluding Remarks	134

Chapter 6	Prognostics of Lumen Maintenance and Chromaticity State with Filter Data-driven Methods	136
6.1	Introductory Remarks	136
6.2	Device under Test and Test Condition	137
	6.2.1 <i>Device under Test</i>	137
	6.2.2 <i>Test Condition</i>	138
6.3	Lumen Maintenance Estimation Using Filter Approaches	139
	6.3.1 <i>Lumen Maintenance Projecting Approach</i>	139
	6.3.2 <i>Unscented Kalman Filter</i>	141
	6.3.2.1 <i>Augmented UKF</i>	143
	6.3.2.2 <i>Non-augmented UKF</i>	146
	6.3.3 <i>Results and Discussion</i>	149
	6.3.3.1 <i>Data pretreatment</i>	149
	6.3.3.2 <i>State initialization</i>	151
	6.3.3.3 <i>Filtering</i>	152
	6.3.3.4 <i>Prognostics</i>	157
6.4	Chromaticity State Estimation Using Filter Approaches	159
	6.4.1 <i>Chromaticity State Shift of High Power White LEDs</i>	160
	6.4.2 <i>Results and Discussion</i>	162
6.5	Concluding Remarks	170
Chapter 7	Optimal Design of Reliability Testing for LEDs in a Six Sigma DMAIC Framework	172
7.1	Introductory Remarks	172
7.2	Case Study	174
7.3	Define Phase	174
7.4	Measure Phase	179
7.5	Analyze Phase	183
	7.5.1 <i>Cost Analysis</i>	183
	7.5.2 <i>Root Cause and Effect Analysis</i>	186
7.6	Improve Phase	187
	7.6.1 <i>Reliability Estimation Methods based on Degradation Data</i>	187
	7.6.1.1 <i>Nonlinear mixed-effect model</i>	187
	7.6.1.2 <i>New reliability estimation with nonlinear degradation data</i>	190
	7.6.2 <i>Design of Experiment (DOE)</i>	194
7.7	Control Phase	201
7.8	Concluding Remarks	202

Chapter 8	Conclusions and Future Work	204
8.1	Conclusions Drawn from Research Work	204
8.2	Suggestions for Future Research Directions	206
References		208
Appendices		
Appendix A		I

List of Figures

Fig. 1-1 Schematic diagram of thesis organization	10
Fig. 2-1 The predicted development trend of LEDs	13
Fig. 2-2 High-resolution transmission electron microscope of InGaN quantum wells separated by GaN barriers	15
Fig. 2-3 The working mechanism of LEDs	15
Fig. 2-4 Band gap of principal semiconductor used in LEDs	16
Fig. 2-5 LEDs packaging: (a) cross-section and (b) top view	17
Fig. 2-6 (a) Packaging structure of Luxeon K_2 and (b) the heat dissipation simulation	18
Fig. 2-7 Chemical structures of (a) typical epoxy and (b) silicone	20
Fig. 2-8 LEDs system architecture	22
Fig. 2-9 (a) Passive cooling and (b) active cooling for LED system	23
Fig. 2-10 White LED lighting	26
Fig. 2-11 The 217Plus approach to failure rate estimation	34
Fig. 2-12 MacAdam ellipses around CCT range 3000K	45
Fig. 3-1 PoF based PHM methodology	53
Fig. 3-2 Support Vector Machines used for classification	65
Fig. 3-3 Recursive operation of Kalman filter	69
Fig. 3-4 Fusion PHM method	71
Fig. 3-5 Six Sigma DMAIC	73
Fig. 3-6 Test procedure recommended by the IES-LM-80-08 Standard	78
Fig. 3-7 High temperature reliability testing for LEDs (a) experiment setup, (b) electrical circuit design and (c) operation profile	80
Fig. 4-1 PoF-based PHM approach	83
Fig. 4-2 Materials and structure of (a) LED chip, LEDs packages, and (b) LED lamps	84
Fig. 4-3 FMMEA for high power white LED lighting systems	87
Fig. 4-4 The mechanisms of (a) radiative recombination and (b) non-radiative recombination	89
Fig. 4-5 Surface Mount Technology module	96
Fig. 4-6 Heat dissipation paths	101
Fig. 4-7 Thermal resistance network of high power white LED lighting system	102
Fig. 4-8 (a) The linear relationship between junction temperature and input power and (b) FEA simulation of heat distribution with 0.2W input power	104
Fig. 4-9 The linear relationship between input current and power	105

Fig. 4-10 Lumen maintenance plotting and prediction for LEDs	106
Fig. 5-1 White LUXEON Rebel and its structure	112
Fig. 5-2 Thermal management of White LUXEON Rebel with (a) ceramic substrate and (b) FR-4 substrate	112
Fig. 5-3 Failure modes of HPWLEDs	113
Fig. 5-4 General degradation path model (a) increasing type; (b) decreasing type	117
Fig. 5-5 Projecting L_{70} with lumen maintenance data from 1,000 to 6,000 hrs	123
Fig. 5-6 Projecting L_{70} with lumen maintenance data from 6,000 to 10,000 hrs	124
Fig. 5-7 Extrapolating degradation path model with 1,000 to 10,000 hrs data	125
Fig. 5-8 Statistical models fitting for “Pseudo Failure Time”	127
Fig. 5-9 Weibull plotting for “Pseudo failure times”	128
Fig. 5-10 Reliability prediction for LUXEON Rebel	129
Fig. 5-11 Weibull plotting for random effect parameters β_i	131
Fig. 5-12 Reliability prediction for random effect parameters β_i	131
Fig. 6-1 White LUXEON Rebel (a) packaging structure and (b) luminescence mechanism	138
Fig. 6-2 IES-TM-21-11 projecting approach	139
Fig. 6-3 Comparison of filter algorithms (EKF, PF and UKF) for prognostics	142
Fig. 6-4 Flowchart of prognostics using the augmented UKF	145
Fig. 6-5 Flowchart of prognostic using the non-augmented UKF	148
Fig. 6-6 Lumen maintenance prognostic procedure	149
Fig. 6-7 Nonlinear curve-fitting of lumen maintenance data from training samples	151
Fig. 6-8 Lumen maintenance prognostics with UKF approaches for test samples (Test sample_1 to Test sample_10 as shown from (a) to (j))	155
Fig. 6-9 Mean square errors of UKF filtering step	156
Fig. 6-10 Lumen maintenance prognostics errors at 10,000hrs	158
Fig. 6-11 CIE 1976 (u' , v') uniform chromaticity diagram	161
Fig. 6-12 Model selection for chromaticity state shift process	163
Fig. 6-13 Prognostic results of chromaticity state shift with UKF approach (from (a) to (o))	167
Fig. 6-14 Prognostics errors of chromaticity state shift at 6,000 hrs	168
Fig. 7-1 Critical-to-quality (CTQ) methodology	177
Fig. 7-2 (a) Traditional LED reliability testing process and (b) operation profile	179
Fig. 7-3 BTS256-LED measurement system used for data collection	180
Fig. 7-4 Lumen degradation process of test units	182

Fig. 7-5 Overview of failure time distribution of test units	183
Fig. 7-6 Simulation contour plot of total operation cost vs. inspection numbers and sample size	185
Fig. 7-7 Cause and effect diagram	186
Fig. 7-8 General nonlinear estimation method with degradation data	191
Fig. 7-9 The main parameters of LED reliability testing process	195
Fig. 7-10 Taguchi orthogonal array $L_{18}(3^3 \cdot 1^2)$ DOE main effects plot for SN ratios	198
Fig. 7-11 Taguchi orthogonal array $L_{18}(3^3 \cdot 1^2)$ DOE interaction plot for SN ratios	199
Fig. 7-12 The improved LED reliability testing process flow	200
Fig. 7-13 Individual control chart for reliability estimation errors	202

List of Tables

Table 2-1 LED lighting systems	14
Table 2-2 LED semiconductor chip materials	16
Table 2-3 Comparison of white LED lightings	27
Table 2-4 Reliability prediction handbooks for electronic devices and equipments	29
Table 2-5 Comparison of reliability prediction methodologies	39
Table 2-6 Nominal CCT Categories	43
Table 3-1 Comparison of MIL-HDBK-217 and Physics-of-failure methods	57
Table 3-2 Six Sigma DMAIC processes	74
Table 3-3 Test conditions recommended by the IES-LM-80-08 Standard	77
Table 3-4 Test condition of the high temperature reliability test	80
Table 4-1 Materials properties of LED chip, packages, and systems levels (at 25°C)	86
Table 4-2 Rank priority for potential failure mechanisms	99
Table 4-3 Lumen data (1000 to 6000 hrs) and exponential extrapolations of L_{70} ages	106
Table 4-4 Fatigue failure models for solder interconnects	108
Table 5-1 IES LM-80-08 Test conditions	123
Table 5-2 Recommended IES TM-21-11 estimation report	124
Table 5-3 List of estimated parameters for degradation path model and pseudo failure time	126
Table 5-4 Estimated parameters of each statistical model by approximate method	128
Table 5-5 Parameters estimation and reliability prediction using the approximation method	129
Table 5-6 Parameters estimation and reliability prediction by the analytical method	132
Table 5-7 Parameters estimation and reliability prediction by the two-stage method	133
Table 5-8 The 95% confidence interval widths of MTTF	133
Table 6-1 Parameters of the measurement model obtained from training samples	152
Table 6-2 Performances of prognostic approaches	159
Table 6-3 Chromaticity state shift process model selection results	163
Table 6-4 Parameters of measurement model obtained from training samples	164

Table 6-5 RMSE results for prognostic of chromaticity state shift	169
Table 7-1 Six Sigma Project Charter	176
Table 7-2 Supplier-Input-Process-Output-Customer (SIPOC) diagram	178
Table 7-3 Results of gauge R&R study	180
Table 7-4 Reliability estimation with time-truncated failure data	183
Table 7-5 Summary of the cost of traditional life testing	185
Table 7-6 The factors and their levels of DOE	195
Table 7-7 Taguchi orthogonal array $L_{18}(3^3 \cdot 1^2)$ DOE	196
Table 7-8 Summary of reliability testing performance from DOE	197
Table 7-9 Response for S/N ratios	199
Table 7-10 Optimum factor level combination	200

List of Abbreviations

ADT	Accelerated Degradation Test
AIC	Akaike Information Criterion
ALT	Accelerated Lifetime Test
ANN	Artificial Neural Network
ANSI	American National Standard Institute
ANSLG	American National Standard Lighting Group
ASSIST	Alliance for Solid-state Illumination Systems and Technologies
CCFLs	Cold Cathode Fluorescent Lamps
CCT	Correlated Color Temperature
cdf	Cumulative Distribution Function
CI	Confidence Interval
CIE	Commission Internationale del' Eclairage
CME	Coefficient of Moisture Expansion
CRI	Color Rendering Index
CTE	Coefficient of Thermal Expansion
CTQ	Critical-to-Quality
DMAIC	Define-Measure-Analyze-Improve-Control
DoE	Department of Energy
DOE	Design of Experiment
DUT	Devices Under Test
DWNN	Dynamic Wavelet Neural Networks
ED	Euclidean Distance
EF	Enhancement Factor
EKF	Extended Kalman Filter
FMMEA	Failure Modes Mechanisms and Effect Analysis
FTA	Fault Tree Analysis
GR&R	Gauge Repeatability and Reproducibility
HPWLED	High Power White LED
IEC	International Electrotechnical Commission
IEEE	Institute of Electrical and Electronics Engineers
IES	Illuminating Engineering Society
JEDEC	Joint Electron Device Engineering Council
KF	Kalman Filter
LED	Light-emitting Diode
LM	Lumen Maintenance
LVQ	Learning Vector Quantization

MD	Mahalanobis Distance
MLE	Maximum Likelihood Estimation
MSE	Mean Square Error
MTTF	Mean Time to Failure
NEMA	National Electrical Manufacturers Association
NGLIA	Next Generation Lighting Industry Alliance
NLS	Nonlinear Least Squares
OA	Orthogonal Array
OLS	Ordinary Least Squares
PCA	Principle Components Analysis
PCB	Printed Circuit Board
pdf	Probability Density Function
PF	Particle Filter
PHM	Prognostics and Health Management
PLS	Partial Least Squares
PNN	Probabilistic Neural Networks
PoF	Physics-of-Failure
RMSE	Root Mean Square Error
RNN	Recurrent Neural Networks
RPN	Rank Priority Number
RUL	Remaining Useful Life
RVM	Relevance Vector Machine
S/N	Signal-to-Noise
SDCM	Standard Deviations of Color Matching
SIPOC	Supplier-Input-Process-Output-Customer
SMT	Surface Mount Technology
SOM	Self-organized Maps
SPD	Spectral Power Distribution
SSL	Solid State Lighting
SVM	Support Vector Machine
TFFC	Thin Film Flip Chip
t_p	the $100p^{th}$ percentiles of failure time distribution
UCS	Uniform Chromaticity Scale
UKF	Unscented Kalman Filter

Chapter 1 Introduction

1.1 Research Background

Solid state lighting (or semiconductor lighting), is considered as the second revolution in the history of lighting, saving €300billion in the global energy bill and reducing 1,000 MT of CO₂ emission every year (Van Driel & Fan, 2012). The high power white light-emitting diode (HPWLED), known as one of the next generation solid state lighting sources, is a novel technology which uses semiconductor and phosphor materials to convert electricity into white light (Mottier, 2009). LED has been widely used as a light source for indoor lighting, street lamps, advertising displays, decorative lighting and monitor backlights (Lenk & Lenk, 2011). Compared to traditional lighting sources (such as incandescent lamps, halogen incandescent lamps, and cold cathode fluorescent lamps CCFLs), LEDs have attracted increasing interest in the field of lighting systems due to their high efficiency, environmental benefits, and long lifetime, with claims of 50,000 hrs or longer (Schubert & Kim, 2005).

Reliability is a fundamental characteristic for the safe operation of any modern technological product (or system) (Zio, 2009), which can be defined as the probability that the product (or system) will perform its intended function for a specified time period when operating under given conditions (Blischke & Murthy,

2000). Reliability is a highly-quantitative engineering discipline with multiple knowledge(Nikulin et al., 1998), which integrates the sciences of probability, statistics, and stochastics with the engineering insights into the design and construction of products and systems. As such, it includes aspects such as: (1) reliability testing; (2) reliability analysis (failure analysis); (3) reliability modeling; (4) reliability prognostics (prediction); and (5) reliability management and maintenance. With the rapid development of today's electronic products that provide high quality products and are successful globally, it is crucial for designers and manufacturers to know the reliability of a new product before release to the market. Thus, reliability testing, assessment and prediction become essential procedures for manufacturers in qualifying their products, with the aims of forecasting the quantification of the probability of failure of the products and their protective barriers.

1.2 Problem Statement

The traditional reliability assessment and prediction methods are usually based on analyzing the failure-time data collected from laboratory life tests, field tracking studies, and warranty data bases, which is required of all failed test products (Nelson, 1990)(Meeker & Escobar, 1998). With developing technology, products are

becoming more reliable than before, with longer lifetimes and higher quality. However, owing to the long lifetime, few or no product failures will occur during the period of reliability test. As a result, it is difficult to assess reliability with traditional approaches which record only failure-time data. Even though improved reliability testing and assessment methods, such as accelerated life testing and censoring technology, have been developed to estimate the rated lifetime distribution for highly reliable products, these approaches may not be feasible for products not failing during life testing due to severe time and cost constraints (Meeker et al., 1998). Sometimes the duration of the reliability test and assessment procedure is longer than the time between product updates, which may delay technology innovation and development. Therefore, developing a fast, accurate and effective reliability assessment and prediction method for highly reliable products is desirable for accelerating technology innovation and development.

In electronic engineering, the current reliability prediction methods have been documented in many handbooks (e.g. MIL-HDBK-217, 217-PLUS Telcordia SR-332, PRISM, GJB-299-87, FIDES and so on), however, they have a lot of limitations in the application for the new electronic products. The reliability prediction handbooks have many drawbacks in current applications due to their limitations in keeping pace with new technologies, accounting for complex usage profiles, and addressing soft

and intermittent faults (the most common failure modes in today's electronics-rich systems) (Cushing et al., 1993). Numerous studies have shown traditional reliability assurance and reliability prediction methods to be significantly flawed (Pecht, 2009). These are: (1) inability to keep pace with new technologies, and their failure modes and failure mechanisms; (2) limitations of previous algorithms and methodologies to assess the reliability of new electronic devices; (3) unreliability of decision-making and maintenance strategies for new technologies or processes. Thus, most of these handbooks have not been upgraded now and some even discontinued.

As introduced above, LEDs possess more benefits compared to traditional lighting sources, however, the mass application of LEDs in our daily lives still face several difficulties due to high cost, failure prediction and maintenance. Meanwhile, due to its longer lifetime, higher reliability, and different failure mechanisms compared to traditional light sources, there has been no standard method to evaluate and predict the reliability of LEDs until now. There are often a large gaps between the warranted life of a LED lighting product and its real application life (DOE, 2009). For example, Xiamen City in China has been installing high power LEDs for street lighting since 2008. The manufacturer promised a system life time of 100,000 hours (over 5 years of reliable operation), but the city government discovered the lights failed within 2 to 3 months after installation (Van Driel & Fan, 2012).

Generally, the challenges to limit the extensive application of LED lighting coming from its unpredictable reliability are:

Challenge 1: Owing to its long lifetime, few or no failures will occur in LEDs during the period of reliability testing. For example, since August 2007, the CALiPER program proposed by the U.S. Department of Energy(DoE) began reliability testing for commercial LED lighting and some products are still producing at least 95% of initial output for over 6,000 hrs (Paget, et al., 2007~201) (normally for general LED lightings, 30% lumen depreciation is defined as failure (ASSIST Recommendation, 2005)). The traditional reliability assessment and prediction approaches which record only failure-time data have difficulties in dealing with these cases;

Challenge 2: Current reliability assessment and prediction methods for LED lighting with large prediction errors and uncertainties have several limitations in applications. For example, since 2011, a projecting approach based on the least-square regression method was recommended by the Illuminating Engineering Society of North American(IESNA), IES-TM-21-11 (IES-TM-21-11, 2011), to predict the lumen maintenance (or lumen lifetime) of LEDs and it has also been widely accepted by many LED manufacturers. For instance, Philips Lumileds (Luxeon, 2011) and CREE (CREE®, 2012) are implementing this projecting approach to predict the lumen maintenance and lumen lifetime of LEDs in their reliability test reports. However,

this projecting approach, depending on least-square regression, introduces large prediction errors and uncertainties;

Challenge 3: Lumen degradation is always used as an important indicator to represent the failure of LED lighting, but it is not the sole characteristic. In the LED reliability field, many previous studies have paid attention only to lumen degradation failure in LED products, ignoring another common failure modes(e.g. chromaticity state shift);

Challenge 4: There is not yet a unified and comprehensive standard system for reliability testing in the LED lighting industry. Different LED manufacturers apply different reliability testing methods for their products, so customers are confused with all kinds of claimed lifetimes from these different LED manufacturers.

1.3 Research Objectives

Therefore, the primary objective of this research is to diagnose the failure modes and failure mechanisms for HPWLED lighting and to develop a fast, accurate and effective reliability assessment and prediction method. The detailed objectives can be summarized as:

- (i) Develop prognostics-based reliability assessment methods for HPWLEDs lighting. As an electronic assembly system, LED lighting system is constructed

by several components (such as, LED chips, phosphors, packaging materials, cooling components and so on). A large number of unknown failure modes and failure mechanisms occur in LED lighting. Thus, this study conducts the diagnosis, analysis and classification of failure modes and failure mechanisms for HPWLED lighting firstly. Then, as introduced above, the reliability testing time for a highly reliable electronic device (such as HPWLEDs lightings) is always too long. To shorten the test time, it is planned to import the prognostics concept into reliability testing and build a prognostics-based reliability assessment method by dealing with the collected degradation data. This helps to solve the challenge (1) in section 1.2;

(ii) Select and verify the prognostics-based reliability assessment methods with both accuracy- and precision-based metrics to reduce the prediction errors and uncertainties that occur in the IES-TM-21-11 projecting approach. The purpose of this part is to solve the challenge (2) as mentioned in section 1.2;

(iii) Take the chromaticity state shift into considering as another indicator of a LED's "end of life" (recommended by the Next Generation Lighting Industry Alliance (NGLIA) of the U.S. Department of Energy (DoE) (Solid-state Lighting Product Quality Initiative, 2011)) besides lumen degradation and develop models to predict both lumen maintenance and the chromaticity state for HPWLEDs

lighting. This step is to solve the challenge (3) shown in section 1.2;

- (iv) Establish an optimal reliability testing procedure for HPWLEDs by considering shortening the testing time, reducing the testing operation cost, and also maintaining the accuracy of the reliability assessment. This step is to solve the problem in the challenge (4) shown in section 1.2.

1.4 Research Contributions

Increasing use of LEDs in lighting applications and the associate unpredicted failures make it difficult for designers and manufacturers to design and produce reliable HPWLEDs lighting for customers. This thesis describes the development of failure diagnosis and reliability prediction methods for HPWLEDs lighting with Prognostics and Health Management (PHM) methodologies. The originality of this work mainly focuses on the establishment of failure criteria and data analysis methods for HPWLEDs lighting. Some of the main contributions from this study are summarized as follows:

- (i) A Physics-of-Failure (PoF) based model is established to assess the reliability of HPWLEDs lighting, which includes the materials and geometries analysis, the failure modes mechanisms and effect analysis (FMMEA) and the damage models built for the prioritized failure mechanisms in the whole LED lighting system level. In this model, three failure modes, (a) Catastrophic failure; (b) Lumen degradation; (c) Chromaticity state shift, are firstly categorized for the whole LED system and the potential failure mechanisms and their contributing loads are presented by the “bottom-up” method. The PoF based damage models

are built for the two failure mechanisms with the highest priority in the degradations in the chip to the whole system.

- (ii) A statistical data-driven method based on the general degradation path model is developed to estimate the lumen lifetime for HPWLEDs lighting. With this method, more reliability messages (e.g. Mean Time to Failure (MTTF), Confidence Interval (CI) and reliability function) can be predicted. In comparison, only the lumen lifetime, L_{70} , can be estimated from the IES TM-21-11 projecting method.
- (iii) Filtering is a widely used prognostic approach for estimating and predicting the state of electronic components or systems based on a state-space model. The Unscented Kalman Filter (UKF) possesses many advantages in the state estimation for nonlinear stochastic systems. To improve the prediction accuracy, this research develops a filter-based data-driven method (recursive UKF) to predict both the lumen maintenance and the chromaticity state of HPWLEDs lighting, instead of the least squares implementation recommended in the IES TM-21-11 projecting method.
- (iv) Finally, an optimal design of reliability testing for LEDs is developed by integrating both statistical and filter data-driven methods within a Six Sigma DMAIC(Define-Measure-Analyze-Improve-Control) framework. With the help of the recursive UKF, the accuracy of reliability estimation can be improved compared to the ordinary least squares(OLS) approach recommended in the IES-TM-21-11 standard. Meanwhile, the reliability testing time and cost can be significantly reduced.

1.5 Organization of the Thesis

According to the objectives mentioned in section 1.3, this thesis is organized into seven chapters as follows (See Fig. 1-1):

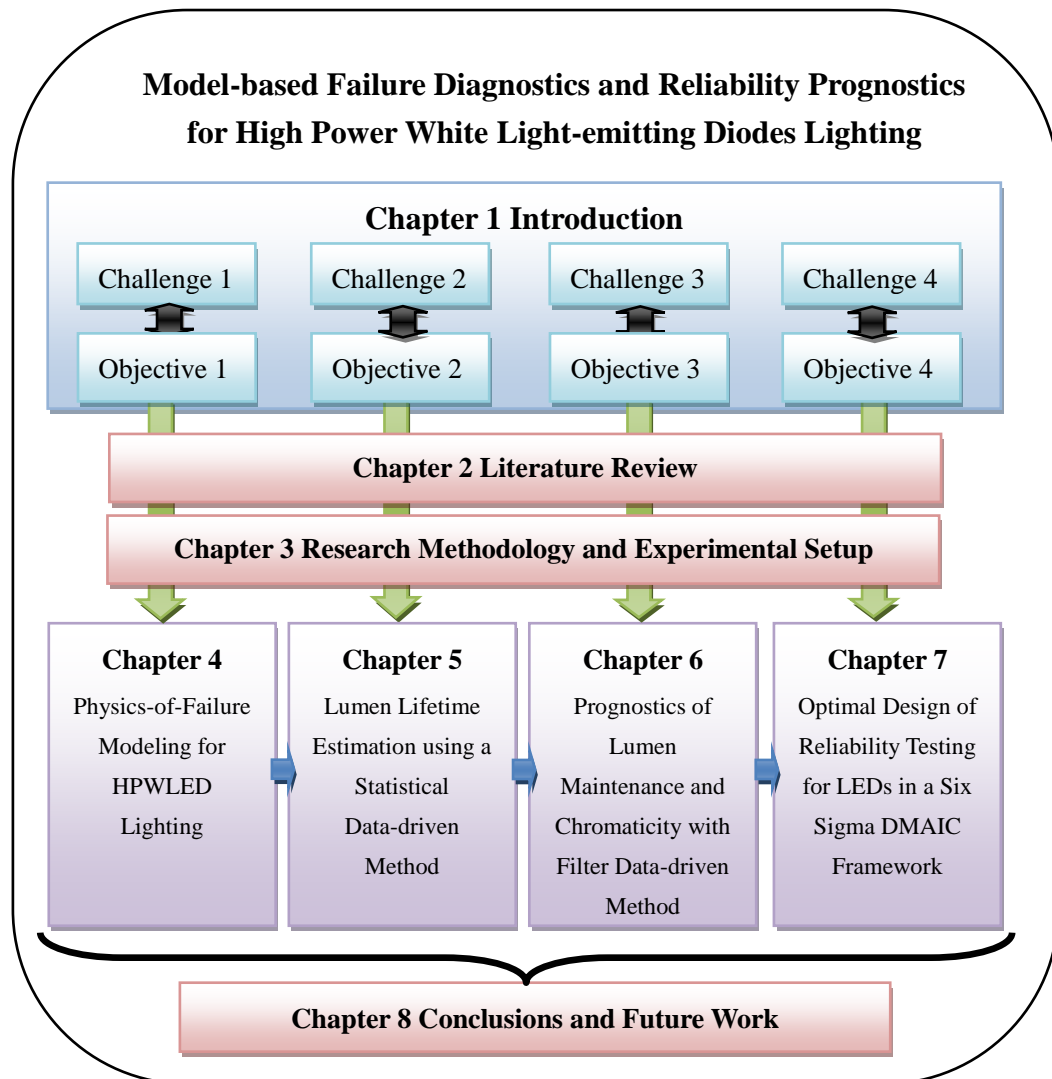


Fig. 1-1 Schematic diagram of thesis organization

Chapter 1 firstly introduces the research background of this project and then states the problems that occur in existing reliability assessment and prediction methods and their difficulties in being applied in LED lighting. Finally, the research objectives and some contributions of this thesis are shown at the end of this chapter.

After the introduction section, literature reviews of LED lighting (from chip to

system), the existing handbook based reliability prediction methods for electronics and the previously published works in the field of failure analysis and reliability prediction for LEDs are given in chapter 2.

Chapter 3 introduces the Prognostics and Health Management (PHM) methodology, the Six Sigma DMAIC methodology and their related applications. Meanwhile, the experimental setup implemented in this research is also described at the end of this chapter.

PHM prognostic methods are proposed and applied to HPWLEDs lighting from chapter 4 to chapter 6. In detail, chapter 4 introduces Physics-of-Failure (PoF) based PHM methods for HPWLEDs lighting, by identifying the failures occurring from the chip level to the system level with the FMMEA approach and establishing the damage models for the prioritized failure mechanisms. After failure diagnosis and analysis, the data-driven prognostic methods and algorithms are proposed in chapter 5 and chapter 6. A statistical data-driven approach is proposed in chapter 5 to predict the lumen lifetime for HPWLEDs. The filter based data-driven methods are applied in chapter 6 to predict both lumen maintenance and the chromaticity state for HPWLEDs. Finally the performances of the proposed models are compared with the IES TM-21-11 standard projecting method.

In chapter 7, by studying a real case in the Six Sigma DMAIC framework, an optimized reliability testing method is developed for HPWLEDs integrating the proposed statistical and filter data-driven methods from the previous chapters.

Finally, chapter 8 draws conclusions from the work undertaken. Possible areas for future research are recommended in this chapter.

Chapter 2 Literature Review

2.1 Framework of the Literature Review

This chapter presents a review of the construction of LED lighting (from chip to system), the existing handbook based reliability prediction methods for electronics and some other's works in the field of failure analysis and reliability prediction for LEDs. The layout of this chapter is organized as follows: Section 2.2 briefly introduces the working mechanism, materials and construction of the LED lighting, from a semiconductor chip to a lighting system. This section also introduces one type of most widely used substitutes for traditional general illumination, the High Power White LEDs (HPWLEDs) lighting. In section 2.3, the handbook-based reliability prediction methods for electronics are reviewed. Finally, section 2.4 reviews the previous study in the field of failure analysis and reliability prediction for LEDs.

2.2 Brief Overview of LED Lighting

Since J. Holonyak and S. Bevacqua (Holonyak & Bevacqua, 1962) invented the first commercial LEDs in 1962, LEDs have undergone remarkable development over the past half century, including the rapid development in epitaxy technology, chip design, packaging structure and materials, and luminaire design (Schubert & Kim, 2005). The development trend of LEDs was predicted by Haitz and Tsao (2011), as following the Moore's law of the traditional semiconductor industry. As shown in Fig. 2-1, the light output per package doubles every year and the cost per lumen (unit of luminous flux) drops ten times every decade.

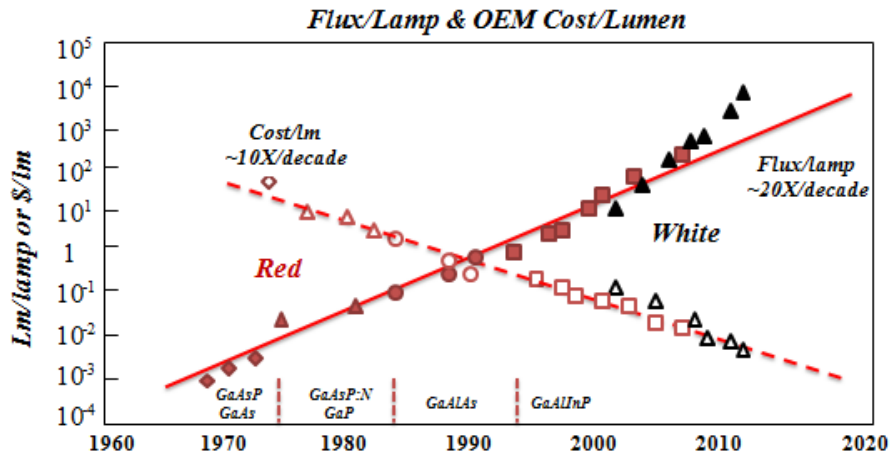
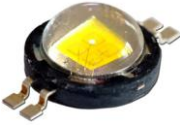
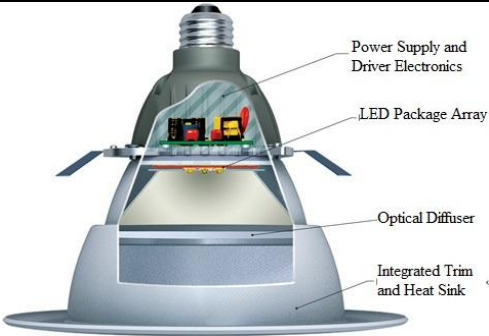


Fig. 2-1 The predicted development trend of LEDs (Haitz & Tsao, 2011)

As an electronic assembly, an LED lighting system is always composed of some subsystems, which can be classified into three levels (Table 2-1): (1) chip level; (2) package level; (3) system level. Usually, as the first level, the chip (or die) is a p-n junction which is always constructed by a thin monocrystalline semiconductor layer and it is working for the photon (light) emission under electronic excitation. In the package level, the packaging materials make contributions in the electrical contacts with the electrodes, thermal dissipation, mechanical resistance, light extraction by lens and reflector, chemical protection and light conversion by phosphor encapsulation (for white LEDs) (Lafont et al., 2012). At the third level of LED lighting, the printed circuit board (PCB) provides the electrical and mechanical supports for the LED module, and by taking thermal, electrical and optical issues into consideration, cooling, electrical drivers and reflectors are introduced to the LED lighting system.

Table 2-1 LED lighting systems

Levels	Subsystems	
Chip level		related to the semiconductor chip (or die)
Package level		related to the LED package (including packaging materials, electrodes and optical lens)
System level		related to the LED systems (including printed circuit board (PCB), cooling, reflector, electrical driver and luminaries house)

2.2.1 LED Chips

An LED semiconductor chip is always composed of a p-junction, an n-junction and an active layer (single quantum well or multiple quantum wells). The illumination mechanism of LEDs is shown in Fig. 2-2. When a p-n junction is biased forwards, electrons in the n-junction with sufficient energy move across the boundary layer into the p-junction, and holes injected in the p-junction move into the n-junction through the active layer (Schubert, 2006, Chang et al., 2012). The recombination of the electron and the hole in the active region leads to the production of a photon (light) (Fig. 2-3).

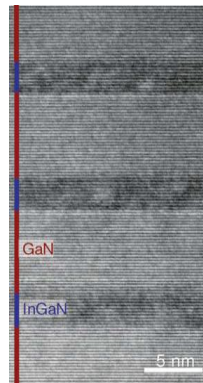


Fig. 2-2 High-resolution transmission electron microscope of InGaN quantum wells separated by GaN barriers (Humphreys, 2008)

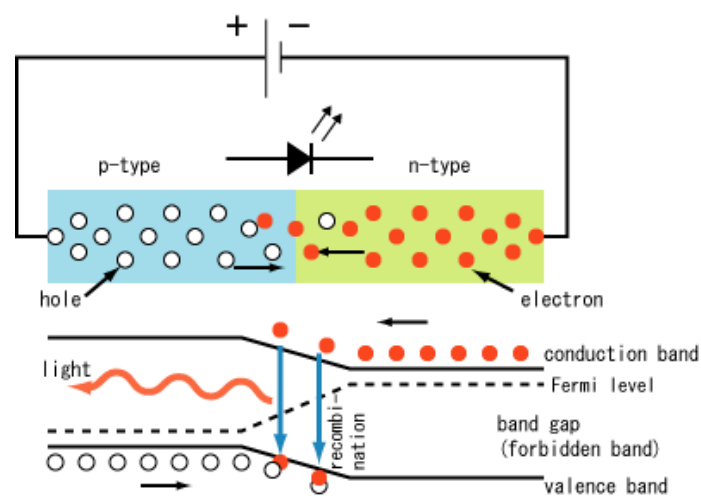


Fig. 2-3 The working mechanism of LEDs (Schubert, 2006)

The photon energy or its wavelength is directly proportional to the band-gap of the semiconductor materials used. The light color of LEDs can be determined by the wavelength of the emitted photon. According to the band gap shown in Fig. 2-4, the semiconductor materials used as LED chips can be distinguished into three main crystal families: (1) cubic diamond structure (Si, Ge, C); (2) cubic zincblende structure (III-Phosphides and III-Arsenides); (3) hexagonal wurtzite structure (III-Nitrides). Among these, the most important semiconductor materials for LEDs

are considered to be the last ones (III-Nitrides type) (see Table 2-2). III-Nitrides semiconductors with wide-band-gap, such as GaN, AlN, and (In, Al, Ga)N, are widely used to fabricate short-wavelength LEDs (UV-to-blue LEDs) (O'Leary et al., 2006, Krames et al., 2007).

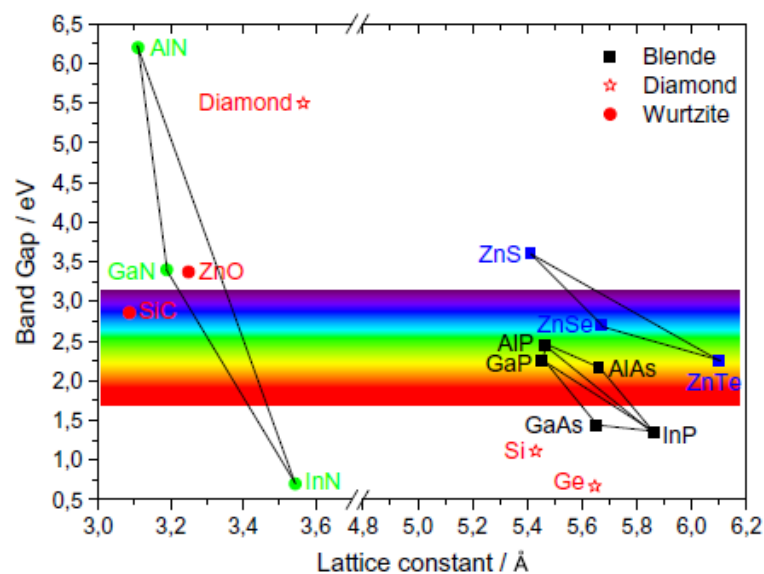


Fig. 2-4 Band gap of principal semiconductor used in LEDs (Schubert, 2006)

Table 2-2 LED semiconductor chip materials (Xie et al., 2011)

Semiconductor Material	Wavelength (nm)	Emission Color
GaAs	840	Infrared
AlGaAs	780,880	Red, infrared
GaP	555,565,700	Green, yellow, red
GaAsP	590-620	Yellow, orange, red
AlGaInP	590-620	Amber, yellow, orange
InGaN	390, 420, 515	Ultraviolet, blue, green
AlGaInN	450, 570	Blue, green
AlGaN	220-360	Ultraviolet
AlN	210	Ultraviolet

2.2.2 LED Packages

A typical LED package can be considered as a subsystem that combines an LED chip, electrical and thermal connections, optical reflector, substrate, phosphors (Xie et al., 2013, Smet et al., 2011) (phosphor-converted white LEDs), encapsulating materials and optical lens (Fig. 2-5) (Lu & Wong, 2009). The functions of packaging process can be summarized into:

- (i) Providing an electrical connection to the LEDs semiconductor chip.

For the LED packaging, the LED chip is attached to the substrate by solder or silver paste (Fig. 2-5), and the lead frame can act as the electrical contact to the outside. The wire bond, one typical electronic interconnection technology, connects the metal pin on the top of the LED chip with the lead frame, which allows the electrical signal to be sent to the LED from the outside.

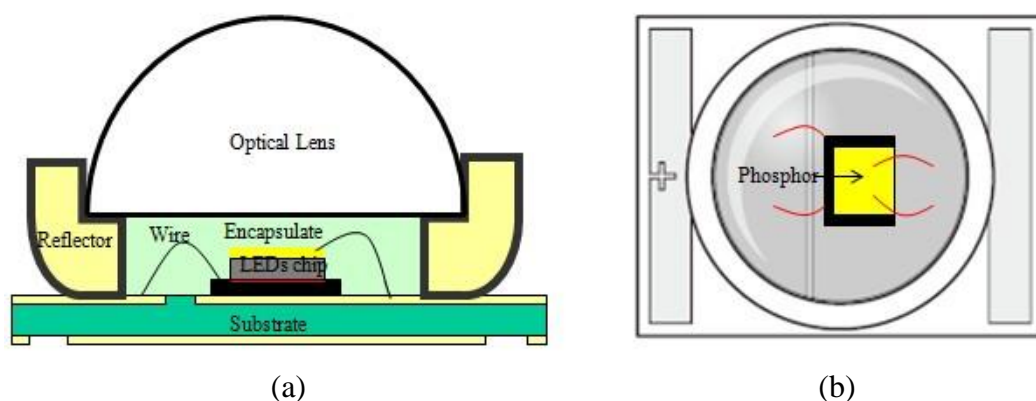


Fig. 2-5 LEDs packaging: (a) cross-section and (b) top view (CREE, 2006)

(ii) Managing the thermal dissipation

Thermal dissipation has become as a serious concern within the reliability of LED lighting systems. The heat produced by the non-radiative process in the active layer may damage the p-n junction, lower the luminous efficiency, increase forward voltage, cause a wavelength shift, reduce lifetime and affect the quantum efficiency of the phosphor (Arik et al., 2004). The main approaches in enhancing the thermal dissipation in LED packages are to make the heat dissipation path as large a surface as possible, to add a heat slug with higher thermal conductivity and to shorten the thermal dissipation path. In 2006, Lumileds (LUXEON, 2008) proposed the most successful high power LED package (Luxeon K_2) (Fig. 2-6 (a)) from the thermal management view, by means of integrating a heat sink slug with high thermal conductivity into the lead frame, which can make the junction temperature of this package to under 150°C with a 1.5 A driven current (Fig. 2-6 (b)).

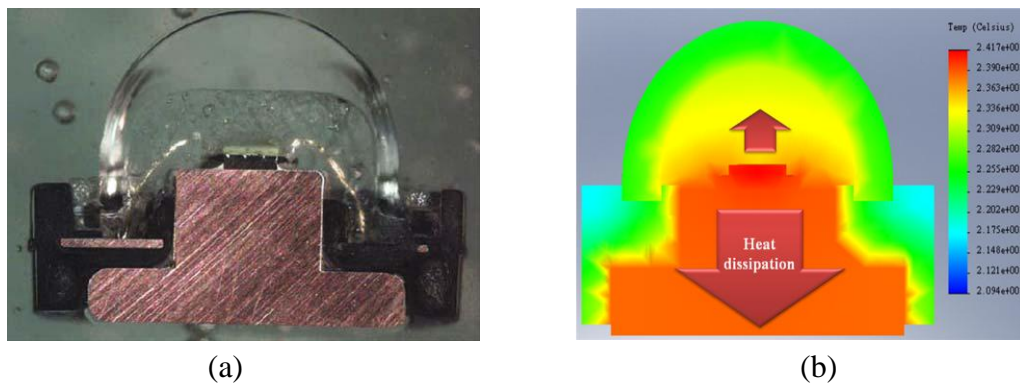


Fig. 2-6 (a) Packaging structure of Luxeon K_2 and (b) the heat dissipation simulation (Schubert, 2006 and Luxeon, 2008)

(iii) Mechanically protecting the LED chip

To protect the LED chip and wire bonds from mechanical vibration or shock, encapsulation materials (such as epoxy or silicone based polymer glue (Chien et al., 2012) are widely implemented into the LED package (as shown in the Fig. 2-6 (a)). For instance, Wong *et al* (Wong, 1995) introduced a modified thermal-mechanical enhanced silicone-based encapsulate to improve the reliability of the LED package.

(iv) Preserving the LED chip from external chemical aggression.

In addition to the mechanical vibration and shock, moisture and dust are two major causes of semiconductor device defects. Among them, moisture is the first suspect in chemical aggression to the LED chip. Electro-oxidation and metal migration are associated with the diffusion of moisture in the LED packages (Yang et al., 2010, Meneghesso et al., 2003, Tan et al., 2009a). Because of their low diffusion rate and low chemical reaction rate with moisture, polymer based materials, such as epoxies and silicones (Fig. 2-7), are widely used for encapsulation in optoelectronic device packaging (Lau et al, 1998). Epoxy based encapsulates are commonly used in the standard LED applications, however, for the high power LEDs (input power >1w), the epoxy encapsulates show photo-thermal induced degradation caused by both high junction temperature from these LED diodes and photo-generated

transmission losses from blue/UV LEDs.

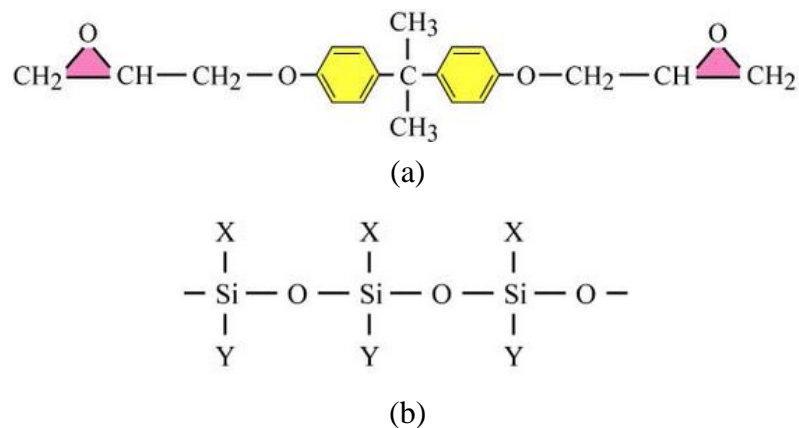


Fig. 2-7 Chemical structures of (a) typical epoxy and (b) silicone (Schubert, 2006)

In contrast to traditional epoxy encapsulates, silicone has become another choice with high resistance to discoloration caused by both the high temperature and blue/UV emissions from high power LED light sources. It has wider operation temperature, higher stress-relieving properties, and better flame resistance. Compared to conventional materials used in optoelectronic applications, the chemical structure of silicone provides several advantages. For instance, the backbone structure of silicone consists of silicon (Si) and oxygen (O). The Si-O bond is inorganic and has a higher bond energy (444kJ/mol) than either C-C bond (356kJ/mol) or carbon C-O bond (339kJ/mol) in epoxy polymers (Momentive Performance Materials, 2005).

(v) Driving the light extraction

As mentioned above, heat generation inside the package affects the reliability of LEDs. One of the contributors to the heat concentration is from the low light extraction, which can be attributed to the LED lumen degradation and color shift. To improve the light extraction, Luo *et al* (Luo et al., 2005) introduced a cup at a certain tilted angle and epoxy surface condition (epoxy-air interface) to the LED package. Other research indicated that the light extraction can be enhanced by using epoxy encapsulates with high refractive index and high transparency.

2.2.3 LED Systems

As mentioned above, LED systems (for example, the LED lamp) always include three major parts (sub-systems): optical part, electrical driver part and thermal management part.

The optical part of the system (LED light engine) contains the light source, PCB, reflector and lens. According to the application requirements, the LED single unit can be connected either in series or in parallel models. The designer always chooses the types and numbers of LEDs based on the application requirements and manufacturing concerns.

The electrical driver part of the LED lighting system prepares the regular power

for the optical part (see Fig. 2-8). Different applications require different power supplies. For instance, in general lighting systems, the main city power supply is 220V/50Hz, However, for automotive applications, the power supplied from a battery is 12~24V. Besides, as the electrical supplier for the optical part of LED system, the electrical part can also dim or control the color of LED optical parts(Winder, 2008, Tarashioon et al., 2012, Fathi et al., 2011).

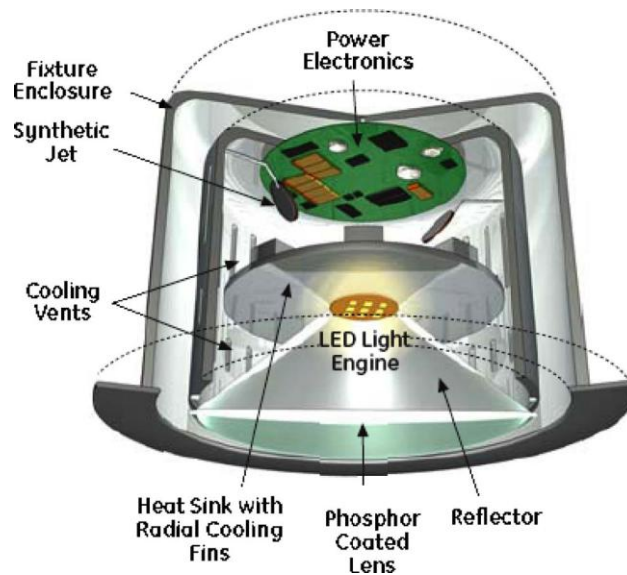


Fig. 2-8 LEDs system architecture (Song et al., 2010)

As discussed previously, heat dissipation is the first challenge for the LED manufacturers or designers, not only at the package level, but also at the system level. Therefore, the thermal management part (either passive cooling or active cooling) becomes the essential subsystem to maintain the LED junction temperature below a

critical value in LED lighting systems. Passive cooling solutions (cooling fins) have been widely implemented in LED lighting systems (such as downlights and lamps)

(Fig. 2-9 (a)).

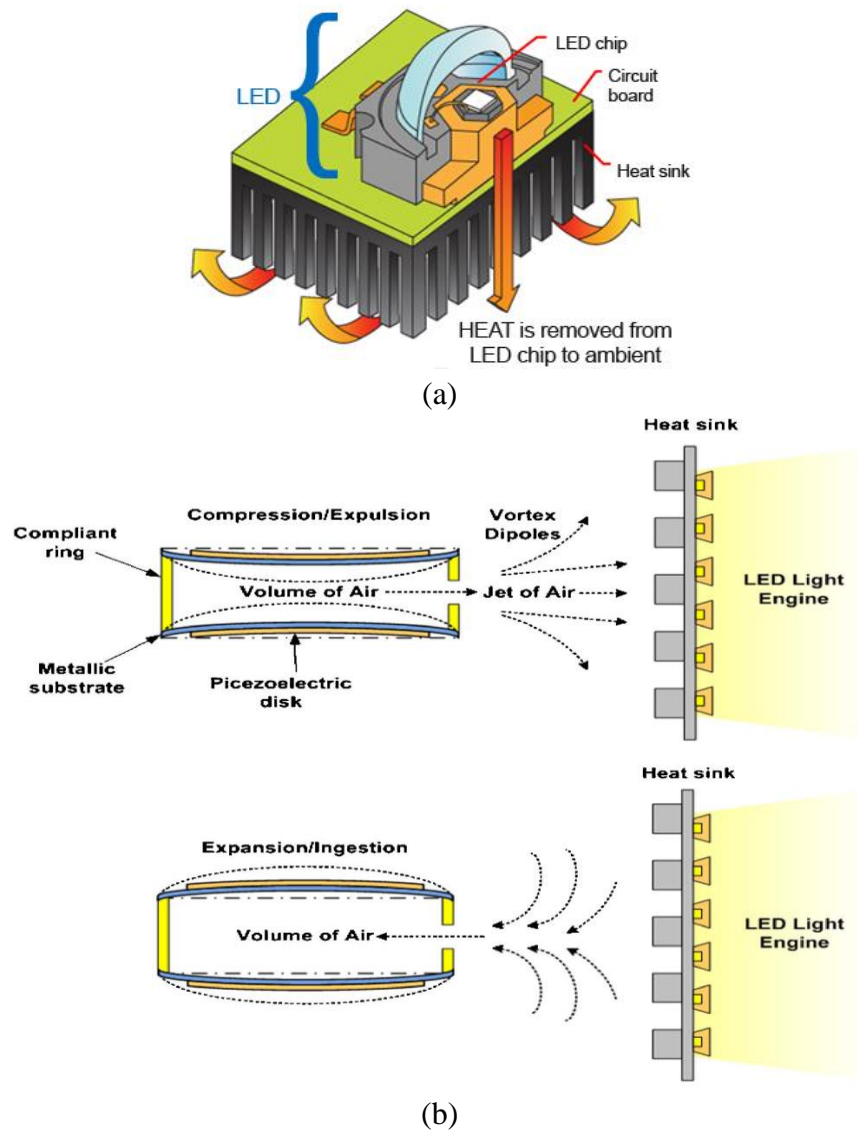


Fig. 2-9 (a) Passive cooling and (b) active cooling for LED system
(Song et al., 2010)

However, due to the limitations of the cooling capacity offered by the passive cooling, the maximum total light output is controlled to under about 600 lm with the highest luminaire efficacy about 54 lm/W. To satisfy the lumen requirement for the

general illumination (lumen: 1200~1500lm, luminaire efficacy: 60lm/W), active cooling with high cooling capacity has become necessary. Potential active cooling methods include thermal-electrics, piezoelectric fans, synthetic jets and small form factor fans. There are some specific requirements for the cooling system: (1) low power consumption; (2) low cost; (3) compact size; (4) high reliability (the lifetime of cooling components should be higher than the LED optical part). For instance, Song *et al* (Song et al., 2010) implemented active cooling(synthetic jet cooling) into the LEDs downlight to solve the thermal problems (Fig. 2-9 (b)).

2.2.4 High Power White LEDs Lighting

One of the most interesting applications of LEDs is in general illumination, which requires white light. During the late 1990s, LED manufacturers began to produce high power white LEDs which have larger lumen packages (10~>100 lumens per package) and greater luminous efficacy (>20 lumens per watt) (Narendran et al., 2004). Since 2000, high power white LED lighting has undergone rapid development.

Because a single LED chip can only generate monochromatic light with a very narrow spectral range or ultraviolet light that the human eye can't see, mixture techniques with two or more colors have been developed to produce white light (Van

Driel & Fan, 2012). To create white light, several promising strategies have been used in the applications, including di-, tri-, and tetra-chromatic approaches (Schubert & Kim, 2005) (Fig. 2-10). These approaches differ in terms of their luminous efficiency, color stability, and color rendering capability (these performance metrics of LED lighting are introduced in the next section).

The di-chromatic approach is one of commonly used methods to generate the white color, which combines two monochromatic colors (blue and yellow) with a certain power ratio. With the help of yellow phosphor materials, the blue light produced from a LED chip can be converted to white. Phosphor is a wavelength converter material, which consists of an inorganic host material doped with an optically active element (Lin & Liu, 2011). Cesium-doped yttrium aluminum-garnet (YAG:Ce³⁺) is a common yellow phosphor (Smet et al., 2011). Nowadays, the phosphor-converted (pc) white LED has become one of most widely used white light sources in general illumination applications, showing advantages in high luminous efficacy (425 lm/W), low cost, easy fabrication and high reliability (Ye et al., 2010). By adjusting the mixing proportion and concentration of phosphor, white LED lighting with different color temperatures can be obtained. However, the degradation of the LED chip or YAG:Ce³⁺ phosphors cause some significant color changes during aging.

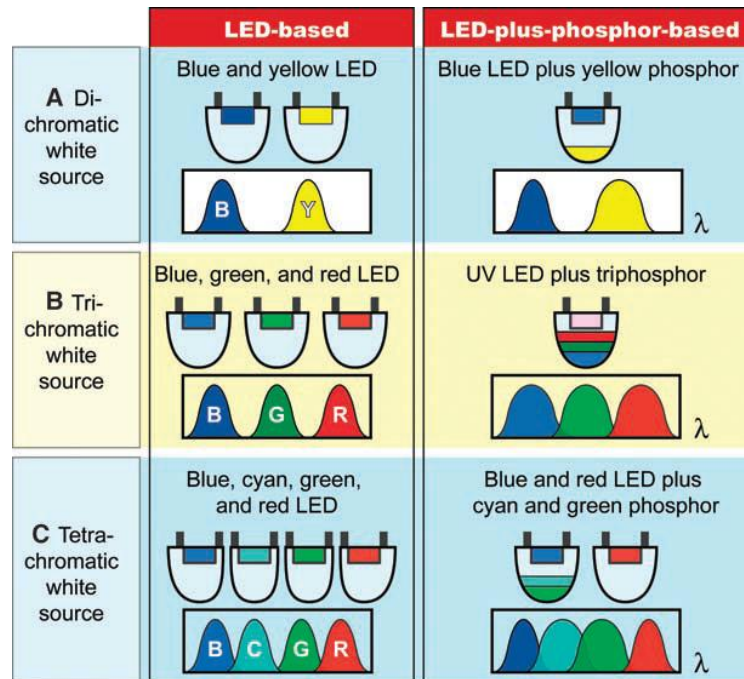


Fig. 2-10 White LED lighting (Schubert & Kim, 2005)

The tri-chromatic approach mixes three colors (reds, greens, and blues) to generate white light. Because the conversion losses associated with the use of phosphors are eliminated, the tri-chromatic approach has both a good color rendering property and high luminous efficacy (300lm/W). However, a disadvantage is that more complex electronics (possibly with feedback mechanisms) have to be used to drive the currents for different color LEDs, which makes the fabrication process complicated. This approach also requires additional electronic circuits to control and counteract the differential aging of the current red, green and blue LEDs. Therefore, the cost is much higher on the associated smart control instruments compared to the previous phosphor converted approach. In order to lower this cost, the tri-chromatic

approach has been developed to produce white light by using an ultraviolet (UV) LED to stimulate RGB tri-chromatic phosphors. Previous research shows that the UV LED with tri-chromatic phosphors has advantages in high efficiency, high color rendering and high chromatic stability (Sheu et al., 2003).

The tetra-chromatic approach combines four colors together (Blue, Cyan, Green and Red) to illuminate white light, which also can give excellent color rendering index (CRI) values suitable for essentially any application. However it has a lower luminous efficacy (275lm/W) than di-chromatic or tri-chromatic sources (Schubert et al., 2006). Because of introducing four color sources, the fabrication and maintenance of LEDs using the tetra-chromatic approach are more complicated and expensive. Table 2-3 lists the advantages and disadvantages of these three white LED lightings.

Table 2-3 Comparison of white LED lightings

Approaches	Advantages	Disadvantages
Di-chromatic white source	Low cost; easy fabrication	Low efficiency; low CRI; low chromatic stability under different driving currents
Tri-chromatic white source	High efficiency; high CRI; high chromatic stability under different driving currents; tunable color temperature	Complex blending of different phosphors; lack of efficient red phosphor
Tetra-chromatic white source	Excellent CRI values suitable for essentially any application	Lowest luminous efficacy; complex blending of different phosphors

2.3 Review of Traditional Reliability Prediction Methods for Electronics

Reliability prediction has a long and controversial history, and is widely applied in electronic devices and equipment. The objectives of reliability prediction methods can be summarized according to the product development states: (1) in the design stage, it helps to determine if a reliability requirement is achievable and to can be used in a reliable design that meets the requirement; (2) in the manufacturing stage, it can help to achieve a reliable manufacturing process; (3) to guarantee the after-sale quality, it assesses potential warranty risks and provides safety analysis and also establishes baselines for logistic product support requirements (Foucher et al., 2002).

Since the 1960s, several reliability prediction handbooks have been published by governments, military organizations and industrial associations, with applications in Aviation and Defense, Telecommunications, Automotives, Electronics and Computers, and Mechanical Equipment (EPSMA, 2005, Cassanelli et al., 2005). These current reliability prediction handbooks for electronic devices and equipment mainly depend on the collection of failure data and generally assume the components of the system have a constant failure rate that can be adjusted by independent “modifiers” to account for various quality, operating and environmental conditions. Some reliability prediction handbooks designed for electronic devices and equipment in different application areas are listed in Table 2-4.

Table 2-4 Reliability prediction handbooks for electronic devices and equipments

Application area	Name
Aviations and Defenses	MIL-HDBK-217F Note2, Reliability Prediction of Electronic Equipment (1995)
	RAC, PRISM Tool (2005)
	RiAC-HDBK-217Plus (2010)
	FIDES Guide, Reliability Methodology for Electronic Systems (2010)
	GJB/Z-299, 電子設備可靠性預計手冊 (1987)
Telecommunications	SN 29500, Siemens Reliability and Quality Specification Failure Rates of Components (1999)
	IRPH, Italtel Reliability Prediction Handbook (2003)
	BellCore TR-332, Reliability Prediction Procedure for Electronic Equipment (1997)
	HRD, Handbook of Reliability Data for Components Used in Telecommunications Systems (British Telecom Reliability Handbook) (1992)
	NTT Procedure, Nippon Telegraph and Telephone Corporation Standard Reliability Table for Semiconductors (1985)
	RDF, Compilation of CNET's Reliability Data (2003)
	Telcordia SR-332, Reliability Prediction Procedure for Electronic Equipment (2011)
Automotives	ARP-1.0, Automotive Reliability Prediction Program (Powertronic Systems Inc., PSI), Society of Automotive Engineer's Technical Paper 870050
Electrics and Computers	IEEE-STD-1413, IEEE Standard Methodology for Reliability Prediction and Assessment for Electronic Systems and Equipment (1996)
	IEEE-STD-1413.1, IEEE Guide for Selection and Using Reliability Predictions Based on IEEE 1413 (2002)
Mechanical Equipments	DTRC-90/010, Handbook of Reliability Prediction Procedures for Mechanical Equipment (1990)
	NSWC-11, Handbook of Reliability Prediction Procedures for Mechanical Equipment (2011)
Electronics	IEC-61709, Reliability – Reference Conditions for Failure Rates and Stress Models for Conversion (1996)
	IEC-62380, Reliability Data Handbook –Universal Model for Reliability Prediction of Electronics Components, PCBs and Equipment (2004)

(i) Note: The year in brackets is the year of the lastly updated

In summary, all reliability prediction handbooks contain one or more of the following set of information for the calculation of predicted results (IEEE 1413.1, 2002):

- (ii) The constant failure rate values for different parts under operation or non operation;
- (iii) Multiplicative factors for different environmental parameters;
- (iv) Multiplicative factors that are applied to a base operating a constant failure rate to obtain the non-operating constant failure rate.

In the following section, an early-published reliability prediction book: MIL-HDBK-217, and three new updated handbooks: RiAC-HDBK-217PLUS (2006), Telcordia SR-332 (2011); FIDES Guides (2010) are reviewed.

2.3.1 MIL-HDBK-217

The Military Handbook MIL-HDBK-217 [Reliability Prediction of Electronic Equipment] was first published by the US Department of Defense (DoD) in the 1960s and the last version of this handbook is MIL-HDBK-217 Reversion F Notice 2 was released on February 28, 1995 (MIL-HDBK-217 F Notice 2, 1995). MIL-HDBK-217 contains two prediction methods with assumption of constant failure rate, including the parts count method and the parts stress method. It proposes

the failure rate prediction models for the electronic components, such as ICs, transistors, diodes, resistors, capacitors, relays, switches, connectors and so on (MIL-HDBK-217 F Notice 2, 1995). These prediction models are based on the averaged accumulated historical field data which were collected from a wide variety of electronic parts and systems. This method assumes that each constant failure rate can be calculated by some factors which account for various quality, operation, and usage conditions.

$$\lambda_p = \lambda_b \pi_T \pi_A \pi_R \pi_S \pi_C \pi_Q \pi_E \quad (2-1)$$

Where λ_p is the part failure rate, λ_b is the base failure rate, and the pi (π) factors are independent parameter modifiers whose values depend on the product and its condition of usage.

Therefore, as summarized by Cushing et al. there are several limitations in MIL-HDBK-217 (Cushing et al., 1993):

- (i) Crucial failure details (like failure site, failure mechanisms, load/environment history, materials and geometries) are not collected and addressed;
- (ii) Failure rate models are point estimates which are based on available data. Hence, they are only useful for the conditions with sufficient historical data, and for the limited devices;
- (iii) The design and usage parameters are also not addressed in this handbook, which

results in an inability to tailor a prediction using these key parameters;

- (iv) This handbook is only suitable for component level, not for equipment or system level.

Because of these limitations, the US army discontinued this particular prediction approach in recent years.

2.3.2 RiAC- HDBK -217PLUS

The 217Plus [Handbook of 217Plus Reliability Prediction Models] is a handbook developed by the Reliability Information Analysis Center (RiAC) to provide methods in assessing the system reliability (RiAC-HDBK-217PLUS, 2006).

Usually, the 217-Plus prediction handbook has two applications: (i) Component reliability prediction; (ii) System-level reliability prediction (Nicholls, 2006).

(i) Component reliability prediction

As mentioned in MIL-HDBK-217, the typical component failure rate is predicted by a base failure rate multiplied by several factors that account for the environmental factors, stresses and component variables that influence reliability (Nicholls, 2006).

However, the predicted failure rate with this multiplicative model form can become unrealistically large or small under extreme value conditions, i.e., when all factors are at their highest or lowest values. To avoid this drawback, the 217-Plus handbook

uses a combination of additive and multiplicative model forms to predict a separate failure rate for each class of failure mechanism (Nicholls, 2006).

$$\lambda_p = \lambda_o \pi_o + \lambda_e \pi_e + \lambda_c \pi_c + \lambda_i + \lambda_{sj} \pi_{sj} \quad (2-2)$$

where λ_p = Predicted failure rate; λ_o = Failure rate from operational stresses; π_o = Product of failure rate multipliers for operational stresses; λ_e = Failure rate from environmental stresses; π_e = Product of failure rate multipliers for environmental stresses; λ_c = Failure rate from power or temperature cycling stresses; π_c = Product of failure rate multipliers for cycling stresses; λ_i = Failure rate from induced stresses, including electrical overstress and ESD; λ_{sj} = Failure rate from solder joints; π_{sj} = Product of failure rate multipliers for solder joint stresses.

(ii) System reliability prediction

Besides component level prediction, the 217-Plus handbook also has a system level reliability prediction model (Nicholls, 2006). To account for non-component effects, the system level prediction models integrate various system-level factors into the initial assessment of the system failure rate. A system level model can be expressed as:

$$\lambda_p = \lambda_{IA} (\Pi_p \Pi_{IM} \Pi_E + \Pi_D \Pi_G + \Pi_M \Pi_{IM} \Pi_E \Pi_G + \Pi_S \Pi_G + \Pi_I + \Pi_N + \Pi_W) + \lambda_{SW} \quad (2-47)$$

where λ_p = Predicted failure rate of the system; λ_{IA} = Initial assessment of the system failure rate; Π_{IM} = Infant mortality factor; Π_E = Environmental factor; Π_G =

Reliability growth factor; λ_{SW} = Failure rate, software; Π_P = Parts process grading factor; Π_D = Design process grading factor; Π_M = Manufacturing process grading factor; Π_S = System Management process grading factor; Π_I = Induced process grading factor; Π_N = No-Defect process grading factor; Π_W = Wearout process grading factor.

The 217-Plus handbook is documented in a similar format as MIL-HDBK-217, and the entire 217-Plus reliability prediction process always includes (RiAC-HDBK-217PLUS, 2006): (1) the prediction process flow diagram, (2) definition of variables, (3) component- and system-level reliability prediction models and model factors, (4) look-up tables that support the calculation of component and system failure rates, and (5) the process and supporting tables for determining and applying process grade factors (see Fig. 2-11).

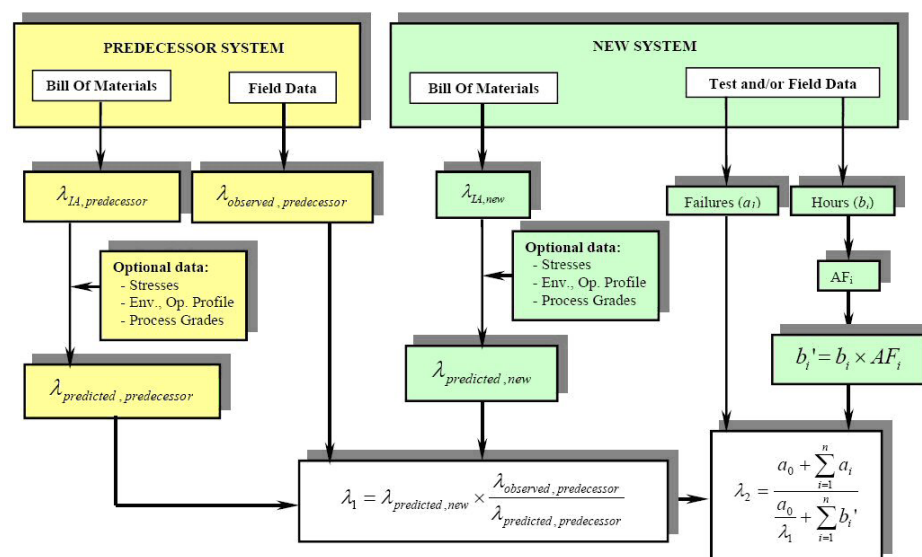


Fig. 2-11 The 217Plus approach to failure rate estimation
(RiAC-HDBK-217PLUS, 2006)

2.3.3 Telcordia SR-332(Bellcore)

The Telcordia SR-332(Bellcore) [Reliability Prediction Procedure for Electronic Equipment] was first published by the Bell Communications Research Center for telecommunications companies in 2001 (SR-332, Issue 1, 2001), and it was upgraded to a new version in 2006 (SR-332, Issue 2, 2006). To meet the appropriate Telcordia generic and system-specific requirements on physical design, manufacture, installation, and reliability assurance practices (SR-332, Issue 1, 2001, SR-332, Issue 2, 2006), this handbook is designed for commercial telecommunication systems with the empirical statistical models. The Telcordia SR-332 proposed a serial model for electronic parts. It developed three prediction methods for the failure rates at the infant mortality stage and at the steady-state stage (Method I, II and III).

- (i) Like the MIL-HDBK-217 parts count and part stress methods. Method I provides the generic failure rates and three part stress factors: device quality factor (π_Q), electrical stress factor (π_S) and temperature stress factor (π_T).
- (ii) Method II provides prediction approach by combining Method I predictions with the laboratory test data collected according to the specific SR-332 criteria.
- (iii) In the Method III, a statistical prediction of failure rate is developed by using field data collected based on specific SR-332 criteria. In this method, the predicted failure rate is a weighted average of the generic steady-state failure

rate and the field failure rate.

The main concepts in Telcordia SR-332 and MIL-HDBK-217 are similar and Telcordia SR-332 applies most equations given in MIL-HDBK-217 in the telecommunications field, however, Telcordia SR-332 also has some developments for solving the prediction problems for systems. For example, a Bayesian analysis to incorporate burn-in, field, and laboratory test data is developed in Telcordia SR-332. It also accounts for the uncertainty in the parameters contributing to reliability, and the upper confidence levels for failure rates are also calculated in Telcordia SR-332 (Bennett, 2008). However it does not address the uncertainty in the failure models used.

2.3.4 FIDES Guides

The FIDES Guides were published by a French alliance which includes Airbus France, Eurocopter, GIAT Industries, MBDA and THALES, and provide reliability prediction methodologies for weapon systems and civil aeronautics systems (FIDES Guide 2004, Issue A, 2004, FIDES Guide 2009, Edition A, 2010). The purpose of the FIDES Guides is to establish a realistic assessment of the reliability of electronic components and systems operating under particular environments. Generally, the FIDES Guides separate the reliability prediction methodologies to two parts: (i)

component reliability prediction guide; (ii) reliability process control and audit guide (Held & Fritz, 2009, Charpenel et al., 2003).

(i) Component reliability prediction guide

The component reliability prediction models proposed in the FIDES Guides are used to calculate the component failure rates based on the component characteristics and application environmental data (such as thermal and electrical stress data). The general model of failure rate in the FIDES Guides consists of the physical contribution $\lambda_{Physical}$, the part manufacturing factor $\Pi_{Part_manufacturing}$ and the process factor $\Pi_{Process}$, which can be expressed as:

$$\lambda = \lambda_{Physical} \times \Pi_{Part_manufacturing} \times \Pi_{Process} \quad (2-3)$$

$$\lambda_{Physical} = \left[\sum_{Physical_contributions} (\lambda_0 \cdot \Pi_{acceleration}) \right] \cdot \Pi_{induced} \quad (2-4)$$

The physical contribution can be expressed as a component basic failure rate λ_0 multiplied by acceleration factors $\Pi_{acceleration}$, where the acceleration factors include the environmental acceleration factors and conditions of usage. The induced factors $\Pi_{induced}$ are the overstress (electrical, mechanical or thermal) factors. The part manufacturing factor represents the quality and technical control of the component's manufacture. The $\Pi_{Process}$ is a factor representing the quality and technical control of reliability in the product lifecycle which includes specification, design, manufacturing, field operation and maintenance, as well as support activities.

(ii) Reliability process control and audit guide

In order to calculate the process factor $\Pi_{Process}$, a guide to audit equipment is recommended in the FIDES Guides. The values of the process factors are assigned by answering questionnaires about the product development, manufacture and operation processes. The audit procedure is standardized in the FIDES Guides: (1) Prepare the audit; (2) Undertake the audit; (3) Gather the proof; (4) Process the collected data; (5) Draw conclusions; (6) Write an audit report; (7) Present the audit results.

Recently, with the increasing number of various reliability prediction handbooks, how to select an appropriate handbook from so many options for their products has become difficult for manufacturers. Thus, the IEEE proposed criteria to assess and compare the reliability prediction methodologies, which was then published as a standard IEEE Std 1413 (IEEE Std 1413, 1998, IEEE Std 1413, 2010). It helps to identify the key required elements for an understandable and credible reliability prediction method and to provide its users with sufficient information to evaluate prediction methodologies (Elerath & Pecht, 2012, Pecht et al., 2002) (see Table 2-5).

Table 2-5 Comparison of reliability prediction methodologies

Criteria	Handbooks	MIL-HDBK-217F	RiAC-21 7PLUS	Telcordia SR-332	FIDES Guides
Does the methodology identify the sources used to develop the prediction methodology?		No	Yes	No	No
Are the sources used to develop the prediction methodology available in public domain or upon request?		No	No	No	No
Does the methodology account for life cycle environmental conditions, including those encountered during 1) manufacturing, 2) product usage (including power and voltage conditions), 3) packaging, 4) handling, 5) storage, 6) transportation, and 7) maintenance conditions?		No	No	No	Yes
Does the methodology account for materials, geometry, and architectures of the parts and assemblies?		No	No	No	No
Does the methodology account for part quality?		Quality levels are derived from specific part-dependent data and the number of the manufacture screens the part goes through	No.	Four quality levels that are based on generalities regarding the origin and screening of parts.	Process factor represents the quality and technical control of reliability in the product lifecycle
Does the methodology have the flexibility to allow incorporation of new reliability data and experience?		No	Yes, through Bayesian method of weighted averaging	Yes, through Bayesian method of weighted averaging	No
Are assumptions used to conduct the prediction according to the methodology identified, including those used for the unknown data?		No	Yes	Yes	No

Table 2-5 Comparison of reliability prediction methodologies (cont')

Criteria	Handbooks	MIL-HDB K-217F	RiAC-21 7PLUS	Telcordia SR-332	FIDES Guides
Are sources of uncertainty in the prediction results identified?		No	Yes	Yes, account for the uncertainty in the parameters contributing to reliability	No
Are limitations of the prediction results identified?		Yes	Yes	Yes	Yes
Are failure modes identified?		No	No	No	No
Are failure mechanisms identified?		No	No	No	No
Are failure causes identified?		No	No	No	No
Are statistical confidence levels and confidence intervals for the prediction results identified?		No	No	Yes, upper confidence levels for failure rates are calculated in SR-332 Issue 2	No

In brief, the handbook-based reliability prediction methods have been widely used in the military and electronic industries for many years. However, with the developing technologies in electronic devices and equipments, most of these reliability prediction handbooks are facing several problems in dealing with today's novel technologies. Several concerns with these handbooks on reliability prediction were reported, such as inappropriate field loading, unreliable material databases, lack of understanding of failure modes and failure mechanisms (Gottfried, 1997, Luthra, 1990). The major conclusion is that these handbooks are inaccurate for predicting actual field failures, such as soft and intermittent faults, which are the most common

failures modes in today's electronics-rich systems, and provide highly misleading predictions, which can result in poor designs and weak logistics decisions (Pecht & Jaai, 2010). Thus, most of these handbooks are no longer upgraded now and some have been discontinued.

2.4 Review of Failure Analysis and Reliability Prediction Methods for LEDs

Reliability is usually defined as the ability of a product (or system) to perform its required functions under the stated conditions for a specified period of time (O'Connor, 2002). In other words, the reliability deficiency eventually results in impaired or lost performance, compromise safety, and lead to the need for such restorative actions as diagnosis, repair, spare replenishment, and maintenance. In reliability engineering, the reliability is always accompany with the term "failure", which means that the device is incapable of performing its required function (Martz & Waller, 1982). Thus, within the failure analysis and reliability prediction for LED lighting, the failures and lifetime of LED should be defined firstly. For LED lighting, its lifetime also can be interpreted as the time when the performance metrics of LED lighting decreased under particular failure thresholds. In 2011, the Next Generation Lighting Industry Alliance (NGLIA) of U. S. Department of Energy (DoE) recommended that both of the lumen degradation and chromaticity shift should be

included in the calculation of LED lighting's lifetime (Solid-state Lighting Product Quality Initiative, 2011).

The Alliance for Solid-State Illumination Systems and Technologies (ASSIST) (ASSIST Recommendation, 2005) recommends two LED lumen lifetimes based on the time to 50% light output degradation (L_{50} : for decorative lighting) or 70% light output degradation (L_{70} : for general lighting) at room temperature:

(a) L_{70} means that the time at which the lumen output declines by 30% from the initial value (or time to 70% lumen maintenance).

(b) L_{50} means that the time at which the lumen output declines by 50% from initial value (or time to 50% lumen maintenance).

Another important characteristic to qualify the performance of LED lighting is the chromaticity, which is a key parameter for high power white LEDs lighting applied in some areas, such as the backlights of monitor display and traffic lighting. Currently, because there is still no specific physical model to describe the chromaticity shift of white LED lighting, a standard to define the chromaticity lifetime is lacking. However, nowadays, there are some specifications applied in the LED industry to classify the different chromaticities of white light and to verify the color consistency of white light, which can be viewed as the definition of chromaticity failure. Firstly, the American National Standard Lighting Group

(ANSI) of the American National Standard Institute (ANSI) began to establish a specification to recommend the acceptable range of chromaticities for LED-based solid state general lighting, specifying indoor lighting applications [ANSI/ANSI C78.377] (ANSI/ANSI C78.377, 2008)(see Table 2-6). This specification was published by the National Electrical Manufacturers Association (NEMA) in 2008 and it was updated to a new version in 2011 (ANSI/ANSI C78.377, 2011).

Table 2-6 Nominal CCT Categories (ANSI/ANSI C78.377, 2011)

Normal CCT (K)	Target CCT and tolerance	Target D_{uv}	D_{uv} tolerance range
2700	2725 ± 145	-0.0001	$D_{uv}(T_x) \pm 0.006$ Where $D_{uv} = 57700 \times (1/T_x)^2 - 44.6 \times (1/T_x) + 0.0085$ T_x : CCT of the source
3000	3045 ± 175	0.0001	
3500	3465 ± 245	0.0004	
4000	3985 ± 275	0.0009	
4500	4503 ± 243	0.0014	
5000	5029 ± 283	0.0019	
5700	5667 ± 355	0.0024	
6500	6532 ± 510	0.0030	
Flexible CCT (2800-6400K)	$T_F^{1)} \pm \Delta T^{2)}$	$D_{uv}(T_F)^{3)}$	
Where 1) T_F is chosen to be at 100K steps (2800 to 6400K), excluding those eight nominal CCTs listed above; 2) $\Delta T = 1.1900 \times 10^{-8} \times T^3 - 1.5434 \times 10^{-4} \times T^2 + 0.7168 \times T - 902.55$; 3) The same equation given in the column of D_{uv} tolerance range			

In this specification, two performance metrics, chromaticity coordinates and correlated color temperature (CCT), are introduced to express the chromaticity of white light in advance. In order to indicate the difference of the chromaticities on the

either side of the Planckian locus, a distance parameter with a positive sign for values above and a negative sign for values below, with respect to the Planckian locus, D_{uv} , is defined in this document. Referring to the nominal CCT categories from 2700K to 6500K, an approximate quadrangle range is established using the target CCT and D_{uv} with their tolerances and the values of each individual white LED samples should within this area.

Through establishing a boundary to distinguish the different color range, the [ANSI/ANSI C78.377] specification is widely used as a criteria for categorizing for the white LED lighting (Cree, 2010), but it has limitations in detecting the color differences within the range. To solve this problem, the International Electrotechnical Commission (IEC) has developed a different approach for characterizing chromaticity and chromaticity shift based on specific chromaticity coordinates, which can be defined in terms of the numbers of “standard deviations of color matching (SDCM)”. It is illustrated as many MacAdam Ellipses in the CIE chromaticity diagram. A product could be considered failed for excessive chromaticity shift if it moves outside a boundary. The boundary is defined in terms of the n -step SDCM (or n -step MacAdam ellipse). Based on different applications, the criteria of chromaticity shift failure can be categorized as follows (see Fig. 2-12):

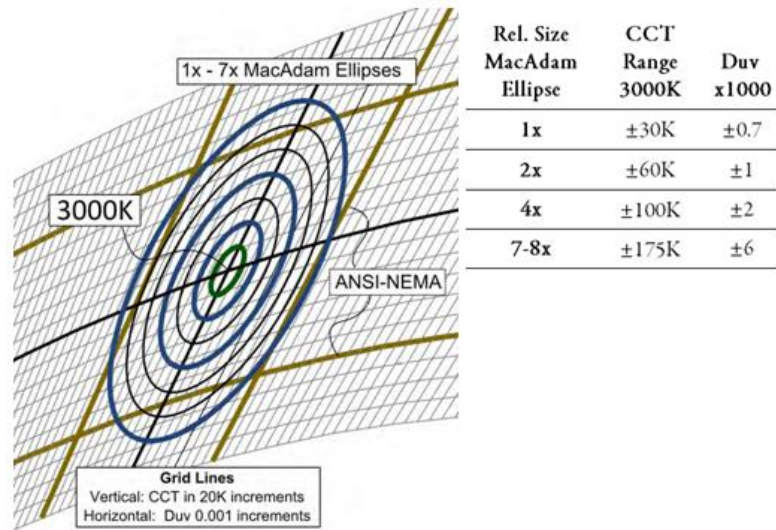


Fig. 2-12 MacAdam ellipses around CCT range 3000K (Steen, 2011)

2-step MacAdam ellipse: it is applied in which the white LED lighting sources are placed side-by-side and are directly visible, or when these lighting sources are used to illuminate an achromatic (white) scene. For example, accent lighting of a white wall and lighting a white cove (Narendran et al, 2004).

4-step MacAdam ellipse: this is used for the situation that the white LED lighting is not directly visible, or when the lighting is used to illuminate a visually complex, multicolored scene. For example, with application of lighting a display case and accent lighting of multicolored objects or paintings (Narendran et al, 2004).

7-step MacAdam ellipse: It covers a very broad area which approximates to the quadrangle range in the [ANSI/ANSI C78.377] specification. Thus, this criteria is accepted by both the ANSI/NEMA and ENERGY STAR Programs of the DoE (DOE,

2008, Wood, 2010).

There have been several papers published on failure analysis and reliability study for the LED lighting. For instance, Narendran *et al* (Narendran et al., 2004) conducted long term life testing for white LEDs to understand the long-term performance. In this study, both the junction temperature and the amplitude of short-wavelength radiation were found to be two major factors influencing the degradation rate of the light output in LEDs. In addition, an overview of the degradation mechanisms of GaN-based LEDs was presented by Meneghini *et al* (Meneghini et al., 2008), in which sets of specific experiments were carried out to analyze the degradation of the performance of LED chips (such as in active layers, ohmic contacts and packaging materials). This study also reported two factors that influences the LED's reliability (current density and temperature). Menghesso *et al* (Menghesso et al., 2010) also presented a review on the physical failure mechanisms of GaN-based LEDs. In this paper, three failure mechanisms, degradation of the active layer, degradation of the package/phosphor system, and electrostatic discharge induced failure, were described. Dal Lago *et al* (Dal Lago et al., 2011) analyzed the failure mechanisms of high-power white LEDs related to both the current and temperature active factors. The results in this study found that the temperature and operation current had different impacts on the optical degradation of LEDs. In detail,

the thermal stress can induce short-term optical power degradation, while the current stress can cause a long-term degradation process. In Horng *et al*'s work (Horng et al., 2012), a thermal transient tester and scanning electron microscope were used to investigate the relationship between thermal resistance analysis and the LED package failure structure. The proposed techniques can be used to detect the thermally induced interface failures in LED packages. In 2012, Chang *et al* (Chang et al., 2012) published a detailed review of the reliability of LEDs at the die and package levels. According to the different failure sites, three types of failures were categorized in this paper (e.g. Semiconductor related failures, Interconnect related failures, and Package related failures). The relationships between the failure causes and their associated mechanisms were also identified.

Besides failure analysis, reliability prediction (or lifetime estimation) for LED lighting is also an essential objective in popularizing LEDs in the lighting market. As introduced earlier, the traditional handbook based reliability assessment and prediction approaches which record only failure-time data have difficulties in dealing with LEDs. To solve this problem, researchers have published papers proposing methods for lumen lifetime prediction and reliability estimation.

Usually, using degradation data for reliability assessment appears to be an attractive alternative in dealing with traditional failure time data, because it benefits

in obtaining more reliability information, identifying the degradation path and providing effective maintenance methods before failures occur (Pan & Crispin, 2011).

For instance, Liao and Elsayed (Liao & Elsayed, 2006) developed a statistical inference procedure to predict the reliability of LEDs with the accelerated lumen degradation data. In this paper, the Accelerated Degradation Test (ADT) model for LEDs was developed with the constant-stress accelerated lumen degradation data.

The results showed that the proposed method could be applied to predict LED reliability in real applications by considering the stress variations. Moreover, Tsaing and Peng (Tsaing & Peng, 2007) also proposed a stochastic diffusion process to model the LED light output degradation path and predicted its lifetime distribution.

With the proposed approximate methods, the LED's lumen lifetime (like, mean-time-to-failure, MTTF and median life, B50) could be estimated by dealing with the light output degradation data. In 2011, IESNA released a standard on predicting lumen lifetime based on the lumen maintenance data collected from IES LM-80-08 (IES-21-11, 2011). In this standard, an exponential model was used to describe the lumen degradation path of LEDs. With the ordinary least squares (OLS) method for fitting the averaged lumen degradation data of LEDs, the model parameters were estimated and the degradation curve was then projected to the threshold to get the lumen failure time. To realize online reliability prediction, T.

Sutharssan *et al* (Sutharssan et al., 2012) proposed a distance-based data-driven method (ED and MD) to detect the lumen failure of high power LEDs with real-time monitoring of the operational and environmental conditions.

In summary, as reviewed, most of previous studies only focused on analysis of the failure mechanisms of LEDs at the chip or package level, not including the system level. As an electronic assembly, a LED lighting system is always established by several subsystems (such as the LED module, electric driver, thermal management module, optical house, and so on), which involves several unknown failure modes, failure mechanisms and failure effects and interactions. Thus, the failure mode and failure mechanism analysis for the system level LED lighting becomes one of the critical issues in the LED reliability field. Moreover, the previous reliability prediction methods only deal with lumen depreciation failure in LED products, ignoring another common failure mode referred to as chromaticity state shift. However, the chromaticity is also a key parameter for high power white LEDs lighting used in some special application areas. Thus, the chromaticity state should be considered as one of health indicators of high power white LEDs in reliability assessment.

2.5 Concluding Remarks

This chapter presents a detailed review of the construction of LED lighting from chip level to system level, the existing handbook based reliability prediction methods for electronics and the previously published works in the field of failure analysis and reliability prediction for LEDs. The findings from this literature review can be summarized as follows:

- (i) As an electronic assembly, a LED lighting system is always established by several subsystems (like, LED module, electric driver, thermal management module, optical house, and so on), which involves several unknown failure modes, failure mechanisms and failure effects and interactions in system level.
- (ii) The traditional handbook based reliability assessment and prediction approaches which record only failure-time data have difficulties in dealing with LEDs, including inappropriate field loading, unreliable material databases, lack of understanding of failure modes and failure mechanisms, high cost and time-consuming analysis.
- (iii) The previous studies just focused on analyzing the failure mechanisms of LEDs in the chip or package level, not including the system level. Most of previous reliability prediction methods only deal with lumen depreciation failure in LED products, ignoring another common failure mode called chromaticity state shift.

Chapter 3 Research Methodology and Experimental Setup

3.1 Research Methodology

To solve the problems mentioned in the literature review chapter, there is an urgent need to develop a new, accurate method to predict the reliability of HPWLEDs lighting. Prognostics and Health Management (PHM) is an effective solution in diagnosing failures, predicting the remaining useful life (RUL) and estimating the reliability for electronic products and systems (Pecht & Jaai, 2010). Therefore, this research develops the failure diagnosis, lifetime estimation and reliability prediction methods for HPWLEDs lighting within the PHM methodology framework. In addition, as a well-organized problem-solving method for improving and guaranteeing product quality, reducing operation cycle time and optimizing process management, the Six Sigma DMAIC methodology is used in this study to design an optimal reliability testing procedure for HPWLEDs lighting.

3.1.1 Prognostics and Health Management

PHM method always solves engineering problems (e.g. failure diagnostics, lifetime estimation and reliability prediction) with multiple discipline approaches which includes physics, mathematics and engineering. It applies physics-of-failure modeling and in-situ monitoring techniques to detect the deviation or degradation of

health and predict the reliability (and remaining life) for electronic products and systems under field operation. Typically, PHM methodology can be categorized into three different methods: (1) Physics-of-Failure (PoF) methods; (2) Data-driven methods and (3) Fusion methods which incorporate the advantageous features from both PoF and Data-driven methods.

3.1.1.1 Physics-of-Failure (PoF) Methods

The Physics-of-Failure (PoF) method is an approach for designing for and assessing reliability by utilizing knowledge of a product's life cyclic loading and failure mechanisms, which is based on the understanding that failures occur due to the fundamental mechanical, chemical, electrical, thermal, and radiation processes (Gu & Pecht, 2008, Pecht, 1994). Based on the PoF method shown in Fig. 3-1, the potential failure modes, failure mechanisms and failure sites of the product are identified as a function of the product's life cycle loading conditions. The PoF methodology can be summarized in the following five steps (White. & Bernstein, 2008):

- (i) Identify the potential failures modes and mechanisms and failure sides merging in the selected device with FMMEA methods(failure modes, mechanisms and effects analysis);

- (ii) Rank the potential failure modes from high risk to low risk and find the dominant root-causes of failure.
- (iii) Develop the appropriate damage models for the identified dominate failure mechanisms with high risk. Calculating the stress at each failure site as a function of both the loading conditions and the product geometry and material properties.
- (iv) Determine the fault generation and propagation with the damage models;
- (v) Predict the reliability by calculating the time-to-failure, or predict the likelihood of failure happened with considering the geometries, material construction, environmental and operational conditions.

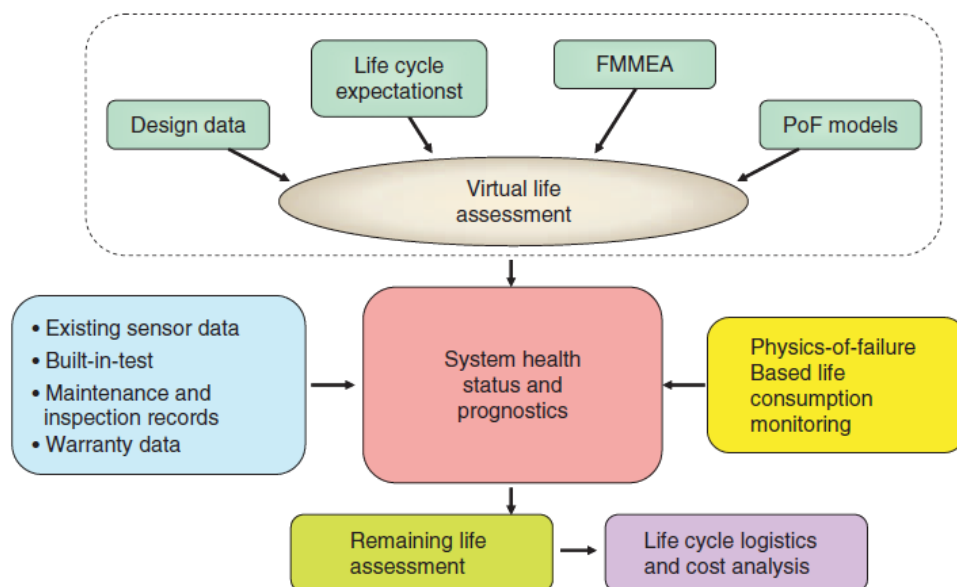


Fig. 3-1 PoF based PHM methodology (Pecht & Gu, 2009)

Most damage models are empirical based models that are widely used for electronic components and systems. Some of these empirical damage models are reviewed below:

(i) Arrhenius model

The Arrhenius model can be used to establish the time to failure model for an electronic device when the failure is induced by temperature factors. It is always used as a relationship between chemical reaction and temperature with the activation energy parameter E_a . Thus the acceleration factor AF between accelerated temperature stress and condition of usage is expressed by the Arrhenius equation (Escobar & Meeker, 2006).

$$t_f \propto e^{\frac{E_a}{kT}} \quad (3-1)$$

$$AF = e^{\frac{E_a}{k} \left(\frac{1}{T} - \frac{1}{T_{use}} \right)} \quad (3-2)$$

Where k is Boltzmann's constant, T is the operating temperature in Kelvin, and T_{use} represents the temperature of use condition.

(ii) Eyring model

The Eyring model calculates the time to failure by taking both temperature stress and other non-thermal stresses (such as humidity, mechanical and electrical stresses) into account. This model can be considered as an extension of the Arrhenius

approach, which imports the theoretical concepts (molecular collisions, activation energy). The time to failures can be expressed as follows:

$$t_f = AT^\alpha \cdot e^{E_a/kT} \cdot e^{(\beta_1+C/T)S_1} \cdot e^{(\beta_2+D/T)S_2} \quad (3-3)$$

Where S_1 and S_2 represent the functions of the non-thermal stresses, and β_1 , β_2 , C , D are the constants related to stress.

(iii) Black's model

Black's model is an empirical relationship to estimate the time to failure of an electronic device because of electro-migration. The failure mode assumption is use a complete open circuit of the metallization

$$t_f = (t_m \cdot w_m) / [j^n \cdot A \cdot e^{-E_a/kT}] \quad (3-4)$$

Where t_m is the thickness of metallization; w_m is the width of metallization; j represents the current density (A/cm^2); n is experimentally determined exponent ($n=2$); A is a constant depending on geometry, substrate, protective coating and film.

(iv) Coffin-Manson model

To modeling the thermo-mechanical fatigue failure in a solder joint or other metals under a thermal cycle condition, the Coffin-Manson model was established and can be used to express the relationship between the number of cycles to failure and the environmental conditions, and is given by (Choi et al., 2011, Cui, 2005):

$$N_f = A f^{-\alpha} \Delta T^{-\beta} G(T_{\max}) \quad (3-5)$$

where N_f is the number of cycles to failure; f is the thermal cycling frequency, α , β are the cycling frequency exponent and temperature range exponent, respectively. $G(T_{\max})$ is the Arrhenius term evaluated at the maximum temperature.

Compared to the traditional handbook based reliability prediction methods, PoF methods have several advantages in increasing the prediction accuracy, detecting root causes contributing to failures and understanding potential failure mechanisms, which are helpful for manufacturers in understanding their products and improving them. Table 3-1 lists the performance comparisons between MIL-HDBK-217 and the PoF method, which indicates that the PoF method can be an alternative to traditional reliability prediction handbooks. Based on the PoF methodology, there are some computer aided modeling and simulation software developed by companies and universities. For example, Computer Aided Design of Microelectronic Packages (CADMP-II) is a set of integrated software programs that assist in assessing the reliability of microelectronic packages (McCluskey & Pecht, 1999). The calcePWA is a PoF based tool designed by the University of Maryland, which can be used to perform simulation based failure assessment of printed wiring assemblies, which combines thermal analysis, vibration analysis and failure assessment (calcePWA, 2004). However, because it requires comprehensive knowledge of the materials and

geometries of a product and the thermal, mechanical, electrical and chemical life cycle environment as well as processes leading to failures in the field in advance, the PoF method requires significant time resources to collection sufficient information, which also increases the operation cost of reliability prediction for manufacturers.

Table 3-1 Comparison of MIL-HDBK-217 and Physics-of-failure methods
(Gottfried, 1997, Cushing et al., 1993)

Issues	MIL-HDBK-217	Physics-of-failure
Model Development	Models can't provide accurate design or manufacturing guidance since they were developed from assumed constant failure-rate data, not root cause, time-to failure data	Models based on science/engineering first principles. Models can support deterministic or probabilistic applications
Device Design Model	The MIL-HDBK-217 assumption of perfect designs is not substantiated due to lack of root-cause analysis of field failures. MIL-HDBK-217 models do not identify wear-out issues.	Models for root-cause failure mechanisms allow explicit consideration of the impact that design, manufacturing, and operation have on reliability.
Device Defect Modeling	Models can't be used to: 1) consider explicitly the impact of manufacturing variation on reliability, 2) determine what constitutes a defect, or how to screen/inspect defects.	Failure mechanism models can be used to: 1) relate manufacturing variation to reliability, 2) determine what constitutes a defect and how to screen/inspect
Device Screening	MIL-Hdbk-217 promotes and encourages screening without recognition of potential failure mechanisms	Provides a scientific basis for determining the effectiveness of particular screen or inspections
Device Coverage	Doesn't cover new devices for approximately the first 5-8 years. Some devices, such as connectors, weren't updated for over 20 years. Developing & maintaining current design reliability models for devices is an impossible task.	Generally applicable-applies to both existing and new devices, since failure mechanisms are modeled, not devices.
Operating Temperature	Explicitly considers only steady-state temperature. Effect of steady-state temperature is 'inaccurate because it's not based on root-cause, time-to-failure data.	The appropriate temperature dependence of each failure mechanism is explicitly considered.
Cost of Analysis	Cost is high compared with value added	Costs are flexible

3.1.1.2 Data-driven Methods

To solve the problems mentioned above, such as expensively conducting a PoF on a complex system, data-driven methods have been proposed to determine anomalies and make predictions about the reliability of systems using historical information. The data-driven methods can intelligently provide valuable decision-making information based on learning from historical data. As shown in previous studies (Wang & Carr, 2010, Si et al., 2011, Hancock & Tran, 1989, Zio & Di Miao, 2010), these data-driven approaches always include: (1) Multivariate statistical methods (e.g., static and dynamic principle components analysis (PCA), linear and quadratic discriminates, partial least squares (PLS) and canonical variated analysis (CVA)); (2) Black-box methods based on neural networks (Yan et al., 2011) (e.g., probabilistic neural networks (PNN), decision trees, multi-layer perceptions, radial basis functions and learning vector quantization (LVQ)); (3) Graphical models (Bayesian networks (Cai et al., 2009), hidden Markov models (Si et al., 2011)); (4) Self-organizing feature maps; (5) Signal analysis (filtering, auto-regressive models, FFT, etc.) and (6) Fuzzy rule-based systems and so on.

Generally, most of data-driven approaches are based on statistical and learning techniques from the theory of pattern recognition. Therefore, the data-driven methods for PHM can be classified into: (1) statistical approaches and (2) learning

approaches.

(i) Statistical approach

Usually, the statistical approaches are composed of parametric methods and nonparametric methods. Where the parametric methods assume that the collected population data follow a certain statistical distribution (like, normal, exponential, weibull or lognormal), the parameters of the distribution can be estimated by fitting the collected data. While the nonparametric methods are not based on the assumption of statistical distributions for the population data, they are just based on their inherent features. In this section, two representative statistical data-driven methods proposed for predicting the reliability (remaining useful life) (general degradation path model as a parametric method and Mahalanobis distance (MD) as a nonparametric method) are reviewed.

(a) General degradation path model

For the devices with long lifetimes, most of the traditional reliability prediction handbook approaches require failure data that are time-consuming and expensive to obtain. In this condition, using degradation data to do reliability assessment appears to be an attractive alternative to deal with traditional failure time data. The general degradation path model as a parametric statistical method was first proposed by Lu

and Meeker (Lu & Meeker, 1993) who modeled the degradation as a function of time and multidimensional random variables, and estimated the failure time distribution with analytical methods by using the relationship between the failure time distribution and the random variables distribution. Usually, several statistical methods have been proposed to estimate reliability based on the degradation data. For example, Freitas *et al* (Freitas, 2010) applied this model to train wheel linear degradation data and assessed its reliability.

The degradation path can be registered as time-performance measurement pairs $(t_{i1}, y_{i1}), (t_{i2}, y_{i2}), \dots, (t_{im_i}, y_{im_i})$, for $i = 1, 2, \dots, n$; and m_i represents the test time points for each unit:

$$y_{ij} = D(t_{ij}; \alpha; \beta_i) + \varepsilon_{ij} \quad (3-6)$$

where a random sample size is n , and the measurement times are $t_1, t_2, t_3, \dots, t_s$. The performance measurement for the i^{th} unit at the j^{th} test time is referred to as y_{ij} . $D(t_{ij}; \alpha; \beta_i)$ is the actual degradation path of unit i at the measurement time t_{ij} ; α is the vector of fixed effects which remains constant for each unit; β_i is a vector of random effects which varies according to the diverse material properties of the different units and their production processes or handing conditions; ε_{ij} represents the measurement errors for the unit i at the time t_{ij} , which is supposed to be a normal distribution with zero mean and constant variance.

To estimate the time to failure distribution, $F(t)$, based on the degradation data, this data-driven method involves two basic steps are involved: (1) estimating the parameters for degradation path model (2) evaluating the time to failure distributions, $F(t)$. Here, a hypothesis needs to be proposed first on the distribution of the random effects parameter β_i . For example, Wu and Shao (Wu & Shao, 1999) assumed the random effects parameter β_i , followed a normal distribution. Wu and Chang (Wu & Chang, 2002) thought it was an exponential distribution, and Yu (Yu, 2006) designed it as a reciprocal *Weibull* distribution.

(b) Mahalanobis distance (MD)

In 1936, P.C. Mahalanobis first proposed MD to represent a single measure of the degree of divergence in the mean values of different characteristics of a population by considering the correlations between the variables (Patcha & Park, 2007, De Maesschalck et al., 2000). This method has been applied successfully over the years in several cases such as anomaly detection, classification and pattern recognition. MD is superior to other distance measures, such as Euclidean Distance ED, because it considers the correlations of the points (Taguchi. & Jugulum, 2002, Taguchi, Chowdhury & Wu, 2001).

$$Z_{ij} = \frac{(X_{ij} - \bar{X}_{ij})}{S_i} \quad (3-7)$$

$$\bar{X}_i = \frac{1}{m} \sum_{j=1}^m X_{ij} \quad (3-8)$$

$$S_i = \sqrt{\frac{\sum_{j=1}^m (X_{ij} - \bar{X}_i)^2}{(m-1)}} \quad (3-9)$$

$$MD_j = \frac{1}{p} Z_j^T C^{-1} Z_j \quad (3-10)$$

$$C = \frac{1}{(m-1)} \sum_{j=1}^m Z_j Z_j^T \quad (3-11)$$

Where \bar{X}_i and S_i are the mean and standard deviation of data matrix; C is the correlation matrix; Z_j is a normalization of raw data matrix; Z_j^T is the transpose of Z_j .

MD has two advantages in detecting differences: first, it reduces a multivariate system to a univariate one; second, MD is more sensitive in detecting changes by taking into account the correlation of several parameters. Thus, MD methods are widely used as a fault alarm to detect anomalies before failure occurs. For example, Niu *et al* (Niu et al., 2011) incorporated the MD method with a Weibull distribution to monitor the health of notebook computers. Kumar *et al* (Kumar et al., 2012) used MD as a health indicator to detect the gradual health degradation of electronic products. Sutharssan *et al* (Sutharssan et al., 2011) developed the distance measure techniques (both MD and ED) for a real-time prognostics system, including assessing the reliability, detecting failures and estimating remaining useful life, for LED lighting.

(ii) Learning approach

The learning approach is based on machine learning algorithms for recognizing patterns in raw data and in making decisions on the state of the system based on the data. The data collected is analyzed with learning approaches using a variety of techniques depending on the type of data: (a) Supervised learning approach, which is for data representing healthy and faulty states of the system; (b) Unsupervised learning approach, which is suitable for the unlabeled data.

(a) Supervised learning approach

Supervised learning is an algorithm to label the outputs of a set of inputs, where healthy and failure datasets are available. Thus, the first step of this approach is training the proposed algorithm with available healthy and unhealthy datasets and in finding boundaries to distinguish them. The next step is to detect any anomaly for a new input dataset with the trained algorithm. Three basic supervised learning approaches are reviewed below (Artificial Neural Network, Support Vector Machine and Relevance Vector Machine).

The Artificial Neural Network (ANN) is a graph based model that establishes a set of interconnected functional relationships between inputs and outputs (Tian & Zuo, 2009). It always consists of input nodes, hidden layers and output nodes. The inputs of neural networks can include process variables, condition monitoring

indicators, asset characteristics and maintenance history features. The outputs depend on the aim of the modeling process, which may be the desired maintenance action or the remaining useful life (Sikorska et al., 2011). As supervised learning, the ANN model is trained with a set of training data to adjust and optimize the associate parameters of the functional relationship (Peel, 2008). Typically, there are two application areas of ANN in prognostics: (1) Estimations and classifications, which work as a nonlinear function approximator to predict system failure features and trends; (2) be used with feedback connections to model dynamic processes of system degradation and predict the remaining useful life (Connor et al., 1994, Peng et al., 2010). There are several types of neural network architectures used for prognostics, such as self-organized maps (SOM), recurrent neural networks (RNN), dynamic wavelet neural networks (DWNN) and so on. For example, an SOM neural network was used by Zhang *et al* as a multivariable trend indicator of fault development to estimate the remaining useful life of a bearing system (Zhang & Ganesan, 1997). Connor *et al* (Connor et al., 1994) proposed recurrent neural networks for time series predictions. Vachtsevanos and Wang (Vachtsevanos & Wang, 2001) used dynamic wavelet neural networks to predict the failures of a bearing system.

The Support Vector Machine (SVM) is a supervised learning method used as a maximum margin classifier with the ability of simultaneously minimizing the

empirical classification error and maximizing the geometric margin (Pecht, 2008).

Given a problem of binary classification with a set of training data, $(x_1, y_1); (x_2, y_2); \dots; (x_M, y_M)$, $y_i=1$ or -1 , $i=1, 2, \dots, M$, a linear separating plane expressed as the equation (3-12) is established to distinguish the input data space.

$$f(x) = w^T x + b = \sum_{j=1}^m w_j x_j + b = 0 \quad (3-12)$$

$$y_i f(x_i) = y_i (w^T x_i + b) \geq 1 \quad (3-13)$$

where w is a weight vector; b is a scalar. Both these two parameters are trained with a training dataset. The training process uses the training dataset to satisfy the constraints which can be described as the equation (3-13).

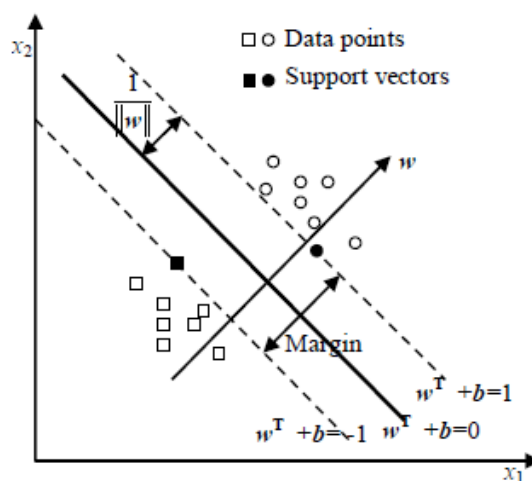


Fig. 3-2 Support Vector Machines used for classification (Qu, 2011)

Fig. 3-2 explains the classification process with SVM methodology. In this figure, the solid squares and the solid circles are support vectors and the two dash

lines cross the support vectors representing two parallel planes and are called boundaries. The distance between the boundaries is called the margin. To get the optimal separating plane, an optimization process with maximizing margin $\frac{2}{\|w\|}$ (minimizing $\|w\|^2$) is used.

As a supervised learning approach, SVM is typically applied to detect any anomaly by distinguishing the features between healthy and unhealthy. For example, a hybrid two stage one-against-all Support Vector Machine (SVM) approach was proposed by Gryllias *et al* (Gryllias & Antoniadis, 2012) for the automated diagnosis of defective rolling element bearings. In the first stage, an SVM classifier was built to separate the normal condition signals from the faulty signals and then the type of the fault is recognized and categorized by a SVM classifier at the second stage.

Recently, because SVM was challenged by the lack of probabilistic outputs that make more sense in health monitoring application, another supervised learning approach (Relevance Vector Machine (RVM)) was proposed within a Bayesian framework. It also uses fewer kernel functions for comparable generalization performance (Tipping, 2001). Given a set of input vectors $[x_n]$ with their corresponding targets $[t_n]$, the learning process is undertaken to infer the parameters of the relationship function between input vectors and the corresponding targets, $F(x)$. Then the likelihood of complete data is built for the next step prediction with the

Bayesian framework.

$$t_n = F(x_n; w) + \varepsilon_n \quad (3-14)$$

$$p(t/w, \delta^2) = (2\pi\delta^2)^{-N/2} \exp\left\{-\frac{1}{2\delta^2}\|t - \Phi w\|^2\right\} \quad (3-15)$$

$$p(t^*/t) = \int p(t/w, \delta_{MP}^2) p(w/t, \eta_{MP}, \delta_{MP}^2) dw \quad (3-16)$$

Where ε_n is the Gaussian noise with mean 0 and variance δ_2 ; w is the weight vector; η is the hyperparameter vector.

(b) Unsupervised learning approach

The unsupervised learning approach deals with unlabeled data and finds clusters by itself. It is used to discover similar groups within the data based on clustering techniques, and separates the data into different groups. Therefore, this approach also can be used to detect any anomaly in the new observation and can predict the reliability and remaining useful life. Here, two popular unsupervised learning approaches according to the different functions in PHM (anomaly detection and prediction) are reviewed.

Principal Component Analysis (PCA) is an unsupervised learning approach used for dimension reduction, data compression, feature extraction, data classification and mapping. The singular value decomposition (SVD) tool is used in this approach to map higher dimension data into lower dimension data while

maximizing the variance of the mapped data. Jiang *et al* (Jiang et al., 2013) improved a principal component analysis (PCA) based chemical process monitoring performance and proposed a sensitive principal component analysis to detect and diagnostic the faults in chemical processes. Liang *et al* (Liang & Wang, 2003) combined PCA with a statistical control chart to reduce the multivariate variables for an industrial rolling mill reheating furnace.

The filter approach has been widely accepted as one of unsupervised learning approaches for estimating and predicting the state of electronic devices or systems by using a state-space model (Daigle et al., 2012, Yang & Liu, 1999, Yang, 2002). The most widely used filter is the Kalman filter (KF), which has effective solutions on estimating the state of linear system with additive Gaussian noise (Simon, 2006, Gibbs, 2011).

As shown in Fig. 3-3, KF is a recursive method to estimate the state of linear system based on prior knowledge of the state of state of the system and the measured information. However, for most nonlinear cases, KF loses its efficacy. Therefore, it is necessary to establish a nonlinear filter to solve state estimation problems in nonlinear systems. Up to now, there have been some approximate nonlinear filters, such as the Extended Kalman Filter (EKF), Uncented Kalman Filter (UKF), and the Particle Filter (PF) (Zio & Peloni, 2011), that have been used to deal with nonlinear

problems.

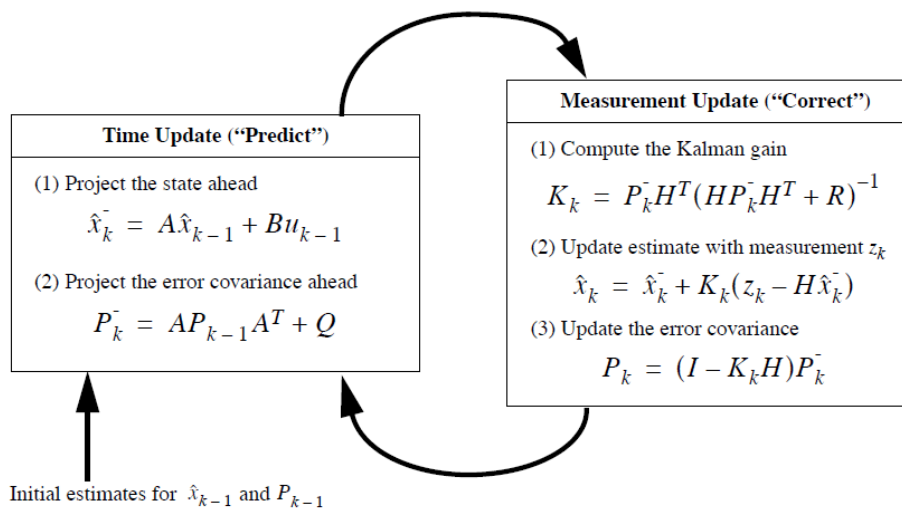


Fig. 3-3 Recursive operation of Kalman filter (Welch & Bishop, 2006)

Among these three nonlinear filters, the EKF linearizes both the state and measurement models by using a first order Taylor approximation. The PF, known as the sequential Monte Carlo method, approximates the state distribution using a set of discrete, weighted samples, called particles. PF approaches have been widely used for state estimation and remaining useful life prediction for battery systems (Miao et al., 2013, Restaino & Zamboni, 2012). The UKF approach was first proposed by Julier *et al.* and developed by Wan *et al.* (Julier & Uhlmann, 2004, Julier et al., 1995, Wan & van der Merwe, 2000) to estimate the state of nonlinear systems by using a deterministic sampling approach (sigma point sampling) to capture the mean and covariance estimates with a minimal set of sample points. Several previous literature

studies have shown that the UKF is considered to be a useful approach for state-space prognostics and estimations for nonlinear systems. For instance, Santhanagopalan *et al.* (Santhanagopalan, & White, 2010) used the UKF method to estimate the state of charge for lithium ion cells. Lall *et al.* (Lall et al., 2012) applied the UKF algorithm to predict the remaining useful life of electronic systems under mechanical shock and vibration conditions. Jafarzadeh *et al.* (Jafarzadeh et al., 2012) developed a UKF-based approach to estimate the nonlinear state of induction motor drives.

In summary, compared to the PoF approaches, the advantages of data-driven approaches are as follows: (1) they do not need know system specific information and can learn the behavior of the system, like black-box models, based on the monitored data; (2) they can be used in complex systems with considering the correlation between parameters and the interactions between subsystems; (3) they can be used to analyze the intermittent faults by detecting the sudden changes in system parameters. However, data-driven approaches have some limitations, as they require historical or operational data to train model. In some cases, there are insufficient training data to obtain health estimates and to determine trend thresholds from failure prognostics. Therefore, the solution to this problem is to incorporate PoF approaches with data-driven approaches.

In this situation, the fusion approach is proposed by absorbing the advance features of both data driven and model based approaches. As shown in Fig. 3-4, the fusion PHM method develops an accurate mathematical model of the system by using both the physical based failure models and data driven prognostic models.

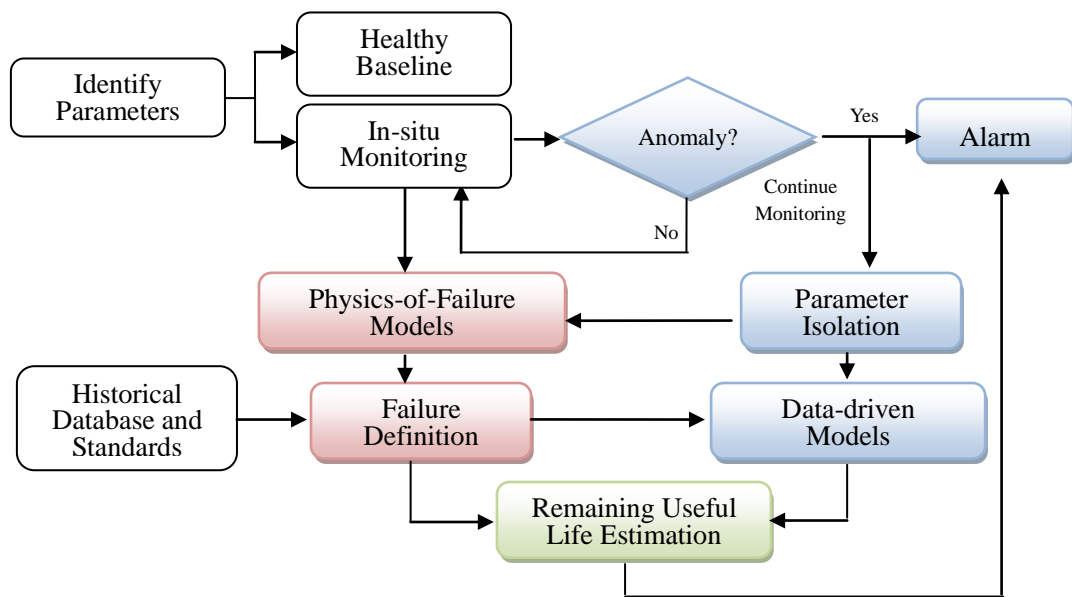


Fig. 3-4 Fusion PHM method (Pecht & Jaai, 2010)

The aim of the fusion approach is to overcome the limitations of both the model and data driven approaches for estimating the remaining useful life (RUL). Cheng *et al* (Cheng & Pecht, 2009) demonstrated the fusion PHM method to predict the remaining useful life of multilayer ceramic capacitors (MLCCs). Xu *et al* (Xu & Xu, 2011) also implemented the fusion based PHM into avionics system to predict remaining useful life. Vasan *et al* (Vasan & Pecht, 2011) developed a generic fusion

PHM approach, which combines stochastic differential models with a recursive nonlinear filtering approach, to allow systems to self-assess performance and recursively estimate remaining useful life.

3.1.2 Six Sigma DMAIC Methodology

The Six sigma DMAIC (Define-Measure-Analyze-Improve-Control) methodology is a well-organized problem-solving methodology for improving and guaranteeing product quality, reducing operation cycle time and optimizing process management in many companies, such as Motorola, General Electric, and Raytheon (Gijo et al., 2011, Easton & Rosenzweig, 2012, Zu, Fredendall & Douglas, 2008, Valles et al., 2009, Antony et al., 2012, Shafer & Moeller, 2012, Montgomery & Woodall, 2008, Jin et al., 2011, Schroeder et al., 2008, Wooles & Allardice, 2008).

As a statistical solution, the term Six Sigma is defined as having less than 3.4 defects per million opportunities or a success rate of 99.997%. The sigma is used to represent the variation about the process average (Antony et al., 2012). The benefits of the Six Sigma approach can be achieved through the utilization of its systematic step-wise DMAIC approach, which enables users to find problems in an old product and process, to improve them with solutions and to maintain the improved gains (Shafer & Moeller, 2012).



Fig. 3-5 Six Sigma DMAIC steps

- (i) *Define phase.* This phase aims to answer “*What is the gap between our customer requirements and what we currently deliver?*”. In detail, a cross-functional Six Sigma team is established first to summarize the problems that occurred in a particular case. The scope and goals of the improvement project based on customer requirements are defined and a process to deliver these requirements is also proposed in this phase.
- (ii) *Measure phase.* This phase is to solve the problem “*What are the types and frequencies of defects?*”. In this phase, the objective is to select the appropriate product characteristics, map the respective process, study the accuracy of the measurement system, record the data, and establish the baseline performance of the process (Table 3-2).

Table 3-2 Six Sigma DMAIC processes

DMAIC steps	Processes	Tools	Deliverables
Define	(1) Define the requirements and expectations of the customer; (2) Define the project boundaries; (3) Define the process by mapping the business flow	CTQ, Process Map, Statistics & Charts, Quality Cost, QFD, Cause & Effect Diagram, Muda	Goal, Project Charter, Quality Function
Measure	(1) Measure the process to satisfy customer's needs; (2) Develop a data collection plan; (3) Collect and compare data to determine issues and shortfalls	Customer survey, Process map & diagnosis, Capability study, Measurement System Analysis, Statistics & Charts, Multi-vari Chart,	Outcomes of Measurements, Data & facts
Analyze	(1) Analyze the causes of defects and sources of variation; (2) Determine the variations in the process; (3) Prioritize opportunities for future improvement	Scatter Diagram, Design of Experiment, Statistics & Charts,	Outcomes of Analysis, Confirmed $Y=f(X1; X2; X3; \dots)$ & their relations
Improve	(1) Improve the process to eliminate variations; (2) Develop creative alternatives and implement enhanced plan	Brainstorming, Action planning	Implemented improvements
Control	(1) Control process variations to meet customer requirements; (2) Develop a strategy to monitor and control the improved process; (3) Implement the improvements of systems and structures	Control Charts, Standard Operation Procedures, Results Calculation	Control Charts, Standard Operation Procedures, Results

(iii) *Analyze phase*. This phase answers the question “*What are the potential root causes of the problems and what are the improvement opportunities?*”. The main purpose of the Analyze phase is to use the data collected from the Measure phase to determine the cause-and-effect relationships in the process and to

understand the different sources of variability.

- (iv) *Improve phase*. In this phase, the solutions are identified and implemented for all the root causes selected during the analyze phase. After creative thinking, this phase always needs make specific changes with the design of experiment to improve the process performance.
- (v) *Control phase*. The purpose of this phase is to maintain the improved gains proposed in the Improve phase.

In summary, the prognostics and health management (PHM) methodology and the Six Sigma DMAIC methodology are introduced in this chapter. The PHM methodology has been proven to have advantages in diagnosing failures, predicting the remaining useful life (RUL) and estimating the reliability for electronic products and systems. The Six Sigma DMAIC methodology can help optimizing the design of experiment with a systematic step-wise approach. Therefore, the ensuring research approach in this thesis is developed with both the PHM and Six Sigma DMAIC methodologies: (1) to diagnosis the failure modes and failure mechanisms for LED lighting; (2) to establish a specific reliability testing for LED lighting, and (3) to develop a fast, accurate and effective reliability assessment and prediction method.

3.2 Experimental Setup

3.2.1 Performance Data Collection based on IES-LM-80-08 Standard

As is known, the reliability of a product is highly dependent on its usage conditions, which means that different lifetimes of a product can be estimated and reported from different test conditions. Nowadays, customers see all kinds of claimed lifetimes, from 10,000 hrs to 100,000 hrs, from different LED manufacturers and suppliers, which confuses buyers. To solve this problem, many institutes and associations of SSL (e.g. IESNA, CIE, IEC, NEMA, ANSI, JEDEC Solid State Technology Association and so on) are making great efforts to specify environmental testing methods for LED lighting.

The IES-LM-80-08 Standard is an approved method for measuring the lumen maintenance of LED light sources, which was published by IESNA in 2008 (IES-LM-80-08, 2008). This standard describes a procedure to test the light output of LED lighting (only for inorganic LED-based packages, arrays and modules) operated under some controlled conditions. The case temperature and its tolerance, testing humidity and airflow are first standardized and recommended in this standard for LED manufacturers (see Table 3-3). Up to now, the IES-LM-80-08 test report has become one of important technical databases for many LED manufacturers to report their product's reliability to customers (Nicha, 2010, Luxeon, 2011, OSRAM, 2010, Cree, 2013).

Table 3-3 Test conditions recommended by the IES-LM-80-08 Standard

Items	Conditions
Case Temperatures	55°C; 85°C and a third temperature selected by manufacturers (108°C is used in the Lumileds LM-80 Test Report) (Luxeon, 2010 and 2011)
Temperature Tolerance	Case temperature controlled to -2°C; Air temperature surrounding case maintained within -5°C
Airflow	Should be minimized
Humidity	< 65% RH
Testing Duration	At least 6,000 hrs
Measurement Interval	Minimum 1,000 hrs
Others	No vibration or shock during life testing; Operating orientation should be specified by manufacturers and be designed to minimize structural components to block airflow.

In our study, the performance data of one type of high power white LED (i.e. lumen flux data and chromaticity coordinate data) were collected in the LM-80 test reports which were published by Lumileds, Philips (Luxeon, 2010 and 2011). The test vehicle used in this experiment was the white LUXEON Rebel which is a type of high power white LED package with high luminous flux (>100 lumens in cool white at 350mA) and with advanced packaging techniques (Chip-on-Board technique without wire bonding) (Luxeon, 2008a).

As recommended in the LM-80 test reports, the experimental procedure includes ten cycles for 10,000 hrs of operation. Each cycle involves three steps: aging, cooling, and testing (Fig. 3-6). For aging, the white LUXEON Rebel LED units were soldered onto a reliability stress board that was thermally controlled by

water cooling. The units were driven by a constant DC current in a thermal chamber. After 1,000 hrs of aging, the reliability test board was removed from the thermal chamber to be cooled to room temperature. For testing, the performance data, including the lumen flux, chromaticity coordinates, and forward voltage of each unit, were measured underneath the integrating sphere. After testing, the reliability stress board was returned to the thermal chamber to undergo the next aging cycle.

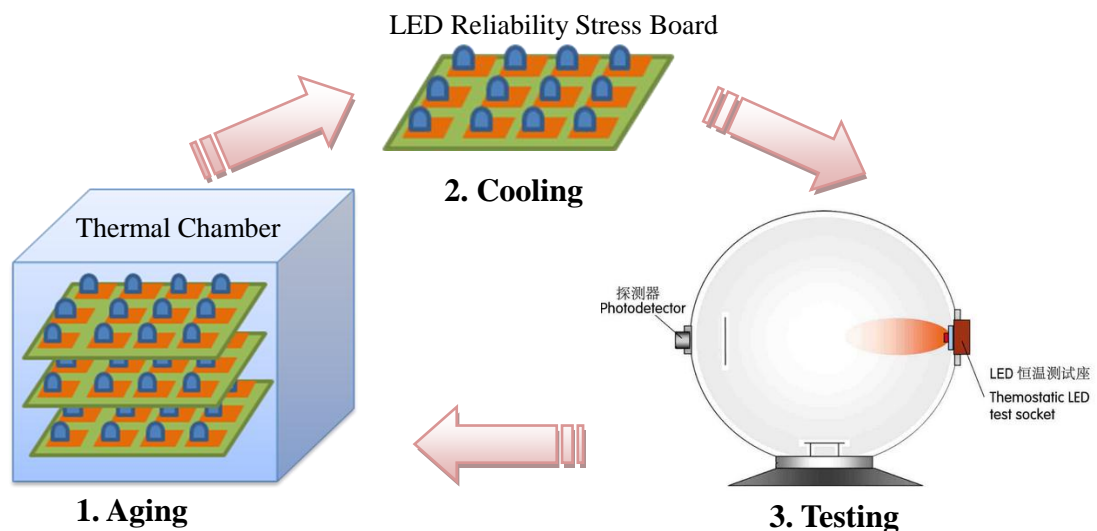


Fig. 3-6 Test procedure recommended by the IES-LM-80-08 Standard

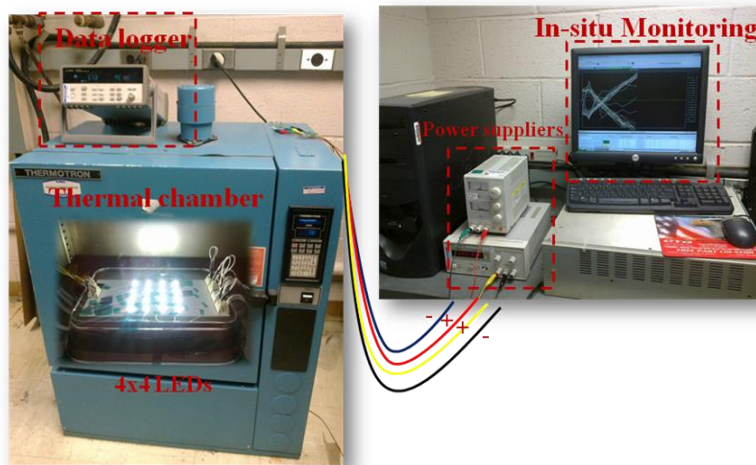
3.2.2 High Temperature Reliability Test

In our study, a high temperature reliability test for LED lighting was also carried out by author in the Center for Advanced Life Cycle Engineering (CALCE) of the University of Maryland in 2012. The objectives of this test were: (1) to determine the

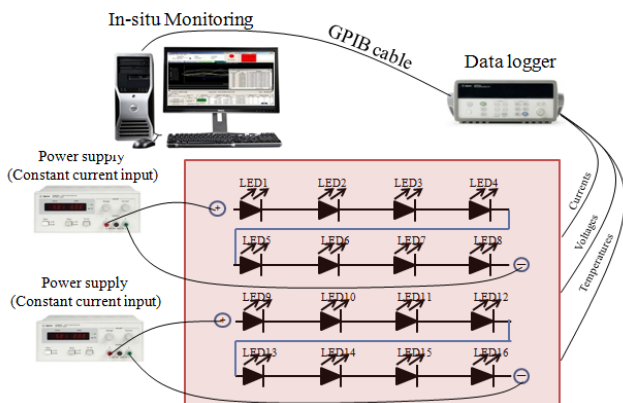
LED's reliability information (such as the failure time distribution, the 100th percentiles of failure time distribution t_p , and mean time to failure MTTF); (2) to estimate rated lifetime for the LEDs in the given accelerated aging condition.

In this experiment (Fig. 3-7a), the sixteen high brightness white LEDs (Type: 3W Mini power ASMT-JN31-NTV01 from Avago) were soldered on an MCPCB reliability stress board and were electrical driven by the same constant direct currents (200mA) provided by two DC power suppliers (Fig. 3-7b). The thermal chamber provided a constant aging temperature for this test (90 °C as required by the customer) (Table 3-4). The experimental procedure is shown in Fig. 3-7c which includes three sections for every operation cycle: aging section, cooling section and testing section. In each operation cycle, the sixteen high brightness white LEDs operated continuously within 23 hrs, under the recommended operation condition. After aging, the LEDs were removed from the thermal chamber to be cooled to room temperature. Then, the direct performance data of LEDs (such as light output, chromaticity coordinates, CCT, CRI, SPD) were manually measured by a Gigahertz-Optik BTS256-LED tester. After testing, the reliability stress board was returned to the thermal chamber to undergo the next aging cycle. The indirect performance data (such as lead temperatures, aging temperature, driven current and forward voltage of each LEDs) were collected online by a Agilent - 34970A Data Acquisition

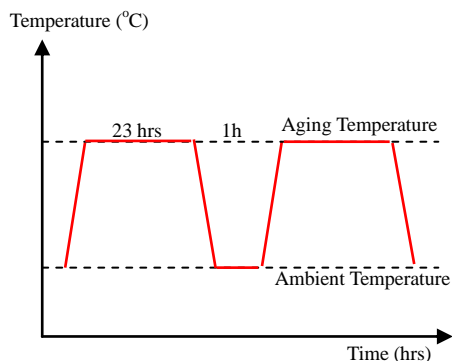
Mainframe (Fig. 3-7b).



(a)



(b)



(c)

Fig. 3-7 High temperature reliability testing for LEDs (a) experiment setup, (b) electrical circuit design and (c) operation profile

Table 3-4 Test condition of the high temperature reliability test

Items	Conditions
Aging Temperature	90°C
Testing Temperature	25 °C
Humidity	20% RH
Driven current	200mA
Others	Testing duration is more than 1,000 hrs and Measurement interval is 23 hrs

Chapter 4 Physics-of-Failure Modeling for High Power White LED Lighting

4.1 Introductory Remarks

High Power White Light-emitting diodes (HPWLEDs) have attracted increasing interest in the field of lighting systems owing to their high efficiency, environmental benefits and long lifetime in a wide range of applications (Schubert & Kim, 2005). Therefore, how to accurately predict the remaining useful lifetime of high power white LED Lighting in the design stage is becoming a key aspect for popularizing this novel product. However, traditional reliability prediction methods for electronic products, including MIL-HDBK-217, RiAC-217PIUS, Telcordia, and FIDES, are not accurate enough for predicting actual field failures (e.g. soft and intermittent faults which are the most common failures modes in today's electronics-rich systems) and provide highly misleading predictions, which can result in poor designs and poor logistics decisions (Pecht & Jaai, 2010).

Prognostics and health management (PHM) is a method for reliability assessment and prediction of products (or systems) under their actual operating conditions (Pecht & Jaai, 2010). This is now becoming one of the critical contributors to efficient system level maintenance. Physics-of-Failure (PoF) based PHM uses the knowledge of a product's life cyclic loading and failure mechanisms to design for and assess reliability (Gu & Pecht, 2008). This approach always includes:

identifying of potential failure modes, failure mechanisms and failure sites of the product as a function of the product's life cycle loading conditions, calculating the stress at each failure site is obtained as a function of both the loading conditions and the product geometry and material properties, and building damage models to determine fault generation and propagation.

The purpose of this chapter is to assess reliability and predict the performance of high power white LED lighting (from chip level, package level to system level) by means of the PoF-based PHM approach (Fan et al., 2011). In this approach, failure modes, mechanisms and effects analysis (FMMEA) is used to identify the potential failures emerging in the high power white LED lighting at all levels and to develop appropriate PoF based damage models for identified failure mechanisms with high risk. The results can help quantify the reliability through evaluation of time-to-failure, or predict the likelihood of failure for a given set of geometries, material construction, environmental and operational conditions.

4.2 Physics-of-Failure based PHM

The PoF-based PHM approach involves several steps (see Fig. 4-1), including failure modes, mechanisms and effects analysis(FMMEA). Damage models are identified and built for each mechanism, feature extraction, and for estimating

remaining useful life (Pecht & Gu, 2009). In this chapter, the focus is on the first step of the PoF-based PHM approach--virtual life assessment, including materials and geometries analysis, FMMEA and on the establishment of failure models for identified failure mechanisms with high risk, for high power white LED lighting from the chip level, the package level to the system level.

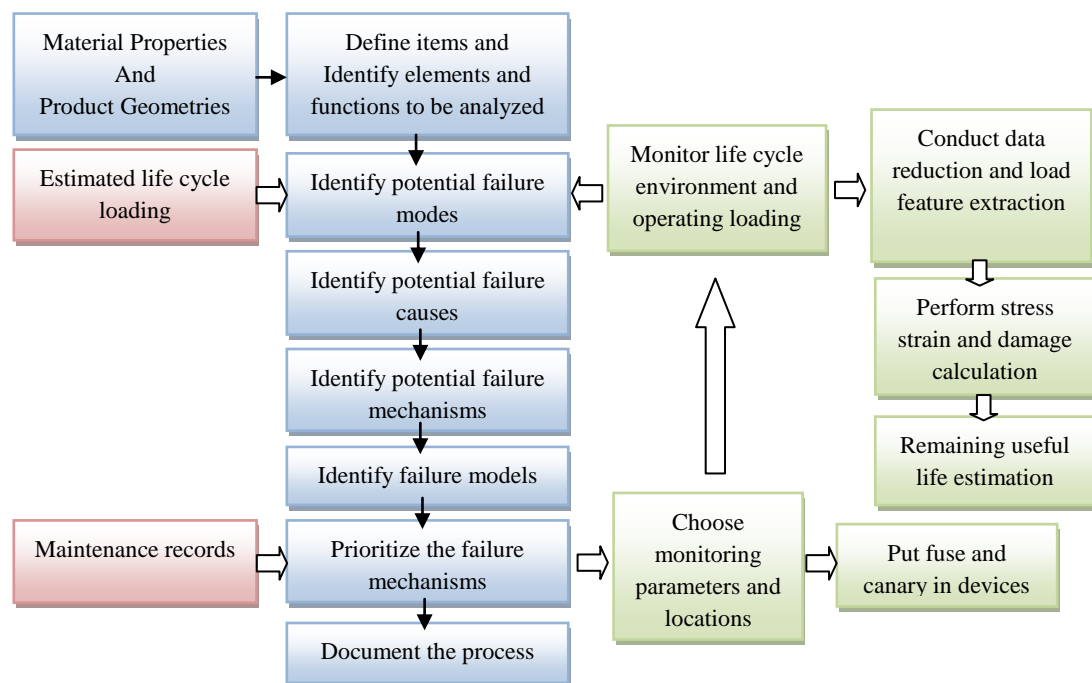


Fig. 4-1 PoF-based PHM approach (Pecht & Gu, 2009)

4.2.1 Materials and Geometries Analysis

To create white light, several promising strategies have been used in the applications, including di-, tri-, and tetrachromatic approaches. Among them, the di-chromatic white source, combining a short-wavelength InGaN blue LED with a

single yellow phosphor (YAG:Ce³⁺), is the most commonly used method on the market. Fig. 4-2(a) shows the cross-section structure and details of the materials of a popular high power white LED product: LUXEON_K2, PHILIPS (Luxeon, 2007).

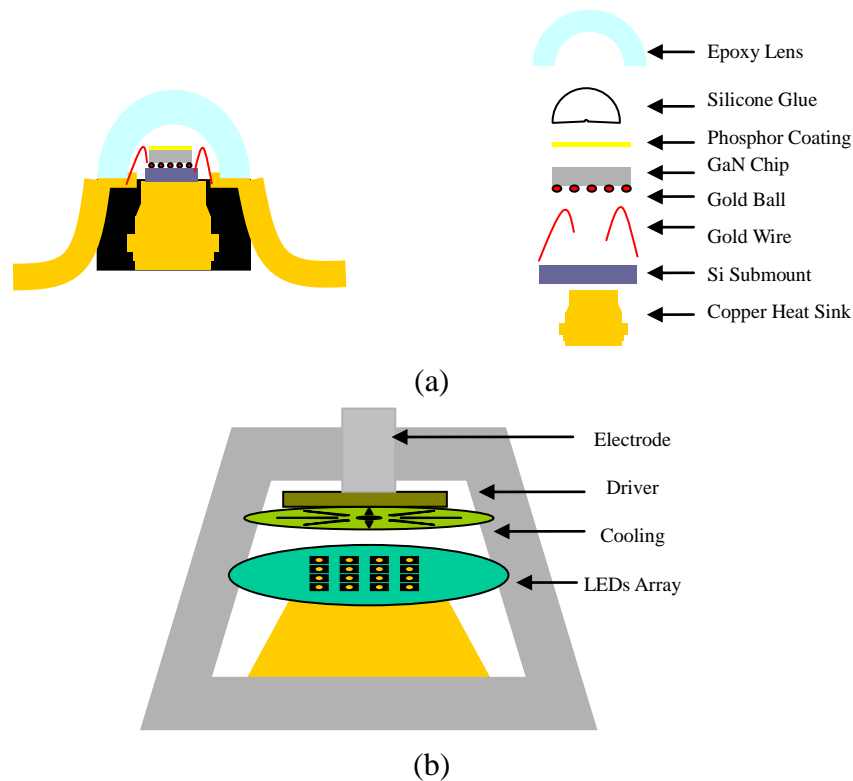


Fig. 4-2 Materials and structure of (a) LED chip, LEDs packages, and (b) LED lamps

To lower the cost and increase power efficiency, Thin Film Flip Chip (TFFC) and Wire Bonding Assembly Technology are used in this package. Meanwhile, three developments in the material selection, containing ceramic-glass phosphor with higher thermal conductivity and more chemical and thermal stability replacing the commonly used phosphor resin, a silicon submount taking the place of the Sapphire

submount, and a wider copper heat sink, lowering the package's thermal resistance ($5.5^{\circ}\text{C}/\text{W}$) and optimizing the module's thermal management (Hu et al., 2007, Tan et al., 2009b, Hu et al., 2008b).

Fig. 4-2(b) illustrates a LED lamp consisting of LUXEON_K2 LED Arrays, a cooling system and the relative power driving module. As shown, the LED packages are mounted on a Sapphire PCB using the series or parallel SMT method to improve the whole system's luminous power. To reduce the accumulated heat generated from the LED arrays, a cooling systems is introduced into this lamp system (Song et al., 2010). The total electric power of the system is supplied and controlled by a power driver located on the top of the cooling system and directly connected to the electrode.

Table 4-1 lists all materials used in this system, from chip to lamp. Any mismatch of the materials' properties (Chemical, Thermal, Mechanical) at any level degrades or damages the system's power efficiency. Therefore, material selection and geometrical design are the first and most critical steps in the PoF-based PHM approach.

Table 4-1 Materials Properties of LED chip, packages, and systems levels (at 25°C)

	<i>CTE</i>	<i>Thermal Conductivity</i>	<i>Elastic Modulus</i>	<i>CME</i>	<i>Density</i>	<i>Specific Heat</i>	<i>Poisson's Ratio</i>
	10^{-6} /°C	W/m°C	Gpa	$\times e^{-3}$ cm ³ /kg	kg/m ³	Cp J/kg °C	
GaN Chip	5.59	130-140	210-295	NA	6150	490	0.31
Epoxy Lens	45	0.17	0.5	0.21	980	1173	0.49
Silicone Glue	300	1.8	6.1×10^{-4}	0.21	1200	92	0.34
Ceramic Phosphor	7.8	13	NA	NA	4500	NA	0.24
Silicon submount	3	124-148	109-190	NA	2330	702-712	0.28
Gold Wire	14.1	318	180	NA	1930	128	0.44
Heat Sink (Cu)	16.5	393	128	NA	8950	390	0.26
Die Attach	30	7.5	40	0.445	2400	300	0.35
Plastic Mould	45	0.23	5.2	0.21	1300	1256	0.35
Lead Frame	18	401	190	NA	8300	385	0.26
Sapphire PCB	7.9	35~46	400	NA	3965	730	0.22

4.2.2 Failure Modes, Mechanisms and Effects Analysis

In electronics-rich systems, a failure mode is the recognizable electrical symptom by which failure is observed, i.e. open or short circuit. Each mode could be caused by one or more different failure mechanisms which could be driven by physical, chemical or mechanical means. Failure mechanisms can be categorized as overstress (catastrophic) failure or wear-out (gradual) failure mechanisms.

Overstress failure arises as a result of a single load (stress) condition, which exceeds the threshold of a strength property. Wear-out failure occurs as a result of cumulative damage related to loads (stresses) applied over an extended period of time. According to recent knowledge, PHM can be applied only in wear-out (time-dependent) failure mechanisms.

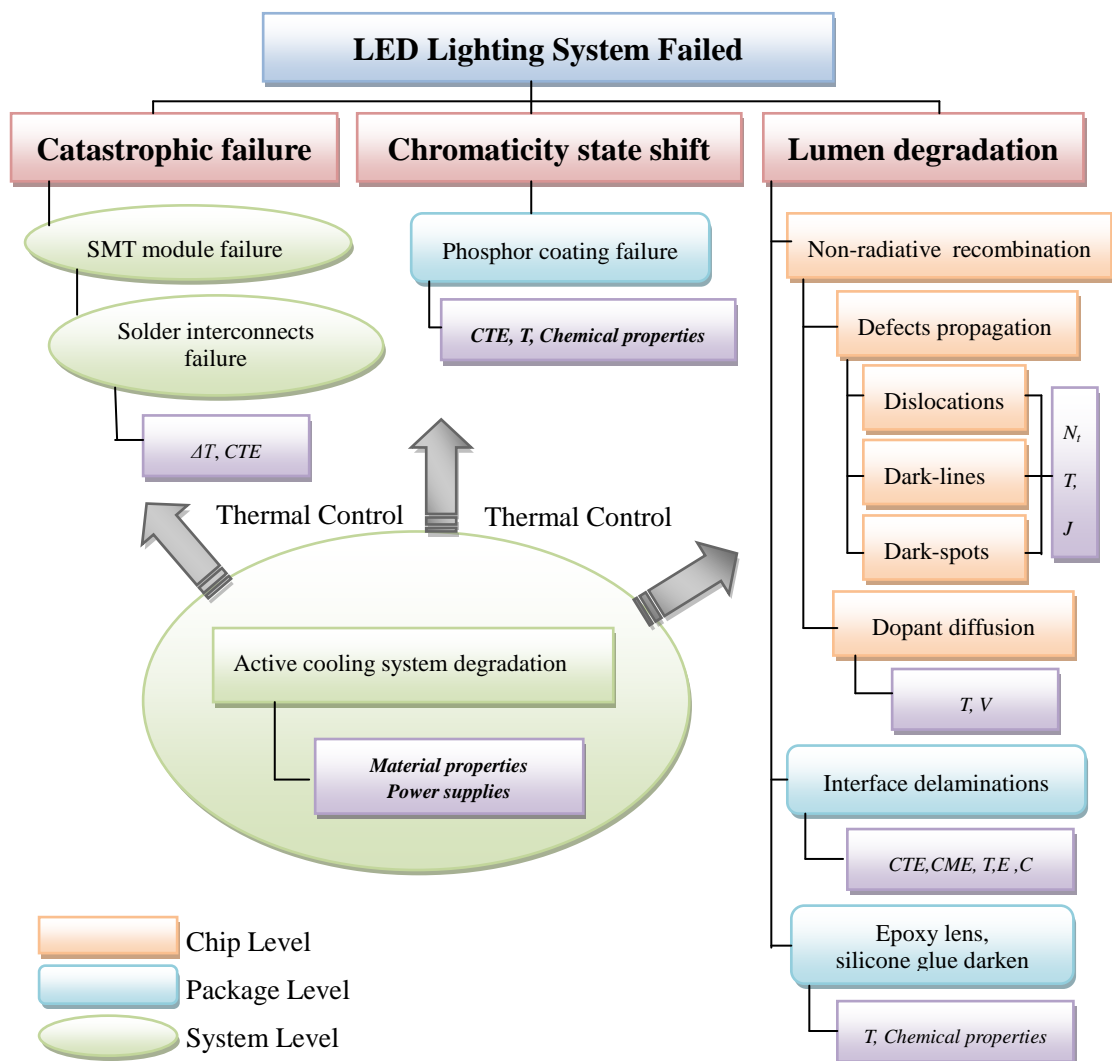


Fig. 4-3 FMMEA for high power white LED lighting systems
 (ΔT : Thermal Cycle; N_t : the defect density; J : Current Density; V : Voltage; E : Elastic Modulus; C : Moisture Concentration)

The failure modes in the mentioned LEDs Lighting systems (i.e lamps) can be categorized as (see Fig. 4-3): (1) Catastrophic failure; (2) Lumen degradation; (3) Chromaticity state shift. Like other electronics-rich systems, the failures of high power white LED lighting also contain the above mechanisms. The following is a summary of the failure modes and the associated wear-out degradation mechanisms from chip to system in accordance with the “bottom-up” methodology.

4.2.2.1 Chip level degradation

As described in the material properties analysis, the LUXEON_K2 chip used is made of GaN-based blue light-emitting diodes with a Multi-quantum Well (MQW) structure. In previous research results (Meneghini et al., 2010, Narendran & Gu, 2005, Yang et al., 2010, Chuang et al., 1997, Hu et al., 2008a), the degradation of the active layer of LEDs due to increased non-radiative recombination lowers the optical output power and power efficiency. The factors responsible for this, which contributes to the non-radiative recombination, were proposed as (Meneghesso et al., 2010):

(i) Defects (dislocations, dark-lines and dark-spots) propagation are some of the factors which are suspected of causing an increase in the non-radiative recombination which converts the most electron-hole recombination energy to heat (Uddin et al.,

2005, Cao et al., 2003). A Carrier-Continuity equation (Equation 4-1) has been widely used to show the qualitative competition among radiative, non-radiative and Auger recombination that occurs in the quantum well active region and carrier leakage out of active layer. As shown in equation 4-2, which expresses the non-radiative recombination coefficient by the Shockley-Hall-Read recombination rate, the increasing defect density N_t contributes to the non-radiative recombination and relatively reduces the light output intensity for a certain value of the forward current. Normally an I/V curve can also imply chip level degradation. A qualitative relationship between the I/V curve degradation and power output loss has been observed in these tests, which depends mainly on two parameters: forward bias and temperature (Nogueira et al., 2009).

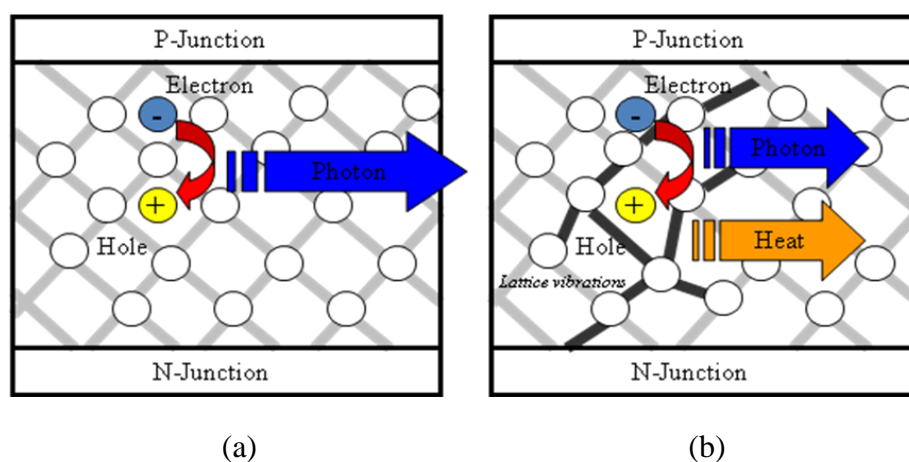


Fig. 4-4 The mechanisms of (a) radiative recombination and (b) non-radiative recombination

$$\frac{dn}{dt} = \frac{J}{ed} - Bn^2(t) - An(t) - Cn^3(t) - f_{leak}(n) \quad (4-1)$$

$$A = N_t v_{th} \sigma \quad (4-2)$$

where the J/ed is the current injection rate, the $Bn^2(t)$ accounts for the spontaneous emission rate (or luminous radiative term), and $An(t)$ represents the non-radiative carrier that accumulates at the defects. A , B and C in each term are the non-radiative, radiative and Auger recombination coefficients respectively. $f_{leak}(n)$ covers the carrier leakage out of the active layer. N_t is the defect density of the traps, v_{th} is the carrier thermal velocity and σ the electron capture cross section

(ii) Another factor which causes an increase in non-radiative recombination emission is the diffusion of dopants or impurities in the quantum well (QW) region. During the aging process, operation at the increasing junction temperature can worsen the electrical properties of the ohmic contact and semiconductor material at the p-side of diodes due to the interaction between hydrogen and magnesium. As is known, in GaN-based LEDs, the GaN epilayer must be covered with a heavy layer of Mg dopant in order to obtain a sufficient carrier density due to the high activation energy of the Mg dopant, but during the growth of high temperature p-type layers, Mg atoms can be easily diffused from the surface to the QW action region. Lee *et al* (Lee et al., 2009) observed that this diffusion could be accelerated along the line of any dislocation defect and one or another of the optical gradual degradations would

operate under very high temperature and voltage.

4.2.2.2 Package level degradation

Packaging is considered as a low cost method to realize the mass production of LEDs and to protect LED chips from damage, including electrostatic discharge (ESD), moisture, high temperature, chemical corrosion, and mechanical shock. When a GaN-based chip is packaged as a LED product, several other materials need to be used together with it. Fig. 4-2(a) and Table 4-1 list most of them, which are Epoxy Lens, Silicone Glue, Phosphor Coating, Die Attach Adhesive, Wire Bond, Silicon submount, Heat Sink, Lead Frame, and Plastic Mould and so on. Any degradation among those materials or interface defects will induce LED package failure and lower its reliability and lifetime. As shown in previous research results, the most common failure mechanisms are (Hu et al., 2007, Arik et al., 2004, Christensen & Graham, 2009, Cassanelli et al., 2008, Yang et al., 2010); (i) Interface delamination which could result in open circuit or heat dispersion problems; (ii) Epoxy lens and silicone glue darkening which worsens the chromatic properties of white LEDs; (iii) Phosphor coating degradations which can cause decay of the spectral properties of white LEDs

- (i) Interface delamination failure, one of the common failures encountered during

electronic packaging, can threaten the packages' electrical and thermal management. As shown in the structure of LUXEON_K2 series LED packages (Fig. 4-2 (a)), there are six different parts packaged together in layers, with five interfaces between adjacent layers. Hu *et al* (Hu et al., 2007) reported on the mechanisms of delamination in LED packages and compared the two driving forces of failure (thermal-mechanical-stress and hygro-mechanical-stress) to accelerate the development of delaminations. By physical analysis, the thermal-mechanical induced stress (σ_T) between layers comes from a mismatch between the Coefficient of Thermal Expansion (CTEs) and the specific heat of different materials. The different capacities of hygroscopic swelling (CME, Coefficient of Moisture Expansion) also contribute to the generation of hygro-mechanical-stress (σ_M). So overall, common delaminations, either driven by thermal-mechanical-stress or hygro-mechanical-stress, produce voids within interface layers. This raises the thermal resistances and finally block thermal passage, especially for the chip-submount layer and submount-heat sink layer, the major heat dissipating route in this package.

$$\sigma_T = E\alpha(T - T_{ref}) \quad (4-3)$$

$$\sigma_M = E\beta(C - C_{ref}) \quad (4-4)$$

$$R_{th} = \frac{T_j - T_0}{Q} = \sum_i^n R_{th,i} \quad (4-5)$$

where E is elastic modulus, α , T and T_{ref} are CTE, temperature and reference temperature, respectively, β , C and C_{ref} are CME, moisture concentration and relative moisture concentration. T_j and T_0 are the highest junction temperature and ambient temperature, respectively, and Q is the input thermal power.

To best qualify the ability of thermal management of white LED packaging, thermal resistance (R_{th}), defined as the temperature difference between junction temperature and ambient environment divided by input thermal power, was introduced, and R_{th} also can be understood as the temperature gradient between the heat resource and its surroundings. This might induce thermal-mechanical-stress to shorten the life of the white LED package. Tan *et al* (Tan et al., 2009b) found that the thermal resistance of the die attachment located between the silicon submount and the copper heat sink would be enhanced greatly when voids exist within the adhesives.

(ii) Epoxy lens and Silicone glue darkening failure. The chromatic properties of white LED lighting products are determined both by the stability of the luminous output produced by blue GaN-based chip and by the capability of light penetration which is controlled by the quality of the lens and silicone glue coatings. The epoxy lenses are applied to the LEDs packages to increase the amount of light emitted to the front (Hsu et al., 2008). Because they are exposed to the air, epoxy lenses suffer

thermal and moisture cycle aging during operation time and some cracks or flocculent were observed in the aging test, which lowers the light output from the GaN-based chips. Similarly, the purpose of introducing transparent silicone glue coatings in the LED package is not only to protect and surround the LED chip, gold ball interconnects and bonding wires, but also to act as a lens through which the light beam is collimated. However, this polymer encapsulate is thermally unstable at high temperatures or in a high forward bias aging period, which could impact on the optical output and the wavelength shift (Meneghini et al., 2008). In conclusion, the above mentioned failure mechanisms are associated with the chemical degradation of materials within the product lifetime, so in order to increase the lifetime of the lens and silicone glue coatings in the LED packages, choosing the correct thermal, mechanical, and chemical stable materials is the most critical step during packaging design.

(iii) Phosphor Coating degradation. The most widely used white LED on the market is a combination of blue LED chips and yellow phosphor (YAG:Ce³⁺) powders mixed with organic resins (Fan et al., 2007). According to previous research (Luo et al., 2005), there are two probable reasons for this. One is that phosphor particles scatter the light emitted by the chip due to the refractive index mismatching between the powders and resins. The other reason is that the thermal degradation of

polymer resins could result in the degradation of the polymer-based phosphor coating during aging. To solve this problem, a glass ceramic phosphor, with higher quantum efficiency, better hydro-stability, excellent heat-resistance, compared to the resin-based one, and with a CTE which matches with the GaN-based chip, is a promising alternative for the future.

4.2.2.3 System level degradation

To satisfy the special applications, i.e Indicators, Lighting, Displays and so on, several LEDs units are mounted together in arrays to increase the luminous flux and the chromatic types. But the accompanying problem is thermal management which is of primary importance to their reliability and efficiency (Christensen & Graham, 2009).

A LED lighting system usually consists of LED arrays mounted on substrates, cooling systems and electrical driving modules, like the high power white LED lamp shown in Fig. 4-2(b). For detail assembly technology, the LED arrays are surface mounted on a sapphire substrate with high thermal conductivity ($35\sim 46 \text{ W/m}^\circ\text{C}$) and an active cooling system is introduced to maintain the junction temperature according to the specification requirements by convection to the surroundings. Finally, to stabilize the power supply, an electrical driver is packaged between the

electrode and the active cooling system. To analyze the degradation mechanisms of the whole system, a hierarchical analysis method was applied to this system by separating it into three subsystems: the SMT module (LED arrays mounted on sapphire substrate) (Fig. 4-5), active cooling systems, and power driving circuit (Song et al., 2010).

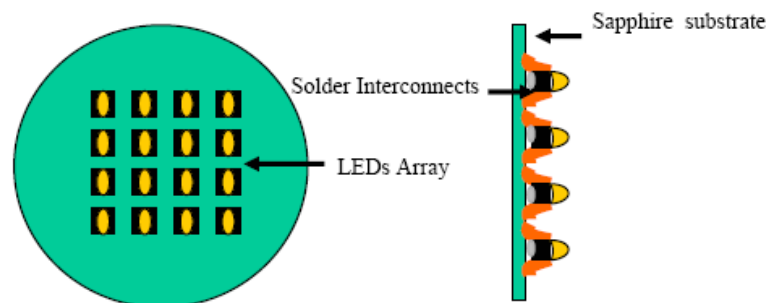


Fig. 4-5 Surface Mount Technology module

(i) Degradation in SMT module

According to the optical design, several high power white LED units are mounted on sapphire substrate by the widely used soldering technology. For this subsystem, the chip level and package level failure mechanisms are summarized in section 4.2.2.1 and section 4.2.2.2 respectively, so the left failure site might be the interconnections between the lead frames and the sapphire substrate. As is known, the solder joint interconnects serve two important purposes (Lee et al., 2000): (1) to form the electrical connection between the component and the substrate, and (2) to build the mechanical bond that holds the component to the substrate. In LED

packaging, they also act as a heat dissipation path from the heat sink to the substrate.

During the product's lifetime, owing to the mismatching of the Coefficient of Thermal Expansion (CTE) between substrate and the LEDs unit, cyclic temperature changes cause cyclic displacement, which can lead to thermal fatigue failures in the solder interconnects. There are two major components to fatigue failures: the initiation of fatigue cracks and the propagation of these cracks under cyclic loading, and both could suddenly cause an open circuit and light-off. Although this seems to be a catastrophic failure for the lighting, time-dependent degradation occurs within solder interconnects under thermal and moisture cyclic aging. Therefore, one of the loads monitored to predict the lifetime in this system would be located in the solder interconnects, not just focused on the output luminous flux.

(ii) Degradation of active cooling systems

As mentioned in Song *et al's* research (Song et al., 2010), a more practical approach to lower the junction temperature of the LEDs chip is to apply an advanced active cooling technology and potentially active thermal management technologies (Luo & Liu, 2007), including thermo-electronics, piezoelectric fans, synthetic jets, and small form factor fans. In order to enhance the whole system's lifetime, the reliability of the cooling systems must be higher than the LED arrays (>50,000 hrs).

With this principle in mind, Song *et al* (Song et al., 2010) chose a much more reliable cooling system (synthetic jets) which comprised two thin piezoelectric actuators separated by a compliant ring of material. The two degradation mechanisms related to the aging of the cooling system were: (1) the depolarization of the piezo-ceramic; (2) change in the elastic modulus of the compliant, rubbery tendon. The contributions that the cooling system made to the whole lighting system were its capacity to remove the heat produced by the LED modules and to lower the junction temperature. This was quantitatively expressed as an enhancement factor (EF), which could contribute to establishing the whole system's thermal induced PoF models (Equation.4-6)

$$EF(P_{cooling-systems}) = \frac{Q_{active}}{Q_{nc}} \quad (4-6)$$

where Q_{active} , Q_{nc} are the heat removed by the active cooling system and by natural convection, respectively. $P_{cooling-system}$ is the performance of the cooling system.

However, this system level degradation analysis didn't take into account the package level degradation, it only correlated with the heat-induced chip level failure, because Song and co-workers (Song et al., 2010) only supposed the chip to be directly mounted on the substrate. When taking into account future maintenance and repair considerations, one should also consider the package level degradation of LED modules.

4.2.2.4 Rank Priority for Potential Failure Mechanisms

After classifying the failure modes and potential failure mechanisms for the whole high power white LED lighting system, the next step is to prioritize the identified failure mechanisms with a rank priority number (RPN), which is widely used in FMMEA to determine the design risk (Modarres, 2010, Stamatis, 2003). Special attention should be given to the failure mechanisms with high RPN values in the reliability design period. In the PoF based PHM approach, damage models are established for those failure mechanisms with high RPN in order to evaluate the system's useful life. From results gleaned from past experience in high power white LED lighting systems, the RPN values are summarized in Table 4-2.

Table 4-2 Rank priority for potential failure mechanisms

Failure Sites	Failure Modes	Failure Mechanisms	Rank Priority Rating			
			<i>S</i>	<i>O</i>	<i>D</i>	<i>RPN</i>
P-N Junction	Power efficiency degradation	Defect propagation	8	3	6	144
P-type Layer		Dopant diffusion	6	2	6	72
Interface		Delamination	7	3	4	84
Epoxy lens & Silicone glue		Darken	6	3	4	72
Phosphor Coating	Chromatic changes	Depolymerization	6	3	4	72
Solder Interconnections	Circuit open	Fatigue	10	5	2	100
Cooling Systems	Heat Increase	Ageing	5	2	3	30

Note: *S*: Severity; *O*: Occurrence; *D*: Detection; $RPN=S \times O \times D$

As shown in Table 4-2, it can be seen that chip level luminous degradation induced by thermal propagation and solder interconnection fatigue damage driven by thermal cycling, are the two potential failure mechanisms which carry the highest degree of risk.

4.2.3 Physics-of-Failure based Damage Modeling

After identifying the failure modes and the potential failure mechanisms and ranking the failure mechanisms, establishing the relevant physics-of-failure models can help quantify the failure through evaluation of time-to-failure or likelihood of a failure for given set of geometries, material construction, environmental and operational conditions. As discussed above, the two most critical failure mechanisms with the highest priority in the degradation from chip to the whole system are: (1) Thermal-induced luminous degradation; (2) Thermal cycle-induced solder interconnect fatigue.

4.2.3.1 Thermal-induced luminous degradation modeling

Referring to the commonly used Solid State Lighting (SSL) standard, lumen depreciation or lumen maintenance is one of the most important criteria to verify the reliability of high power white LED Lighting (Chips, Packages, or Systems).

According to the laminate standard, IES LM-80-08, the lifetime of LED packages, arrays or modules can be defined as the time for 70% lumen maintenance.

As already mentioned, in failure mechanisms, thermal dissipation is a serious issue in high power white LED Lighting from the chip to system, and higher junction temperature accelerated by poor thermal dissipation of packages or cooling systems was responsible for deterioration in luminous efficacy and in shortening the lifetime of the system. Normally, there are two paths for heat dissipation(Fig. 4-6): (1) by conducting heat through the upper phosphor coating and silicone glue, and the epoxy lens; (2) the other is from the materials attached to the die, the silicon submount and through the heat sink to the substrate.

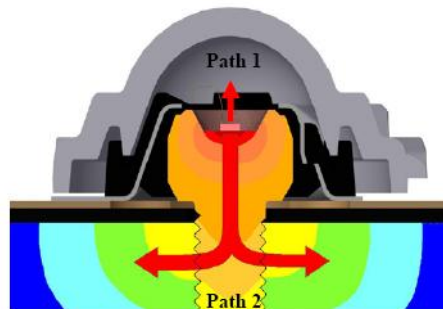


Fig. 4-6 Heat dissipation paths

However, evidence showed that the first path was blocked because of the heat insulation of the polymer materials. To establish PoF based damage models between lumen maintenance and the capacity for thermal dissipation of the system, a thermal

resistance network was first built to evaluate the performance of heat dissipation (Fig. 4-7). The submodel for the lumen maintenance (L_m) of LED chips has an empirical exponential form:

$$L_m = \frac{L_{output}}{L_0} = e^{-\alpha(T_j)t} \tag{4-7}$$

$$TTF = \frac{\ln 0.7}{-\alpha(T_j)} \tag{4-8}$$

$$T_j = f\{A; R_{th}; I_c; T_0\} \tag{4-9}$$

$$R_{th} = \sum_i^n (R_{chip} + R_{ball} + R_{SiC} + R_{adhesive} + R_{heat\ sink})_i + R_{solder\ interconnects} + R_{substrate} - EF \tag{4-10}$$

where α is the junction temperature-dependent light output degradation rate, t is the operation time measured in hours, and when $L_m=0.7$, TTF is the time to failure. T_0 is the ambient temperature. I_c is the forward current. A represents the non-radiative coefficient which contributes to produce intrinsic heat. R_{th} is the thermal resistance of the whole system.

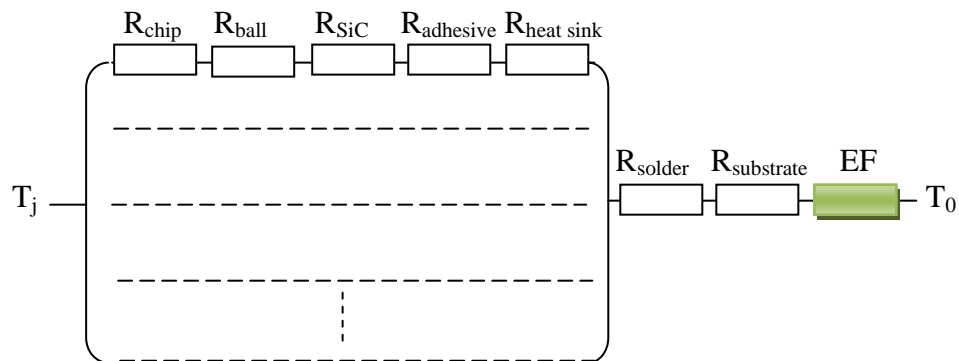


Fig. 4-7 Thermal resistance network of high power white LED lighting system (EF: Enhancement factor of cooling systems)

The enhancement factor EF is a performance factor of the cooling system, which is defined as the ratio of the heat removed using active cooling systems to the heat removed through passive means alone. The degradation of the active cooling system, including material wearout, determines the enhancement factor. As shown in Fig. 4-7, enhancement performance can also be achieved in series in the thermal resistance network, as negative thermal resistance.

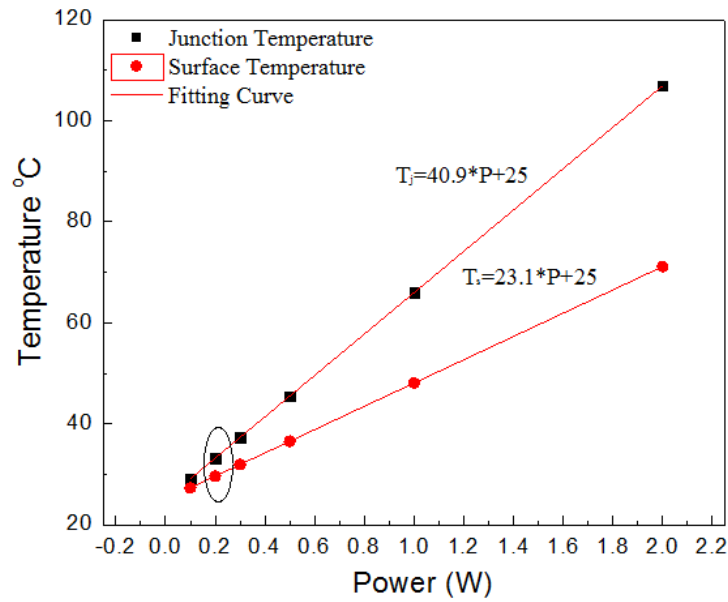
Equation 4-9 reveals that several parameters determinate the junction temperature, and testing the junction temperature accurately is a difficult task when a GaN chip is packaged in the LED unit during aging. This section used the finite element method based on COSMOS software to simulate the junction temperatures under different driving powers and the temperature distribution result is shown in the Fig. 4-8 (b), after materials properties were put into the simulation model. Finally, the actual surface temperature of the LED unit measured by the NEC MRI 9100 thermal tracer was used to verify the simulation results. The result showed little difference between the simulation result (31.92 °C) and the real test result(32.4 °C) under the same 0.3 watt driving power.

$$T_j = 40.9 * P + 25 \quad (4-11)$$

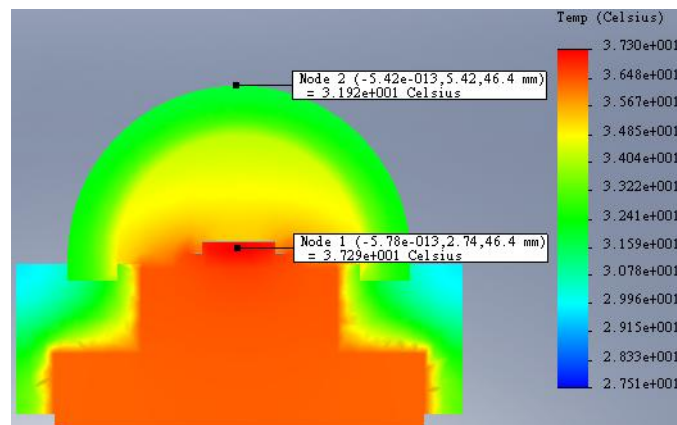
$$T_s = 23.1 * P + 25 \quad (4-12)$$

$$P = 0.003 * I_c - 0.003 \quad (4-13)$$

$$T_j = 0.1227 * I_c + 24.877 \quad (4-14)$$



(a)



(b)

Fig. 4-8 (a) The linear relationship between junction temperature and input power and (b) FEA simulation of heat distribution with 0.2W input power

Fig. 4-8 and Fig. 4-9 illustrate the relationships between junction temperature, input power and input current. The linear relationship between the junction temperature and input current can be inferred by inserting equation 4-13 into equation 4-11, calculated from fitting the simulation data. Therefore, equation 4-14

can be used to evaluate the junction temperature based on the input current for the LUXEON_K2 LED unit.

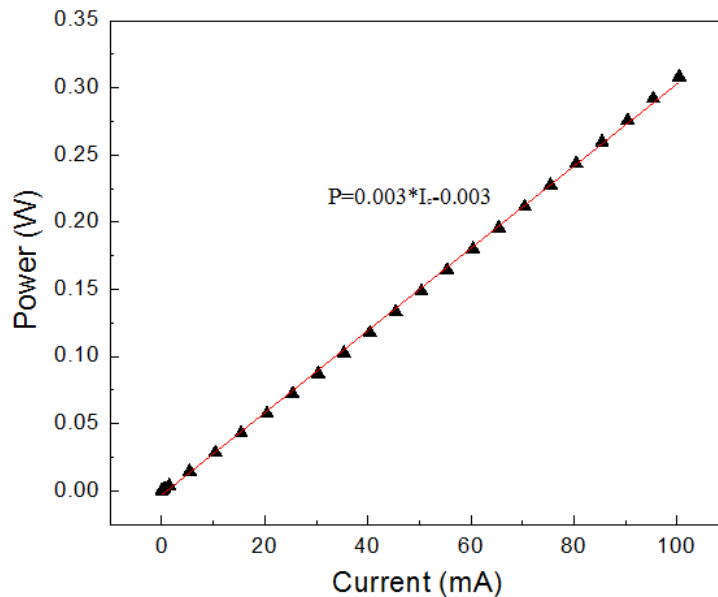


Fig. 4-9 The linear relationship between input current and power

Fig. 4-10 shows the LM-80 test results of 10 LEDs from PHILIPS LUXEON lifetime database under the operation conditions: $T_j=68^\circ\text{C}$, $T_0=55^\circ\text{C}$, $I_c=0.35\text{A}$. The exponential degradation model was used to fit the lumen maintenance data from 1000 to 6000 hrs. Then the two parameters (α , β) were estimated for each degradation curve by the least square method and the goodness of fit was determined by R^2 , which was close to 1, if the regression curve fitted well to the data. Based on extrapolations of the curves, the lumen maintenance of each test samples at 10,000 hrs was predicted and compared with the test results, revealing little difference

between the estimated and real data. With the same method, TTFs (L_{70} age) were calculated, but until now no field results has provided verification (Table 4-3).

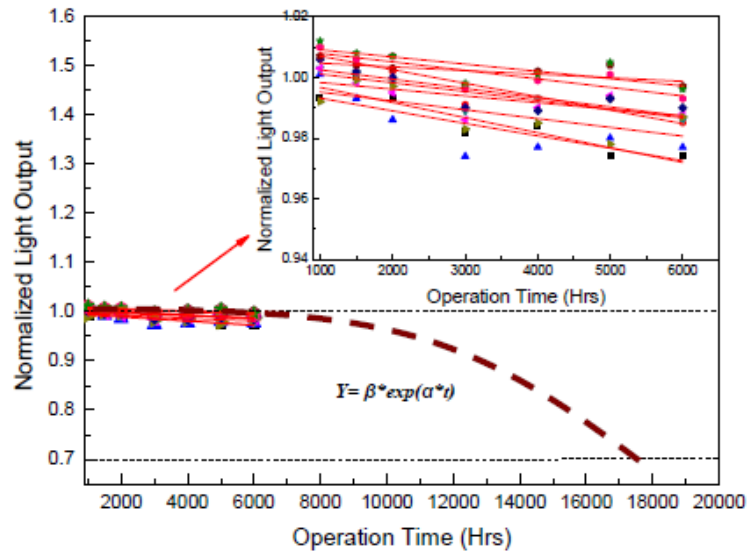


Fig. 4-10 Lumen Maintenance Plotting and Prediction for LEDs

Table 4-3 Lumen data (1,000 to 6,000 hrs) and exponential extrapolations of L_{70} ages ($T_j=68\text{ }^\circ\text{C}$, $T_0=55\text{ }^\circ\text{C}$, $I_c=0.35\text{A}$, data normalized to 1 at 24hrs)

	$Y = \beta * \exp(\alpha * t)$		R^2	Y (10000 hrs)	Test results (10000 hrs)	Error	TTF
	β	α $*10^{-6}$					
S1	1.00174	5.2876	0.82310	0.950	0.956	-0.00616	67783.8
S2	1.01149	4.4541	0.81384	0.967	0.964	0.00354	82643.4
S3	0.99726	4.1726	0.51570	0.957	0.96	-0.00365	84822.5
S4	1.00406	2.9143	0.70202	0.975	0.968	0.00740	123779.9
S5	1.00055	2.2251	0.37781	0.979	0.962	0.01690	160544.7
S6	0.99807	2.9347	0.40313	0.969	0.966	0.00331	120880.9
S7	1.00554	3.0600	0.62529	0.975	0.974	0.00127	118365.9
S8	1.00585	1.1931	0.22685	0.994	0.974	0.02004	303826.8
S9	1.01075	2.7981	0.65066	0.983	0.969	0.01410	131293.7
S10	1.01154	2.3735	0.51541	0.988	0.974	0.01398	155109.3

Note: Error=(Y-Test result)/Y; TTF=(L_{70} ages, hrs)

4.2.3.2 Thermal cycle-induced solder interconnects fatigue modeling

Although this failure mechanism induces catastrophic electrical power-off for LED lighting systems, time-dependent fatigue degradation of solder interconnects results in this type of crack failure during cyclic aging. Thus, capturing the time to failure of solder interconnects also helps to evaluate the lifetime of LED lighting systems. Lee (Lee et al., 2000) presented the solder joint fatigue models, summarized their features and applications and classified them into five categories, including stress-based, plastic strain-based, creep strain-based, energy-based, and damaged-based.

For the package type of LUXEON_K2: leaded packaging, three physical failure models were fitted to identify the failure mechanisms (Table 4-4): *The Coffin-Manson model*, *the Coffin-Manson-Basquin model*, and *the Engelmaier model*. Among these three models, the *Coffin-Manson fatigue model* is the best known and most widely used approach, but it assumes that fatigue failure is strictly controlled by plastic deformation and the elastic strains contribute little to fatigue. To avoid this shortcoming, *Basquin's* equation which considers the elastic deformation's contribution is added to the *Coffin-Manson fatigue model* and the *Coffin-Manson-Basquin model* is formed. The third failure model, the *Engelmaier model*, also is an improvement on the *Coffin-Manson fatigue model* by including

cyclic frequency effects, temperature effects, and elastic-plastic strain.

Table 4-4 Fatigue failure models for solder interconnects

Failure Types	Failure models and equations	Required Parameter	Coverage
Plastic Strain Driven	1 <i>Coffin-Manson model</i> $\frac{\Delta \varepsilon_p}{2} = \varepsilon_f' (2N_f)^c$	Plastic strain	Low thermal cycle fatigue
Plastic + elastic Strain Driven	2 <i>Coffin-Manson Basquin model</i> $\frac{\Delta \varepsilon_p}{2} = \frac{\sigma_f'}{E} (2N_f)^b + \varepsilon_f' (2N_f)^c$	Strain range	High and low thermal cycle fatigue
Total shear strain Driven	3 <i>Engelmaier model</i> $N_f = \frac{1}{2} \left[\frac{\Delta \gamma_s}{2 \varepsilon_f'} \right]^{1/c}$	Total shear strain	Low thermal cycle fatigue

where, N_f = number of cycles to failure; $\Delta \varepsilon_p$ = plastic strain amplitude; ε_f' = fatigue ductility coefficient; c = fatigue ductility exponent, $\Delta \varepsilon$ = strain range; σ_f' = fatigue strength coefficient; E = elastic modulus; b = fatigue strength exponent (Basquin's exponent); T_s = mean cyclic solder joint temperature in °C; f = cyclic frequency in cycles/day;

4.3 Concluding Remarks

In this chapter, the Physics-of-failure based PHM approach, including an analysis of materials and geometries, FMMEA and failure models built for the prioritized failure mechanisms, was used to assess the reliability of high power white LED Lighting from the chip level to the system level. Three failure modes, (1) Catastrophic failure; (2) Lumen degradation; (3) Chromaticity state shift, were firstly categorized to the whole system and the potential failure mechanisms and their contributing loads were presented by the “bottom-up” method. Then, the

physics-of-failure based damage models were built for the two failure mechanisms with highest priority in the degradations from the chip to the whole system. These findings have been published by author on the journal of IEEE Transactions on Device and Materials Reliability in 2011 (Fan et al., 2011).

Notwithstanding that the PoF based PHM method requires comprehensive knowledge of the materials and geometries of products and the thermal, mechanical, electrical and chemical life cycle environment as well as processes leading to failures in the field in advance, this always increases the time and cost in the actual applications. To solve the problems in the complexity of conducting a PoF modeling, the data-driven methods have been reviewed and proven as alternatives to determine anomalies and make predictions about the reliability of systems with the historical information. Therefore, in the next chapter, the data-driven PHM methodologies on the lumen lifetime estimation for high power white LED lightings are developed.

Chapter 5 Lumen Lifetime Estimation Using a Statistical Data-driven Method

5.1 Introductory Remarks

Traditional reliability assessment techniques, like the Failure Mode Mechanism and Effect Analysis (FMMEA), Fault Tree Analysis (FTA), Lifetime Test, and Accelerated Lifetime Test (ALT), are always time and cost consuming during operation (de Oliveira & Colosimo, 2004). In addition, with highly reliable products, there may be only a few failures during reliability tests. Another drawback of ALT is that the failure mechanisms are different when the devices are under different accelerating stress levels, which may not properly imitate the actual failure process. In this situation, using degradation data to do reliability assessment appears to be an attractive alternative to deal with traditional failure time data, like that with more reliability information, and benefits in identifying the degradation path and providing effective maintenance methods before failures occur (Pan & Crispin, 2011).

Using degradation data to perform reliability assessment was proposed by statisticians some years ago. Nelson (Nelson, 1990) reviewed two methods for modeling the degradation data. One was called a ‘general degradation path model’ which was developed by Lu and Meeker (Lu & Meeker, 1993) who modeled the degradation as a function of time and multidimensional random variables. However,

little research has been carried out on these methods to assess the reliability of high power white LEDs (HPWLEDs) which usually follow a nonlinear degradation path.

In this chapter, a statistical data-driven method based on the general degradation path model was used to analyze the lumen maintenance degradation data of HPWLEDs (Fan et al., 2012). In detail, it deals with the degradation data using three different approaches (the approximation method, analytical method and the two-stage method) to estimate the failure time distribution and evaluate the product's reliability (e.g. Mean Time To Failure (MTTF), Confidence Interval (CI) and reliability function). Another method named the IES TM-21-11 method provided by the Illuminating Engineering Society of North America (IESNA) was also used to estimate the lifetime of the same product with the same degradation data. The estimation results from both methods are discussed and compared.

5.2 Device under Test Description

LUXEON Rebel is one type of high power white LED package with high luminous flux (>100 lumens in cool white at 350mA) and advanced packaging techniques (Chip-on-Board technique without wire bonding) (Luxeon, 2008a). From the cross-section of this device, the packaging structure is shown in Fig. 5-1. Fig. 5-2 shows the simulation of heat distribution of LUXEON Rebel with the improved

thermal management.

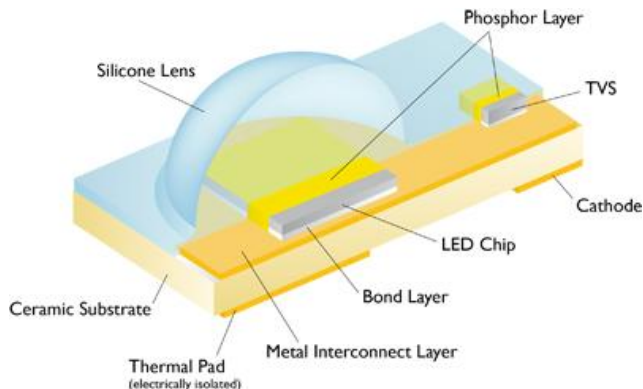


Fig. 5-1 White LUXEON Rebel and its structure (Luxeon, 2008a)

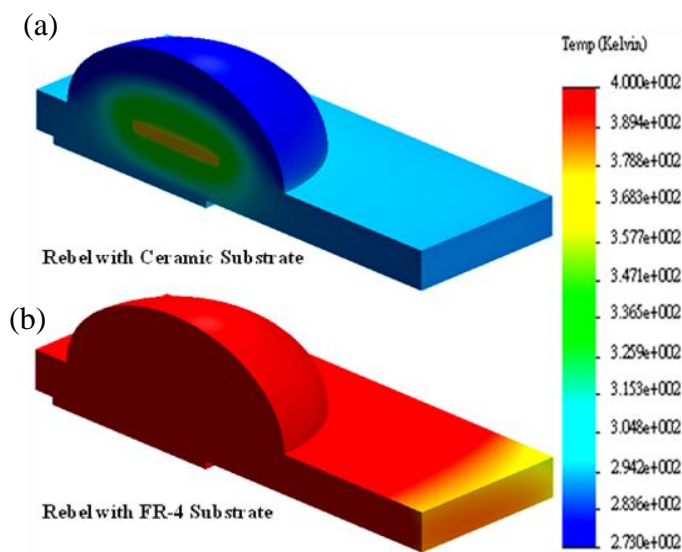


Fig. 5-2 Thermal management of White LUXEON Rebel with (a) ceramic substrate and (b) FR-4 substrate

An LED InGaN chip is attached to the surface of the metal interconnect layer (copper) by the bond layer (silver adhesive) and in order to improve the thermal dispersion capacity of the whole package, a ceramic with higher thermal conductivity

(>20W/m.K) compared to the traditional glass fiber reinforced epoxy material (FR-4) (0.35 W/m.K) is introduced as the substrate. At the same time, a copper thermal pad is set at the bottom of the ceramic substrate in order to conduct the heat produced by a LED InGaN chip to the air effectively. The top surface of the LED InGaN chip is covered with phosphor to convert the blue light to a white color.

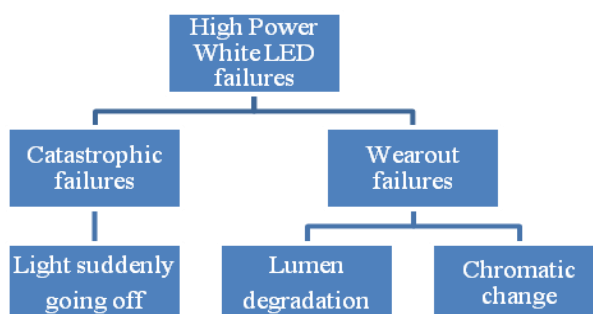


Fig. 5-3 Failure modes of HPWLEDs

From the FMMEA results mentioned in the previous chapter, it can be seen that the common failures modes of HPWLED as shown in Fig. 5-3 include: catastrophic failure, lumen degradation failure and chromatic change failure. However, for the LUXEON Rebel, InGaN types of LED without wire bonding interconnects, the probability of catastrophic failure (like the light suddenly going off due to an open circuit) under standard aging test conditions recommended by IES LM-80-08 is low, especially at the beginning of the test period (before 6,000 hrs). The lumen degradation and chromatic change are the two dominating failures in the LUXEON

Rebel LED. This section is focused on predicting the lumen degradation failure which is one of the most disturbing technical problems for both LED manufacturers and LED reliability engineers, and the chromatic change failure is analyzed in the next chapter.

5.3 Theory and Methodology

5.3.1 IES TM-21-11 Method

IES TM-21-11, Projecting Long Term Lumen Maintenance of LED Light Sources, is a lumen lifetime estimation standard proposed by the IESNA, which provides a method to determine the LED luminaire operating life (lumen output decreases by some percentage, 50% or 70%, of the initial one over a certain length of operation time) based on the lumen maintenance data collected from IES LM-80-08. The main implementation procedure of the IES TM-21-11 method provided by the TM-21 working group is as follows:

- (a) Selecting the sample size. Minimum sample size is recommended as 20 and the lumen maintenance data are collected based on the IES LM-80-08 test standard.
- (b) Preprocessing the lumen maintenance data. Firstly, for each unit, remove the initial data (0~1,000hrs) to reduce the noise from the non-chip decay failure mechanisms (like encapsulant decay); and then normalize all data to 1 at the time

zero test point. The next step is to average the data from all 20 samples at each test point (normally, additional measurements after the initial 1,000 hours at intervals smaller than 1,000 hours (including every 1,000 hour points)) as the fitting data (not considering the influence of variance between the samples).

(c) Fitting model. Previous work on the high power white LEDs indicated that the degradation of lumen performance followed an exponential curve. Therefore, in this section, applying the LED exponential lumen degradation path model (Equation (5-1)) is applied to fit the averaged degradation data using the ordinary least squares (OLS) method (Appendix A).

$$D(t) = \alpha \cdot \exp(-\beta \cdot t) \quad (5-1)$$

where $D(t)$ is the averaged normalized luminous flux at time t , α is initial constant, and β is the degradation rate which varies from unit to unit.

(d) Projecting the lumen maintenance life L_p .

$$L_p = \ln\left(\frac{100 \times \alpha}{p}\right) / \beta \quad (5-2)$$

where p is the maintained percentage of the initial lumen output (i.e. 50, 70).

(e) Adjusting the result with the “6-times rule”. The “6-times rules” means that if the lumen maintenance data before 6,000 hrs are used to fit the model, the projected lumen maintenance life L_p must be smaller than 36,000 hrs (from 6,000 x 6). If the lumen maintenance data during 6,000 to 10,000 hrs is collected, the maximum

projected lumen maintenance life L_p is 60,000 hrs (from 10,000 x6 hrs).

5.3.2 Statistical Data-driven Method

Statistical Data-driven method used in this section is based on the general degradation path model presented by Lu and Meeker, introduced in the literature review. For the general degradation path model, a random sample size is supposed as n , and the measurement times are $t_1, t_2, t_3, \dots, t_s$. The performance measurement for the i^{th} unit at the j^{th} test time is referred to as y_{ij} . So the degradation path can be registered as the time-performance measurement pairs $(t_{i1}, y_{i1}), (t_{i2}, y_{i2}), \dots, (t_{imi}, y_{imi})$, for $i = 1, 2, \dots, n$, and m_i represents the test time points for each unit

$$y_{ij} = D(t_{ij}; \alpha; \beta_i) + \varepsilon_{ij} \quad (5-3)$$

where $D(t_{ij}; \alpha; \beta_i)$ is the actual degradation path of unit i at the measurement time t_{ij} . α is the vector of fixed effects which remains constant for each unit. β_i is a vector of random effects which vary according to the diverse material properties of the different units and their production processes or handling conditions. ε_{ij} represents the measurement errors for the unit i at the time t_{ij} which is supposed to be a normal distribution with zero mean and constant variance, $\varepsilon_{ij} \sim \text{Normal}(0, \delta_\varepsilon^2)$.

The failure definition for the general degradation path models is when the performance measurement y_{ij} exceeds (or is lower than) the critical threshold D_f at

time t , and pdf is the probability density failure distribution of the sample. The cumulative probability of the failure function $F(t)$ is given as follows(Fig. 5-4):

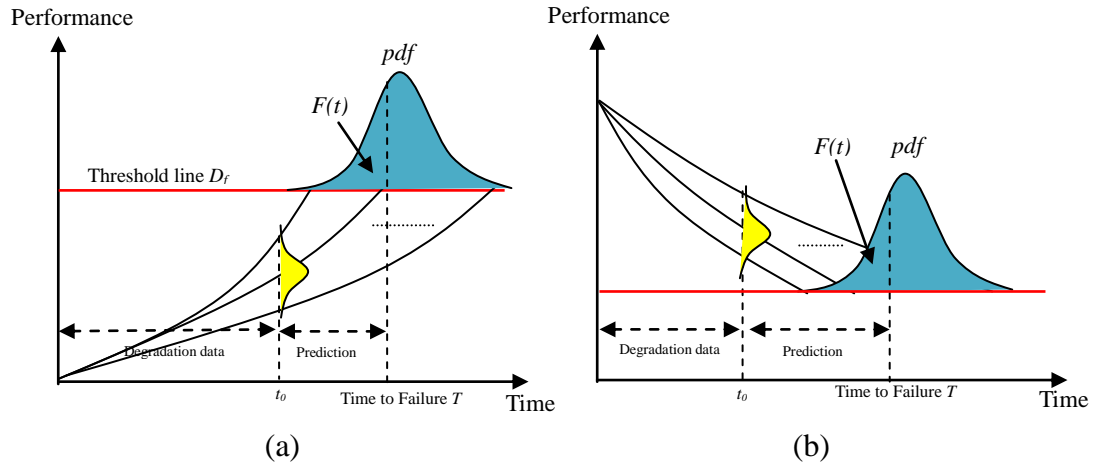


Fig. 5-4 General degradation path model (a) increasing type and (b) decreasing type

The increasing type of performance measurement

$$F(t) = P(t \leq T) = P[D(t_{ij}, \alpha, \beta_i) \geq D_f] \tag{5-4}$$

$$\text{Time to Failure} \quad T = \inf(t \geq 0; D(t_{ij}, \alpha, \beta_i) \geq D_f)$$

The decreasing type of performance measurement

$$F(t) = P(t \leq T) = P[D(t_{ij}, \alpha, \beta_i) \leq D_f] \tag{5-5}$$

$$\text{Time to Failure} \quad T = \inf(t \geq 0; D(t_{ij}, \alpha, \beta_i) \leq D_f)$$

To estimate the time to failure distribution, $F(t)$, based on the degradation data, several statistical methods have been proposed by researchers, including (1)the approximation method; (2)the analytical method; (3)the two-stage method and others.

After reviewing these methods, it can be concluded that two basic steps are involved:

(1) estimating the parameters for the degradation path model (2) evaluating the time to failure distributions, $F(t)$.

5.3.2.1 Approximation method

The approximation method predicts each unit's time to failure based on the general degradation model and projects to the "pseudo" failure time when the degradation path reaches the critical failure threshold, D_f . Normally, the steps in the analysis are as follows:

- (a) Use the NLS method to estimate the parameters (fixed effect parameter α and random effect parameter β_i) of the degradation path model, based on the measured path data $(t_{i1}, y_{i1}), (t_{i2}, y_{i2}), \dots, (t_{im_i}, y_{im_i})$ for each unit, and the estimated results are α and β_i respectively.
- (b) Extrapolate the degradation path model of each unit to the critical failure threshold, D_f . When $D(t_{ij}; \alpha; \beta_i) = D_f$, the "pseudo" failure (not the real failure) time for each unit $(t_1, t_2, t_3, \dots, t_s)$ can be predicted.
- (c) Fit the probability distribution for these "pseudo" lifetime data and estimate the associated parameters for each distribution.
- (d) Assess the sample's reliability, based on the analysis reliability function $R(t)$, hazard function $h(t)$, mean time to failure (MTTF), and the confidence interval

(CI).

The approximation method is simple to implement not only for statisticians but also for manufacturers. However, there are also some requirements for this method if believable prediction results are to be achieved. Firstly, the degradation path model, $D(t_{ij}; \alpha; \beta_i)$, needs to be relatively simple. Secondly, sufficient degradation data is the essential requirement to get accurate parameter estimation results for α and β_i . Last but not least is that both the magnitudes of error ε_{ij} and the extrapolation width, which means the time period from the cut time of the data collection to the projected failure time, need to be small.

5.3.2.2 Analytical method

Regarding simple degradation path models, researchers have found that there are certain relationships between the random effect parameters of the degradation path models and the cumulative probability of failure distribution $F(t)$. Therefore, the reliability information of a sample can be obtained by analyzing the statistical properties of the random effects parameters β_i . The LED empirical lumen degradation path model is used to show the details of the inference procedure of this method.

(a) The first step of the analytical method is also to estimate the parameters (fixed

effect parameter, α , and random effect parameter, β_i) using the NLS method for each unit, like the first step of the approximate method.

(b) It is assumed that the random effect parameter β_i , which varies from unit to unit, follows the widely used two-parameter Weibull distribution with shape parameter δ_β and scale parameter λ_β , $\beta \sim \text{Weibull}(\delta_\beta, \lambda_\beta)$. Next, estimate the two parameters in $\delta_\beta, \lambda_\beta$ using the maximum likelihood estimation (MLE) method.

(c) Infer the cumulative probability of failure distribution, $F(t)$, from **Weibull** ($\delta_\beta, \lambda_\beta$).

$$F(t) = P(t \leq T) = P\left[t \leq \frac{\ln(D_f / \alpha)}{-\beta}\right] = P\left[\beta \leq \frac{\ln(D_f / \alpha)}{-t}\right] = 1 - \exp\left[-\left(\frac{\ln(D_f / \alpha)}{-t\lambda_\beta}\right)^{\delta_\beta}\right] \quad (5-6)$$

In this situation, the reciprocal of time to failure, T , is also Weibull distribution with shape parameter $\delta_{1/T} = \delta_\beta$, scale parameter $\lambda_{1/T} = \lambda_\beta / \ln(\alpha / D_f)$, $1/T \sim \text{Weibull}(\delta_{1/T}, \lambda_{1/T}) = \text{Weibull}(\delta_\beta, \lambda_\beta / \ln(\alpha / D_f))$. Thus the time to failure distribution can be inferred from the probability distribution of the random effect parameter, ignoring the step of extrapolating the degradation path model. However, the analytical method does not consider the measurement errors ε_{ij} .

5.3.2.3 Two-stage method

To solve the shortcomings in the above two methods, Meeker *et al* (Meeker & Escobar, 1998) proposed a two-stage method for the parameter estimation.

(a) In the first stage, for each unit, the degradation path model is also fitted with the

nonlinear least squares method to estimate the parameters (fixed effect parameter, α_i , and random effect parameter, β_i). However, the difference between this method and the two methods mentioned above is that the measurement errors, ε_{ij} , are taken into consideration and the error variance, σ_{ε}^2 , for the i^{th} unit is estimated by

$$\sigma_{\varepsilon_i}^2 = \left[\sum_{j=1}^{m_i} \{y_{ij} - D(t_{ij}; \alpha_i; \beta_i)\}^2 / (m_i - q) \right] \quad (5-7)$$

where $q = p + k$, p and k are the number of estimated fixed effect parameters and the random effect parameters respectively.

Then by some appropriate re-parameterization, transfer the distribution of the random effect parameter, β_i , into a multivariate normal distribution with asymptotic mean, μ_{φ} , and variance covariance matrix, \sum_{φ} , $\varphi = H(\beta_i) = \mathbf{Normal}(\mu_{\varphi}, \sum_{\varphi})$.

(b) In the second stage, estimate the parameters including α , μ_{φ} , and \sum_{φ} , for the degradation path model.

$$\alpha = \sum_{i=1}^n \alpha_i / n \quad (5-8)$$

$$\mu_{\varphi} = \sum_{i=1}^n \varphi_i / n \quad (5-9)$$

$$\sum_{\varphi} = \left(\sum_{i=1}^n (\varphi_i - \mu_{\varphi})(\varphi_i - \mu_{\varphi})^i / (n-1) \right) - \left(\sum_{i=1}^n \text{var}_{\varepsilon}(\varphi_i) / n \right) \quad (5-10)$$

(c) Randomly generate N (normally 100,000) simulated realizations φ^* of φ from $\mathbf{Normal}(\mu_{\varphi}, \sum_{\varphi})$ and then the corresponding N simulated realizations β^* of β from $H^{-1}(\varphi)$.

- (d) Calculate the simulated failure time t^* by inserting the β^* into the $D_f = D(t; \alpha; \beta)$.
- (e) With Monte Carlo simulation, the time to failure distribution $F(t)$ can be expressed by:

$$F(t) = (\text{Number of simulated first crossing times} \leq t) / N \quad (5-11)$$

and the confidence interval can be calculated by the bootstrap method.

5.4 Results and Discussion

5.4.1 Lumen Maintenance Data

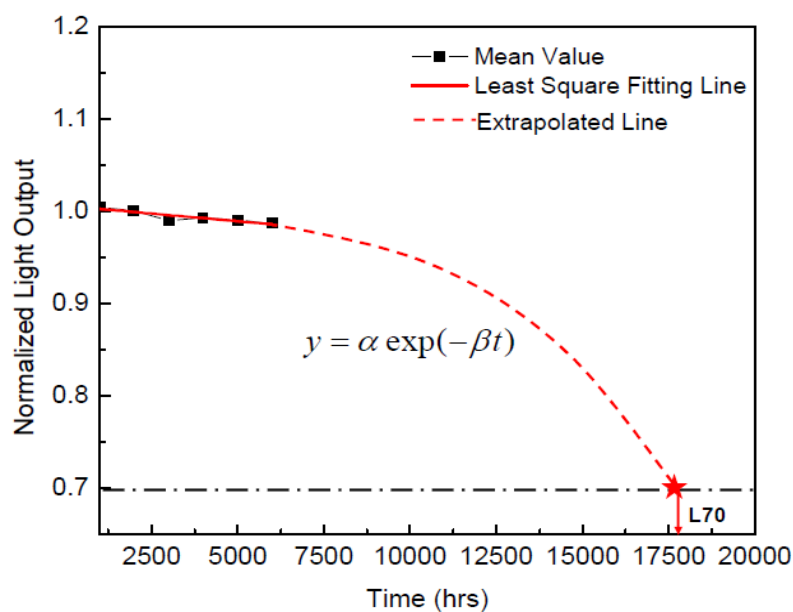
The lumen maintenance data of the LUXEON Rebel LEDs were collected from the LM-80 test report [DR03: LM-80 Test Report (Luxeon, 2010)] which was published by Lumileds, Philips (see Fig. 3-6). The data analyzed in this section were obtained under a test condition shown in Table 5-1. According to the IES LM-80-08 standard, lumen degradation failure is defined as when the lumen output decreases to 70 percent of the initial value over a certain length of operation time, which is also the lumen lifetime L_{70} . Therefore, in this study, L_{70} is the critical failure threshold of the lumen degradation model, D_f . The sample size was chosen as 20. For each unit, lumen maintenance data was collected every 1,000 hrs up to 10,000 hrs (totally 10 test time points) and normalized to 1 at the time zero test point.

Table 5-1 IES LM-80-08 Test conditions (Luxeon, 2010)

LM-80-08 Test Temperature	Input Current	Ambient Temperature	Case Temperature	Relative Humidity
55 °C	350 mA	64 °C	60 °C	18%

5.4.2 Lumen Lifetime Estimation with the IES TM-21-11 Method

Following the IES TM-21-11 operation procedure shown in section 5.3.1, the mean value of the lumen maintenance data from 20 units at each test time was used to fit the degradation path model using the nonlinear least squares method. Fig. 5-5 and Fig. 5-6 are the projected lumen lifetime L_{70} based on two different test time intervals (1,000 to 6,000 and 6,000 to 10,000 hrs respectively). The parameter estimation of the degradation path model and the lumen lifetime L_{70} projection results are shown in Table 5-2.

Fig. 5-5 Projecting L_{70} with lumen maintenance data from 1,000 to 6,000 hrs

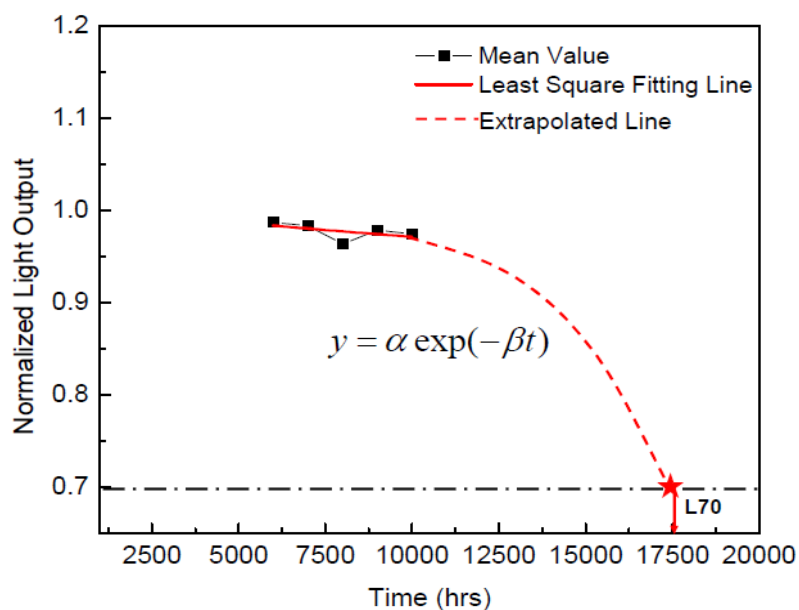


Fig. 5-6 Projecting L70 with lumen maintenance data from 6,000 to 10,000 hrs

Table 5-2 Recommended IES TM-21-11 estimation report

Tested Device	LUXEON Rebel, LUMILEDS, PHILIPS	
Sample Size	20	
Driven Current (mA)	350	
Test Case Temperature (°C)	60	
Test Duration (hrs)	10,000	
Test Duration used for Projection (hrs)	1,000~6,000	6,000~10,000
α	1.00633	1.00216
β	3.35252*e-6	3.11021*e-6
Lumen Lifetime L70 (hrs)	108,272.3	115,372.5
6 times limitation	36,000	60,000

By applying the “6 times rule” required in IES TM-21-11, both projected results exceed the 6 times limitation (like $L_{70}(6k) > 36,000$ hrs). Therefore, more test time and more lumen maintenance data are required to estimate the lumen lifetime under

these test conditions for the LUXEON Rebel LED device. Another drawback of IES TM-21-11 is that as it does not consider the variance of each test unit, so some reliability information for this device, including MTTF, confidence interval, and reliability function and so on, could not be obtained. This may be not effective for maintenance decision making by either LED manufacturers or designers.

5.4.3 Lumen Lifetime Estimation with the Approximation Method

To overcome the problems encountered in the IES TM-21-11 method, the approximation method was used to estimate the lumen lifetime using the same data as shown in the previous section (Fig. 5-7).

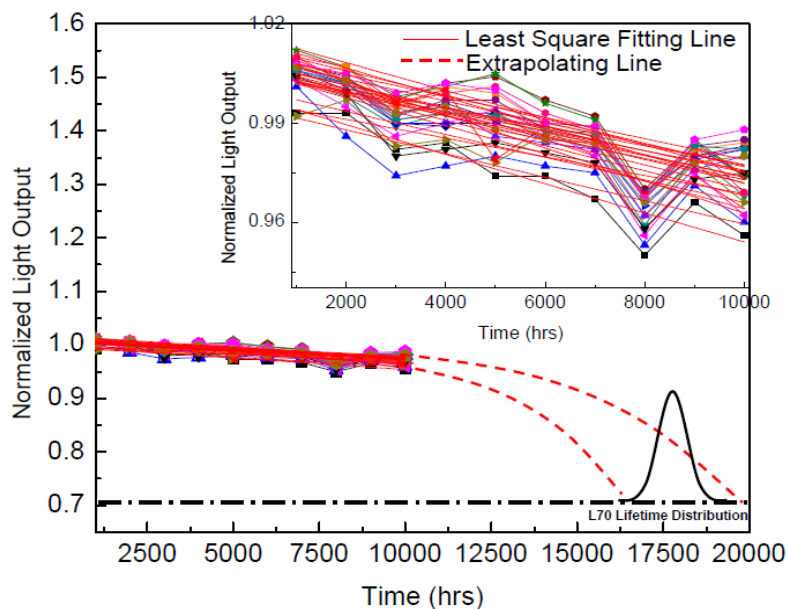


Fig. 5-7 Extrapolating degradation path model with 1,000 to 10,000 hrs data

Using the nonlinear least squares estimator, the parameters of the general degradation path model (α_i, β_i) were estimated for each unit. This is different from the IES TM-21-11 method which just considers the average data. Further, by extrapolating the model of each unit to the critical failure threshold (30% light decrease), “pseudo failure times” can be predicted (Table 5-3).

Table 5-3 List of estimated parameters for degradation path model and pseudo failure time

Sample No.	α	β	Pseudo failure time (hrs)
1	0.99858	4.57E-06	77816.5
2	1.01269	5.06E-06	72988.9
3	0.99518	3.66E-06	96138.6
4	1.00629	3.88E-06	93511.0
5	1.00624	4.28E-06	84788.7
6	0.99682	2.88E-06	122853.4
7	1.00572	3.22E-06	112472.9
8	1.01317	3.67E-06	100867.2
9	1.01559	4.42E-06	84287.7
10	1.0167	4.17E-06	89440.3
11	1.00823	3.34E-06	109122.0
12	1.00993	3.30E-06	111008.9
13	1.00618	2.90E-06	125152.1
14	1.00721	3.77E-06	96535.9
15	1.00053	3.52E-06	101485.3
16	1.00859	3.54E-06	103196.0
17	1.00537	3.29E-06	110133.4
18	1.0056	3.01E-06	120175.9
19	1.01107	3.23E-06	113760.5
20	1.00772	3.62E-06	100602.0

The next step of the approximation method is to fit the probability distribution for the “pseudo failure times” obtained from the extrapolating method. In this section,

three types of statistical models (Weibull, Lognormal and Normal) were selected to fit the “pseudo failure times” (Fig. 5-8) and the fitting results were justified by the Akaike Information Criterion (AIC) which is a method proposed by Akaike *et al* (Akaike, 1974) to verify the goodness of fit of a proposed statistical model. The AIC is quantitatively defined as follows:

$$AIC = -2\log(L) + 2 \cdot k \quad (5-12)$$

Where L is the maximum likelihood estimation (MLE) of the fitting model and k is the number of independently adjusted parameters within the model.

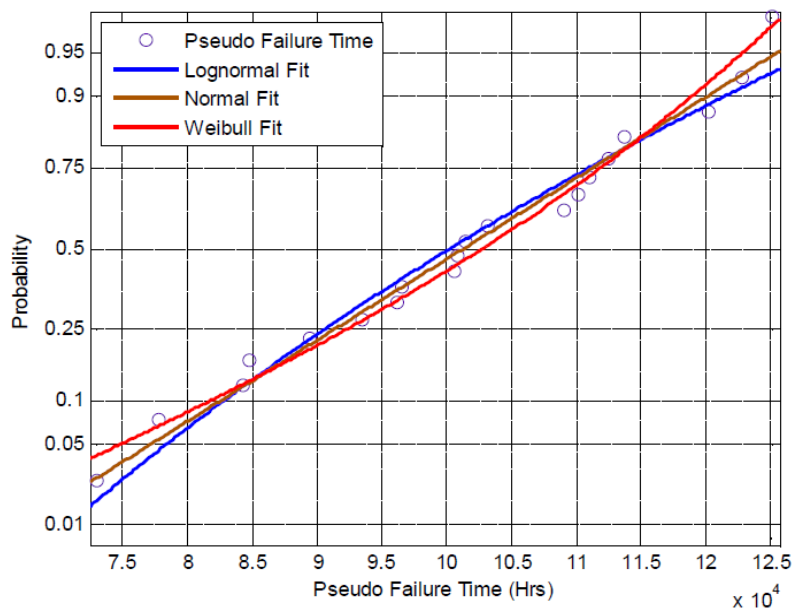


Fig. 5-8 Statistical models fitting for “Pseudo Failure Time”

The judgment standard of this theory is to compare the AIC value of the proposed fitting models and the lowest AIC value as means to obtain the best model-fitting.

According to the AIC value shown in Table 5-4, the Weibull model with the lowest AIC value presents the best fitting performance among the various models.

Table 5-4 Estimated parameters of each statistical model by approximate method

Parameters	Weibull	Lognormal	Normal
k	2	2	2
$\text{Log}(L)$	-219.554	-220.171	-219.712
AIC	443.108	444.342	443.4242

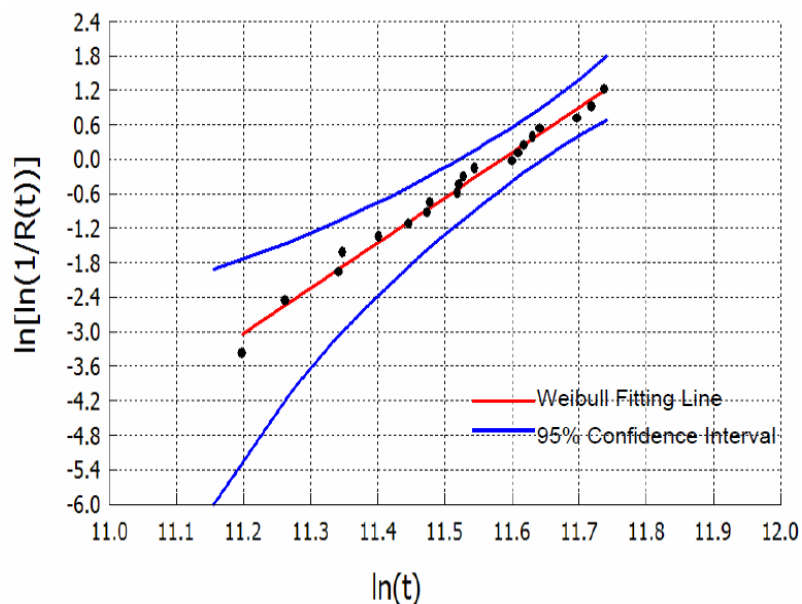


Fig. 5-9 Weibull plotting for “Pseudo failure times”

As shown in Fig. 5-9, the “pseudo failure times” followed the Weibull distribution with shape parameter δ and scale parameter λ , $T \sim \text{Weibull}(\delta, \lambda)$. The reliability function is shown as follows:

$$R(t) = \exp \left[- \left(\frac{t}{\lambda} \right)^\delta \right] = \exp \left[- \left(\frac{t}{107,500} \right)^{8.223} \right] \quad (5-13)$$

Fig. 5-10 reveals the reliability and the 95% confidence limit prediction results for our research device. The parameters of the reliability function, which were estimated by the maximum likelihood estimator (MLE), are listed in Table 5-5.

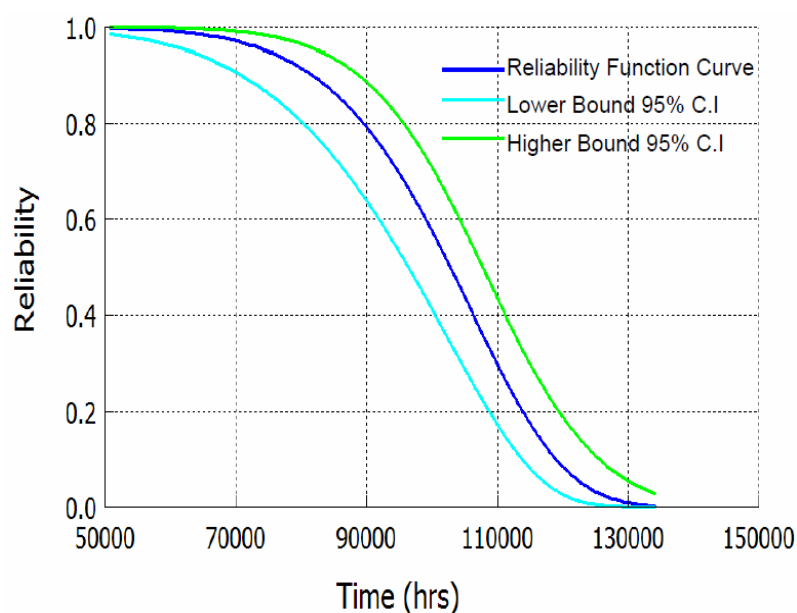


Fig. 5-10 Reliability prediction for LUXEON Rebel

Table 5-5 Parameters estimation and reliability prediction using the approximation method

Parameters	Estimation Results
α	8.223
β	107,500
MTTF (hrs)	101,300 (95,870, 107,000)
$t_{0.1}$ (hrs)	119,000 (113,500, 124,700)
$t_{0.5}$ (hrs)	102.800 (97,530, 108,400)

By comparing the predicted results, considering the sample's variance, the approximation method provides more reliability information (i.e. reliability function, MTTF and confidence interval) than the IES TM-21-11 method. This benefits not only manufacturers in making decisions but also customers in understanding products clearly. However, due to assuming the fitting model $D(t_{ij}; \alpha; \beta_i)$ as the degradation path and ignoring the measurement errors ε_{ij} , the approximation method also has some limitations.

5.4.4 Lumen Lifetime Estimation with the Analytical Method

The analytical method is similar to the approximation method by replacing the extrapolating step as the probability analysis for the random effect parameters, β_i . The parameter, α_i , was considered as a fixed effect and equal to 1, as all lumen degradation data of each unit were normalized to 1 at the original test point. So after parameter estimation for the degradation path model, the Weibull probability curve was used to fit the random effect parameters, β_i , shown in Fig. 5-11. Then the two parameters, δ_β , λ_β , for the Weibull distribution, were estimated with the maximum likelihood estimation (MLE) method (Table 5-6). The reliability function with its 95% confidence limits was predicted (Fig. 5-12).

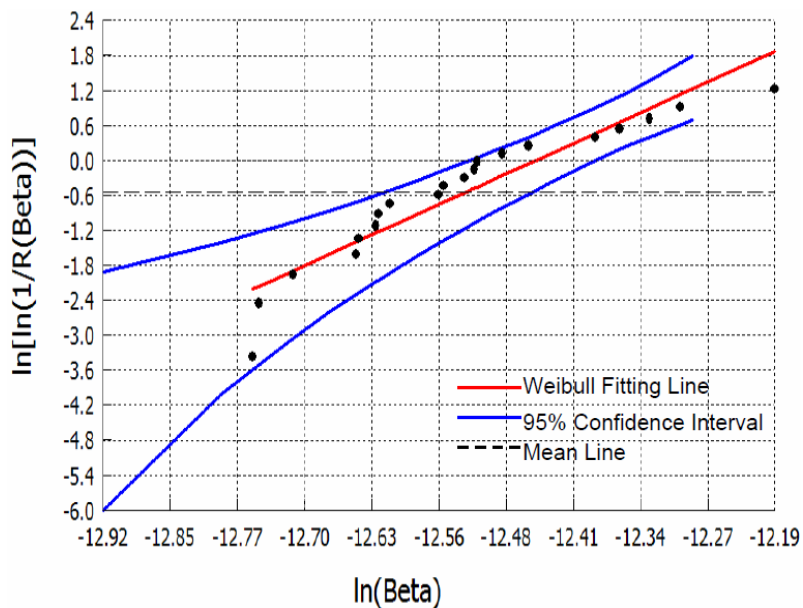


Fig. 5-11 Weibull plotting for random effect parameters β_i

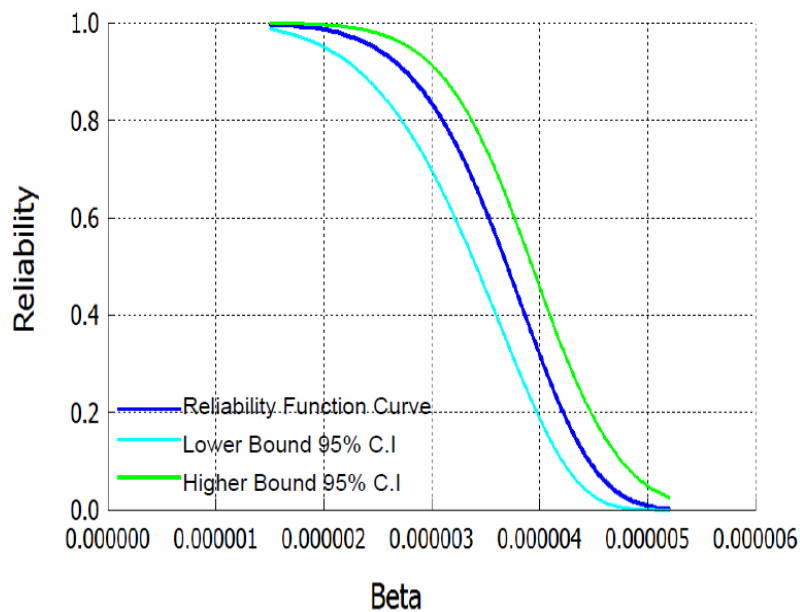


Fig. 5-12 Reliability prediction for random effect parameters β_i

As discussed previously, if the random effect parameters, β_i , follow a two-parameter Weibull distribution, $\beta \sim \text{Weibull}(\delta_\beta, \lambda_\beta)$, the reciprocal of time to

failure is also a Weibull distribution, $1/T \sim \text{Weibull}(\delta_{1/T}, \lambda_{1/T}) = \text{Weibull}(\delta_\beta, \lambda_\beta / \ln(\alpha / D_f))$. Both reliability functions can be calculated as follows:

$$R(\beta) = \exp \left[- \left(\frac{\beta}{\lambda_\beta} \right)^{\delta_\beta} \right] = \exp \left[- \left(\frac{\beta}{3.918 * e^{-6}} \right)^{6.433} \right] \quad (5-14)$$

$$R(1/t) = \exp \left[- \left(\frac{1/t}{\lambda_{1/T}} \right)^{\delta_{1/T}} \right] = \exp \left[- \left(\frac{1/t}{1.098 * e^{-5}} \right)^{6.433} \right] \quad (5-15)$$

Table 5-6 Parameters estimation and reliability prediction by the analytical method

Random Effect parameter β Estimation		Reciprocal Time to Failure $1/T$ Estimation	
δ_β	6.433	$\delta_{1/T}$	6.433
λ_β	$3.918 * e^{-6}$	$\lambda_{1/T}$	$1.098 * e^{-5}$
Mean	$3.649 * e^{-6}$ ($3.404 * e^{-6}$, $3.912 * e^{-6}$)	<i>MTTF</i> (hrs)	97,745.9 (91,174.6, 104,781.1)
$\beta_{0.1}$	$4.46 * e^{-6}$ ($4.206 * e^{-6}$, $4.731 * e^{-6}$)	$t_{0.1}$ (hrs)	79,972.0 (75,391.0, 84,801.5)
$\beta_{0.5}$	$3.701 * e^{-6}$ ($3.46 * e^{-6}$, $3.959 * e^{-6}$)	$t_{0.5}$ (hrs)	96,372.6 (90,092.2, 103,085.2)
$R(1.5 * e^{-6})$	0.998 (0.987, 0.999)	$R(1/80,000)$	0.100 (0.035, 0.207)

5.4.5 Lumen Lifetime Estimation with the Two-stage Method

As mentioned above, the random effect parameters, β_i , follow a Weibull distribution with scale parameter, λ_β , and shape parameter, δ_β , $\beta \sim \text{Weibull}(\delta_\beta, \lambda_\beta)$. So it was possible to move to the third step of this method directly, randomly generating $N(=100,000)$ realizations β^* of β from two-parameter $\text{Weibull}(6.433, 3.918 * e^{-6})$ with the S-PLUS (software for statistical computing from Bell Laboratories) random number generation function (Gentle, 1998). The corresponding N simulated failure

time t^* was calculated by substituting each β^* into $D_f = D(t; \alpha; \beta)$. The time to failure distribution, $F(t)$, was estimated with a Monte Carlo simulation. The lifetime estimation results are shown in Table 5-7.

Table 5-7 Parameters estimation and reliability prediction by the two-stage method

Parameters	Estimation Results
MTTF (hrs)	101,763 (101,618, 101,908)
$t_{0.1}$ (hrs)	79,977.8
$t_{0.5}$ (hrs)	96,375 (96,265, 96,510)
$R(80,000)$	0.900

Through comparing the prediction results of the two-stage method with the other methods, the estimated results of MTTF by the two-stage method and the approximation method are very close, but the widths of the 95% confidence intervals obtained by using the two-stage method are smaller than the others (Table 5-8), which means the last method has the highest prediction accuracy.

Table 5-8 The 95% Confidence interval widths of MTTF

Methods	MTTF (hrs)	Widths (hrs)
IES TM-21-11	108,272.3 ⁽ⁱ⁾	N.A.
	115,372.5 ⁽ⁱⁱ⁾	
Approximation method	101,300	11,130
Analytical method	97,745.9	13,606
Two-stage method	101,763	290

Note: (i) is estimated based on the data from 1,000 to 6,000 hrs, (ii) is estimated based on the data from 6,000 to 10,000 hrs.

5.5 Concluding Remarks

In this chapter, the lumen lifetime of the HPWLED unit (LUXEON Rebel, LUMILEDS, PHILPS) was estimated by a statistical data-driven method including the approximation method, the analytical method and the two-stage method, and the estimation results were compared to those obtained when using the IES TM-21-11 method.

From the IES TM-21-11 method, only the lumen lifetime, L_{70} , could be estimated by projecting the empirical degradation model without other reliability information. Moreover the prediction results based on two sets of periodical degradation data revealed different prediction results, both of which exceeded the maximum requirements of the “6 times rules”. This suggests that the prediction results are not acceptable without extending the data collecting time. However, with the proposed statistical data-driven method, more reliability messages, in addition to the lumen lifetime (e.g. Mean Time to Failure (MTTF), Confidence Interval (CI) and reliability function), can also be predicted. Among these three methods, the two-stage method with the smallest widths of the 95% confidence intervals produced the highest degree of prediction accuracy. This proposed statistical data-driven method (DDDM) has been published on the journal of IEEE Transactions on Device and Materials Reliability in 2012 (Fan et al., 2012).

Notwithstanding the promising results above, lumen lifetime is not the extracted “end of life” of LEDs. Both the lumen degradation and the chromaticity state shift need to be considered as health indicators of high power white LEDs. Secondly, the statistical data-driven method needs to select or assume a statistical distribution for the collected data, which limits the applications of this method. Thirdly, the prediction errors and uncertainties oriented from the ordinary least squares regression are large. Therefore, a machine learning based data-driven method (filter based data-driven method) is proposed in the next chapter to predict both the lumen maintenance and the chromaticity state for HPWLEDs.

Chapter 6 Prognostics of Lumen Maintenance and Chromaticity State with Filter Data-driven Methods

6.1 Introductory Remarks

From previous studies, lumen degradation is known as one of the two dominant wearout failure modes in high power white LEDs (HPWLEDs). Usually, the LED lumen lifetime is measured based on the lumen maintenance, which can be defined as the remaining percentage of initial light output over time. The Alliance for Solid-State Illumination Systems and Technologies (ASSIST) recommends two LED lumen lifetimes based on the time to 50% light output degradation (L_{50} : for display lighting) or 70% light output degradation (L_{70} : for general lighting) at room temperature (ASSIST Recommendation, 2005). To predict the lumen maintenance (or lumen lifetime) of LEDs, a projecting approach based on the least-square regression method is now recommended by IES (IES-TM-21-11) and is also widely accepted by many LED manufacturers.

For instance, Philips Lumileds and CREE are implementing this projecting approach to predict the lumen maintenance of LEDs in their reliability test reports. However, this IES-TM-21-11 projecting approach, dependent on least-square regression, introduces large prediction errors and uncertainties. Secondly, the reliability concerns of LED lighting are considered as involving both lumen

maintenance and the chromaticity state. However, previous research on the health of LEDs has not taken chromaticity state shift into consideration.

Therefore, both lumen maintenance and the chromaticity state are considered as the health indicators of high power white LEDs in this chapter. As reviewed before, the filter approach has become one of the most widely used learning based data-driven prognostic methods for estimating and predicting the state of electronic components or systems based on a state-space model. To reduce the prediction errors and uncertainties introduced by the IES-TM-21-11 projecting approach, a nonlinear filter-based data-driven approach (recursive Unscented Kalman Filter (UKF)) is used to predict the lumen maintenance (Fan et al., 2014b) and chromaticity state of HPWLEDs (Fan et al., 2014a).

6.2 Device under Test and Test Condition

6.2.1 Device under Test

We selected the same test device as used in the chapter five, one type of high power white LED from Lumileds, Philips, the White LUXEON Rebel. It has high luminous flux (>100 lumens in cool white at 350mA). Fig. 6-1 shows the packaging structure and luminescence mechanism of the White LUXEON Rebel. The mechanism of generating white light is a combination of blue light emitted by a

GaN-based chip and the excited emission from YAG:Ce³⁺ phosphor (Luo et al., 2005, Ye et al., 2010).

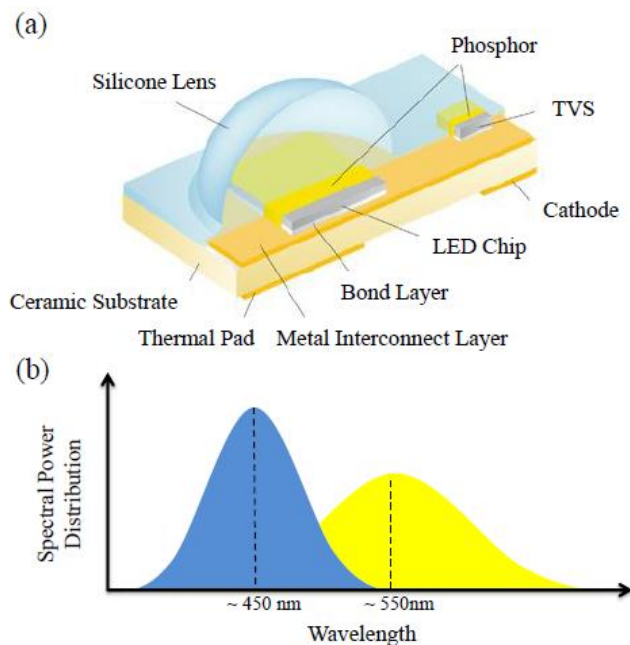


Fig. 6-1 White LUXEON Rebel (a) packaging structure and (b) luminescence mechanism (Luxeon, 2008a)

6.2.2 Test Condition

In this section, the lumen maintenance data of the LUXEON Rebel LEDs were collected from the LM-80 test report [DR03: LM-80 Test Report (Luxeon, 2010)] as shown in Fig. 3-6. This study selected the lowest stress³ aging conditions from the LM-80 test report (a driven current I_F of 350mA and an aging temperature of 55 °C), which was considered as the condition most similar to normal operation. Other high stress aging conditions will be considered in future accelerated testing work.

6.3 Lumen Maintenance Estimation Using Filter Approaches

6.3.1 Lumen Maintenance Projecting Approach

As recommended by IES-TM-21-11 (see Fig. 6-2), the lumen maintenance data collected from the IES-LM-80-08 test report are fitted with a curve and then the curve is extrapolated to the given future time points (i.e., 10,000 hrs, 25,000 hrs, and 35,000 hrs). The operation procedure can be specified as follows:

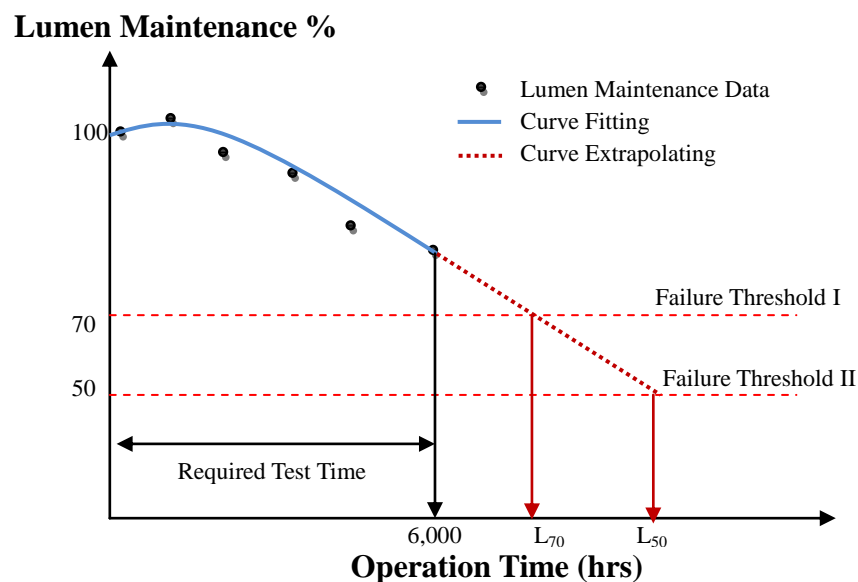


Fig. 6-2 IES-TM-21-11 projecting approach (IES-TM-21-11, 2011)

Step 1: Normalization

Normalize all collected lumen flux data to 1 (with the initial lumen maintenance value defined as 100%) at the time zero test point for each test unit. As mentioned before, lumen maintenance, LM , can be defined as the maintained percentages of

initial light output over time:

$$LM(t) = \frac{\Phi(t)}{\Phi(0)} \times 100\% \quad (6-1)$$

where $\Phi(0)$ is the initial light output and $\Phi(t)$ is the lumen flux at time t .

Step 2: Curve-fitting

Previous work on high power white LEDs indicated that the degradation trajectory of the lumen performance followed an exponential curve (Ishizaki et al., 2007, Narendran et al., 2004). Therefore, this study applied the LED exponential lumen degradation path model (Equation (6-2)) to fit the lumen maintenance data and estimated the parameters of the model using the ordinary least squares(OLS) estimation method (Appendix A).

$$LM(t) = A \cdot \exp(-B \cdot t) \quad (6-2)$$

where the fixed effect parameter, A , is the initial constant, and the random effect parameter, B , is the degradation rate, which varies from unit to unit.

Step 3: Curve-extrapolating

We extrapolated the curves based on the obtained parameters of each test unit to get the future lumen maintenance data and project the lumen maintenance life L_p :

$$L_p = \ln\left(\frac{100 \times A}{p}\right) / B \quad (6-3)$$

where p is the maintained percentage of the initial lumen output (i.e. 50, 70 recommended by ASSIST).

6.3.2 Unscented Kalman Filter

The most well-known filter is the Kalman filter (KF), which is considered to be an effective method of conducting linear state-space estimation with additive Gaussian noise. However, for most nonlinear cases, KF loses its efficacy. Therefore, it is essential to establish a nonlinear filter to solve prognostic problems in nonlinear systems. Up to now, there have been some approximate nonlinear filters, such as the Extended Kalman Filter (EKF), the Particle Filter (PF) (ZIO & Peloni, 2011), and UKF, that have been used to deal with nonlinear problems. Among them, the EKF uses a first order Taylor approximation to linearize both the state and measurement models. The PF approximates the state distribution using a set of discrete, weighted samples, called particles. The UKF approach was first proposed by Julier *et al.* and developed by Wan *et al.* (Julier & Uhlmann, 2004, Julier *et al.*, 1995, Wan & van der Merwe, 2000) to estimate the state of nonlinear systems by using a deterministic sampling approach (sigma point sampling) to capture the mean and covariance estimates with a minimal set of sample points.

Compared to the other two nonlinear state estimation methods, UKF possesses many advantages (Fig. 6-3): first, UKF eliminates the calculation of Jacobian and Hessian matrices in EKF and makes the estimation procedure easier; second, it increases the estimation accuracy by considering at least the second order Taylor

expansion; third, it develops an optimal sampling approach (sigma point sampling), whereas the Monte Carlo random sampling approach used in PF does not.

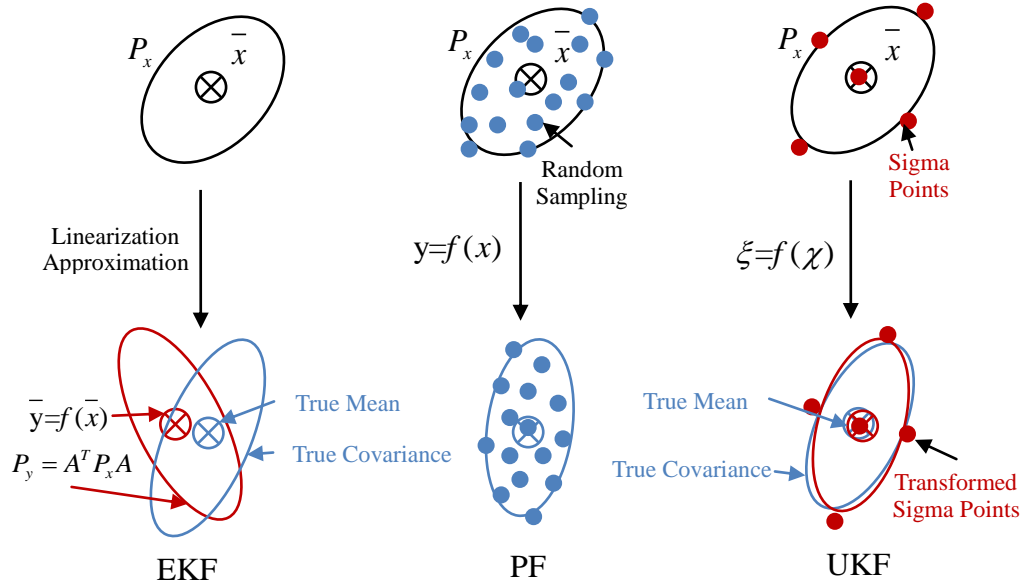


Fig. 6-3 Comparison of filter algorithms (EKF, PF and UKF) for prognostics (Wan & van der Merwe, 2000)

The UKF algorithm involves estimation of the state of a discrete-time nonlinear dynamic system, which can be represented by both a state model and a measurement model:

$$\text{State model} \quad x_k = f_k(x_{k-1}, v_{k-1}) \quad (6-4)$$

$$\text{Measurement model} \quad y_k = h_k(x_k, n_k) \quad (6-5)$$

where x_k represents the unobserved state of the system, y_k is the observed measurements, v_{k-1} and n_k are the state noise and observation noise, respectively, and $v_{k-1} \sim N(0, Q_{k-1})$ and $n_k \sim N(0, R_k)$ are assumed to be the mean zero white Gaussian

noises.

This study uses two types of UKF to predict the long-term lumen maintenance of HPWLEDs, (1) augmented UKF; and (2) non-augmented UKF. The algorithm implementations of these two UKFs can be expressed as follows:

6.3.2.1 Augmented UKF

Step 1: Initialization

The initial state is described by its mean and covariance:

$$\bar{x}_0 = \mathbf{E}[x_0] \quad (6-6)$$

$$\mathbf{P}_0 = \mathbf{E}[(x_0 - \bar{x}_0) \cdot (x_0 - \bar{x}_0)^T] \quad (6-7)$$

Supposing that both noises are non-additive, the initial state vector and covariance matrix can be expressed as an augment vector:

$$\bar{x}_0^a = \mathbf{E}[x_0^a] = [\bar{x}_0 \quad 0 \quad 0]^T \quad (6-8)$$

$$\mathbf{P}_0^a = \begin{bmatrix} \mathbf{P}_0 & 0 & 0 \\ 0 & \mathbf{Q}_0 & 0 \\ 0 & 0 & \mathbf{R}_0 \end{bmatrix} \quad (6-9)$$

Step 2: Sigma point sampling

To undergo a nonlinear transformation, we develop a matrix χ_k^a with $2n_a+1$ sigma points

$$\chi_{k-1}^a = [\bar{x}_{k-1}^a \quad \bar{x}_{k-1}^a + \sqrt{n_a + \lambda} \cdot \sqrt{p_{k-1}^a} \quad \bar{x}_{k-1}^a - \sqrt{n_a + \lambda} \cdot \sqrt{p_{k-1}^a}] \quad (6-10)$$

$$n_a = n_x + n_v + n_n \quad (6-11)$$

$$\lambda = \alpha^2 (n_a + \kappa) - n_a \quad (6-12)$$

Then the sigma points are weighted by:

$$W_0^{(m)} = \frac{\lambda}{n_a + \lambda} \quad (6-13)$$

$$W_0^{(c)} = \frac{\lambda}{n_a + \lambda} + (1 - \alpha^2 + \beta) \quad (6-14)$$

$$W_i^{(m)} = W_i^{(c)} = \frac{1}{2(n_a + \lambda)} \quad i=1, 2, \dots, 2n_a \quad (6-15)$$

where λ is the composite scaling parameter, which can be calculated from Equation (6-12). The constant α determines the spread of sigma points around the mean ($1 \geq \alpha \geq 10^{-4}$); κ is a secondary scaling parameter which is usually set to $3 - n_a$; and β is used to incorporate prior knowledge of the distribution of the state vector x (for Gaussian distribution, $\beta = 2$). Here, we set $\alpha=0.01$, $\kappa=3-n_a$, and $\beta=0$.

Step 3: Time update

The transient state $\bar{x}_{k/k-1}$ and measurement $\bar{y}_{k/k-1}$ are estimated as:

$$\chi_{k/k-1}^x = f(\chi_{k-1}^x, \chi_{k-1}^v) \quad (6-16)$$

$$\bar{x}_{k/k-1} = \sum_{i=0}^{2n_a} W_i^{(m)} \chi_{i,k/k-1}^x \quad (6-17)$$

$$P_{k/k-1} = \sum_{i=0}^{2n_a} W_i^{(c)} [(\chi_{i,k/k-1}^x - \bar{x}_{k/k-1}) \cdot (\chi_{i,k/k-1}^x - \bar{x}_{k/k-1})^T] \quad (6-18)$$

$$y_{k/k-1} = h(\chi_{k/k-1}^x, \chi_{k-1}^n) \quad (6-19)$$

$$\bar{y}_{k/k-1} = \sum_{i=0}^{2n_a} W_i^{(m)} y_{i,k/k-1} \quad (6-20)$$

Step 4: Measurement update

The cross-covariance of the state and measurement $\mathbf{P}_{k/k-1}^{xy}$ and the Kalman gain

K_k and compute the predicted mean \bar{x}_k and covariance \mathbf{P}_k are calculated as.

$$\mathbf{P}_{k/k-1}^{yy} = \sum_{i=0}^{2n_a} W_i^{(c)} [(y_{i,k/k-1} - \bar{y}_{k/k-1}) \cdot (y_{i,k/k-1} - \bar{y}_{k/k-1})^T] \quad (6-21)$$

$$\mathbf{P}_{k/k-1}^{xy} = \sum_{i=0}^{2n_a} W_i^{(c)} [(x_{i,k/k-1}^x - \bar{x}_{k/k-1}) \cdot (y_{i,k/k-1} - \bar{y}_{k/k-1})^T] \quad (6-22)$$

$$K_k = \mathbf{P}_{k/k-1}^{xy} (\mathbf{P}_{k/k-1}^{yy})^{-1} \quad (6-23)$$

$$\bar{x}_k = \bar{x}_{k/k+1} + K_k (y_k - \bar{y}_{k/k-1}) \quad (6-24)$$

$$\mathbf{P}_k = \mathbf{P}_{k/k+1} - K_k \mathbf{P}_{k/k-1}^{yy} K_k^T \quad (6-25)$$

Step 5: Recursive filtering

By inputting the new measurements (Fig. 6-4), steps 1–4 are repeated in the next time step using the updated covariance \mathbf{P}_k and Kalman gain K_k .

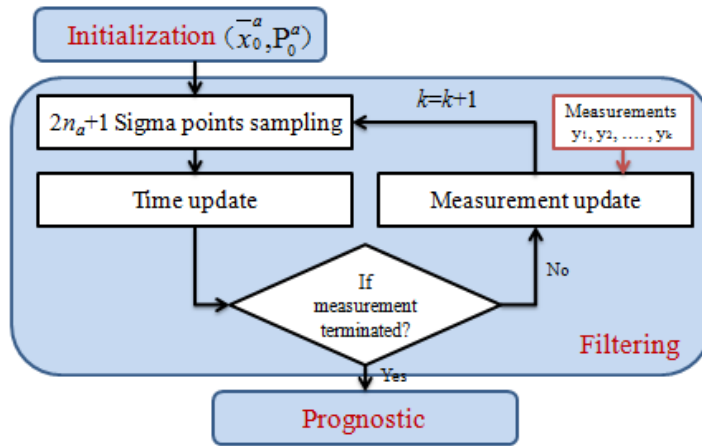


Fig. 6-4 Flowchart of prognostics using the augmented UKF

Step 6: Prognosis

Then, when the measurement update is terminated, the future $k+1 \dots n$ step states

are predicted within the k -step measures and the time updates from $k+1$ to the desired step (Fig. 6-4).

6.3.2.2 Non-augmented UKF

Usually, the computational complexity of the augmented UKF algorithm can be reduced by using the non-augmented form, which can reduce the number of the sigma points as well as the total number of sigma points used ($n_{\text{sigma points}} = n_x$). Meanwhile, the covariances of the noise are incorporated into the state covariance using a simple additive form (Wu et al., 2005).

Step 1: Initialization

The initial state is described by its mean \bar{x}_0 and the covariance p_0 as defined by Equation (6-6) and Equation (6-7) shown in the augmented UKF algorithm.

Step 2: Sigma point sampling

A matrix χ_k with $2n_x+1$ sigma points is generated:

$$\chi_{k-1} = [\bar{x}_{k-1} \quad \bar{x}_{k-1} + \sqrt{n_x + \lambda^*} \cdot \sqrt{p_{k-1}} \quad \bar{x}_{k-1} - \sqrt{n_x + \lambda^*} \cdot \sqrt{p_{k-1}}] \quad (6-26)$$

where n_x is the number of the state. The composite scaling parameter can be expressed as:

$$\lambda^* = \alpha^2 (n_x + k) - n_x \quad (6-27)$$

Then the sigma points are weighted by:

$$W_0^{(m)*} = \frac{\lambda^*}{n_x + \lambda^*} \quad (6-28)$$

$$W_0^{(c)*} = \frac{\lambda^*}{n_x + \lambda^*} + (1 - \alpha^2 + \beta) \quad (6-29)$$

$$W_i^{(m)*} = W_i^{(c)*} = \frac{1}{2(n_x + \lambda^*)} \quad i=1, 2, \dots, 2n_x \quad (6-30)$$

Step 3: Time update

The transient state $\bar{x}_{k/k-1}$ and measurement $\bar{y}_{k/k-1}$ are estimated as:

$$\chi_{k/k-1}^* = f(\chi_{k-1}) \quad (6-31)$$

$$\bar{x}_{k/k-1} = \sum_{i=0}^{2n_x} W_i^{(m)*} \chi_{i,k/k-1}^* \quad (6-32)$$

$$P_{k/k-1} = \sum_{i=0}^{2n_x} W_i^{(c)*} [(\chi_{i,k/k-1}^* - \bar{x}_{k/k-1}) \cdot (\chi_{i,k/k-1}^* - \bar{x}_{k/k-1})^T] + Q_0 \quad (6-33)$$

Step 4: Sigma point re-sampling

A new set of sigma points is redrawn to incorporate the effect of the additive process noise.

$$\chi_{k/k-1} = [\bar{x}_{k-1} \quad \bar{x}_{k-1} + \sqrt{n_x + \lambda^*} \cdot \sqrt{p_{k-1}} \quad \bar{x}_{k-1} - \sqrt{n_x + \lambda^*} \cdot \sqrt{p_{k-1}}] \quad (6-34)$$

$$\xi_{k/k-1} = h(\chi_{k/k-1}) \quad (6-35)$$

$$\bar{y}_{k/k-1} = \sum_{i=0}^{2n_x} W_i^{(m)*} \xi_{i,k/k-1} \quad (6-36)$$

Step 5: Measurement update

The covariance of measurement $P_{k/k-1}^{yy}$ and the cross-covariance of the state and measurement $P_{k/k-1}^{xy}$ is calculated as:

$$P_{k/k-1}^{yy} = \sum_{i=0}^{2n_x} W_i^{(c)*} [(\xi_{i,k/k-1} - \bar{y}_{k/k-1}) \cdot (\xi_{i,k/k-1} - \bar{y}_{k/k-1})^T] + R_0 \quad (6-37)$$

$$P_{k/k-1}^{xy} = \sum_{i=0}^{2n_x} W_i^{(c)*} [(\chi_{i,k/k-1} - \bar{x}_{k/k-1}) \cdot (\xi_{i,k/k-1} - \bar{y}_{k/k-1})^T] \quad (6-38)$$

The Kalman gain K_k can be computed by inserting the calculated $P_{k/k-1}^{yy}$ and $P_{k/k-1}^{xy}$ into Equation (6-23). The predicted mean \bar{x}_k and covariance P_k can be obtained based on Equation (6-24) and Equation (6-25), respectively.

Step 5: Recursive filtering

Like augmented UKF (see Fig. 6-5), by inputting the new measurements, the steps 1–4 are repeated for the next time step using the updated covariance P_k and the Kalman gain K_k .

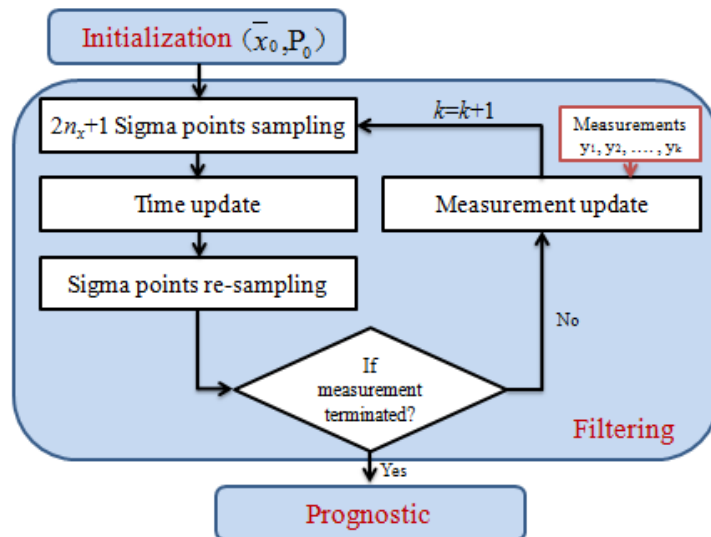


Fig. 6-5 Flowchart of prognostic using the non-augmented UKF

Step 6: Prognosis

Then, when the measurement update is terminated, the future $k+1 \dots n$ step states are predicted with the k -step measures and the time updates from $k+1$ to the desired step.

6.3.3 Results and Discussion

To evaluate our proposed approach, we developed a procedure to compare the prognostic results. The procedure includes four steps: (1) data pretreatment; (2) state initialization; (3) filtering; and (4) prognostics (Fig. 6-6).

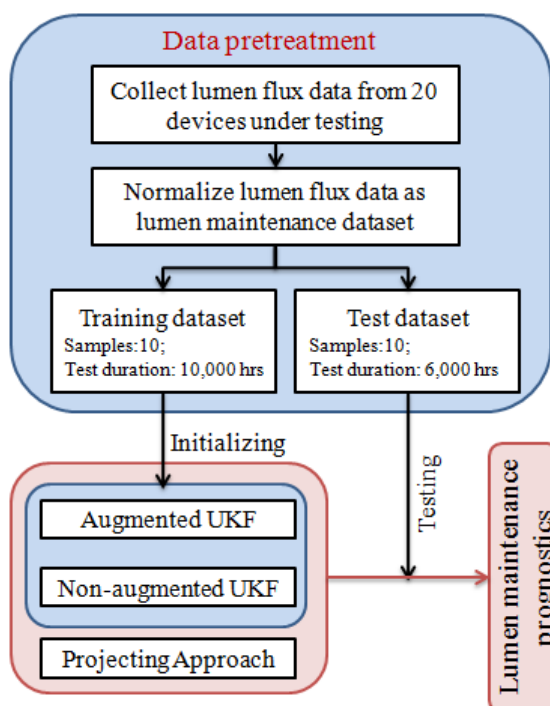


Fig. 6-6 Lumen maintenance prognostic procedure

6.3.3.1 Data pretreatment

Firstly, we pretreated the raw data collected from the LM-80 test report [DR03: LM-80 Test Report (Luxeon, 2010)] in section 3.2.1, and used the lumen flux data sets of the twenty DUTs collected periodically within 10,000 hrs (1,000 hrs per cycle). After collection, the lumen flux data at each cycle were normalized to 1 at the

24 hrs test point for each DUT (as shown in the LM-80 test report, to reduce initial testing errors, this study used the data collected after 24 hrs initial running as the first test point). Then the time series lumen flux data can be transferred to the time series lumen maintenance for each DUT.

Next, all twenty DUTs were separated into two groups: the training samples (ten units) and the test samples (ten units). The calculated lumen maintenance data of the training samples from initial to 10, 000 hrs were used as the baseline database to train the lumen degradation model, as mentioned in Equation (6-2), and initialize the model's parameters. The prognostic performances of proposed models were then compared and evaluated based on the data from the test samples.

As shown in the UKF algorithms (Equations (6-4) and (6-5)), the measurement model in our case was expressed as the lumen maintenance degradation model (Equation (6-2)). The parameters of the degradation model (the fixed effect parameter, A , and the random effect parameter, B) were seen as the states.

$$\text{State model:} \quad x_k = [A_k, B_k] \quad (6-39)$$

$$A_k = A_{k-1} + v_{k-1}^A \quad v_{k-1}^A \sim N(0, Q_v^A);$$

$$B_k = B_{k-1} + v_{k-1}^B \quad v_{k-1}^B \sim N(0, Q_v^B);$$

$$\text{Measurement model:} \quad y_k = A_k \cdot \exp(-B_k \cdot 1000 \cdot k) + n_k \quad (6-40)$$

where k is the measurement cycle (from 0 to 10,000 hrs).

6.3.3.2 State initialization

To begin with, the UKF approach needs to initialize the state model with the training dataset. The initial state can be expressed by the parameters of the lumen degradation model of each training sample. As shown in Fig. 6-7, these parameters were estimated by the least square curve-fitting approach.

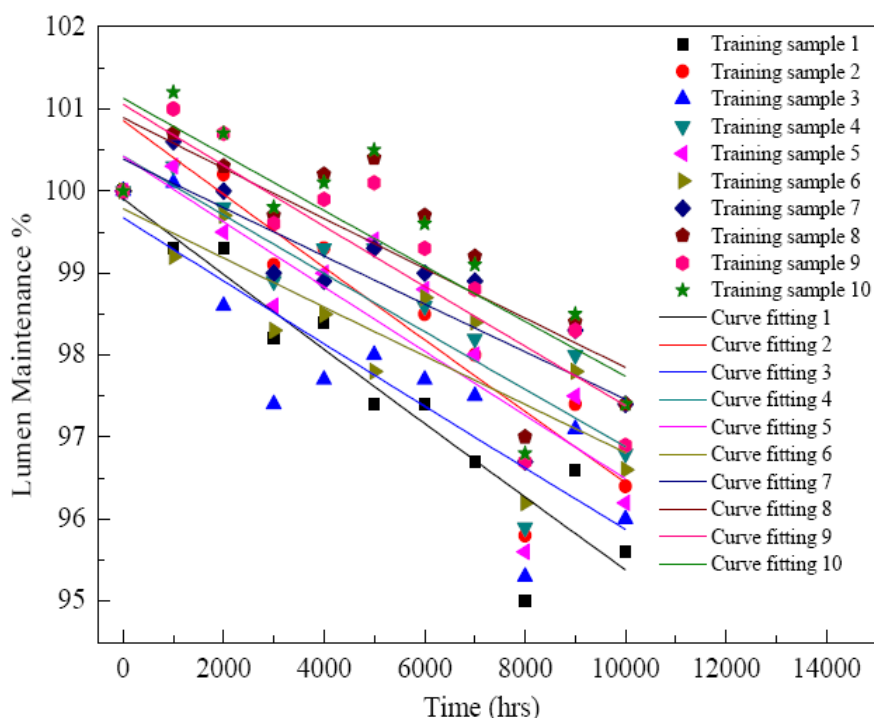


Fig. 6-7 Nonlinear curve-fitting of lumen maintenance data from training samples

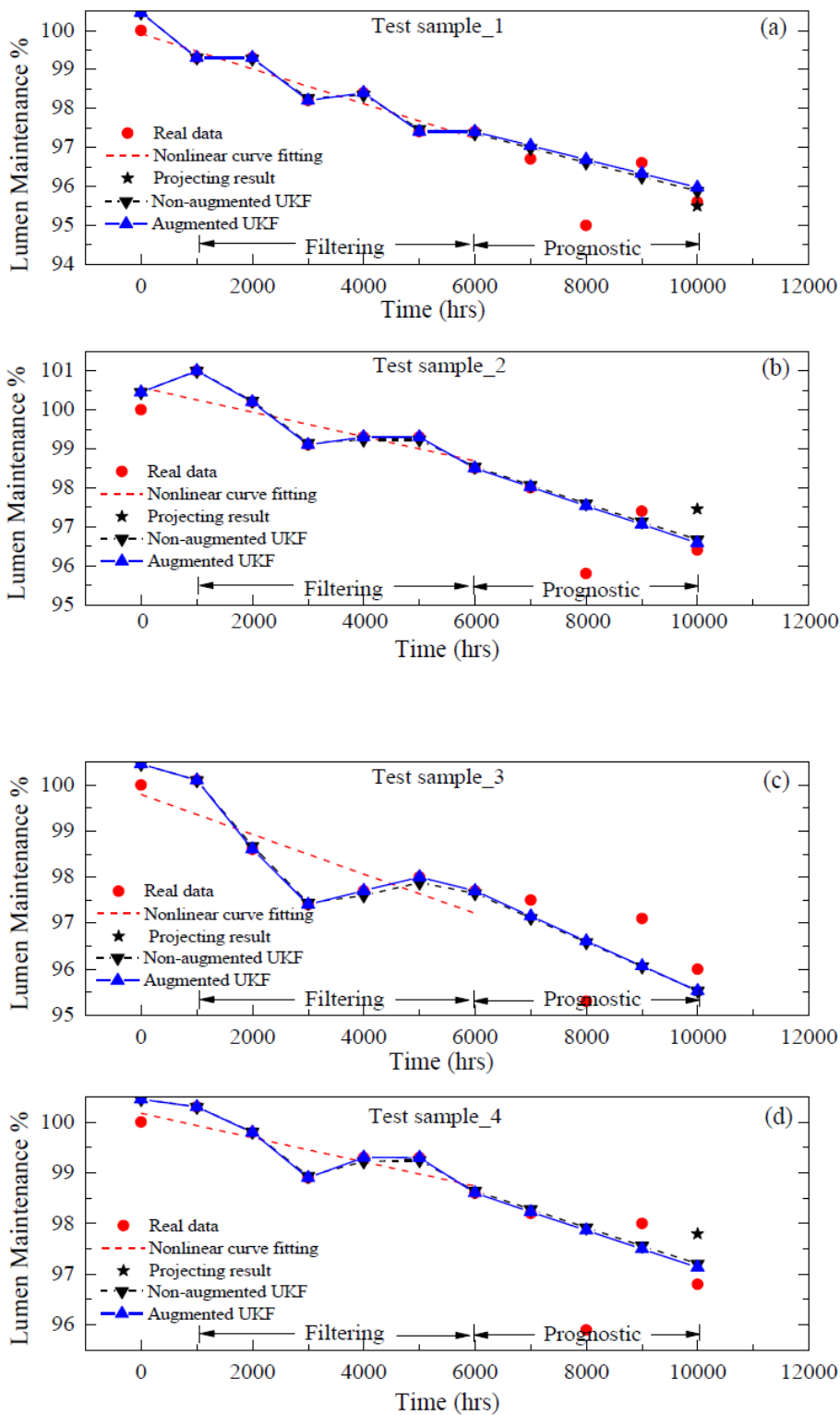
Then, the calculated parameters were averaged as the initial states of the test samples, and can be described by the means and covariances ($A_0=100.453$, $P_{A_0}=0.2821$; $B_0=3.67E-06$, $P_{B_0}=3.428E-13$) (Table 6-1).

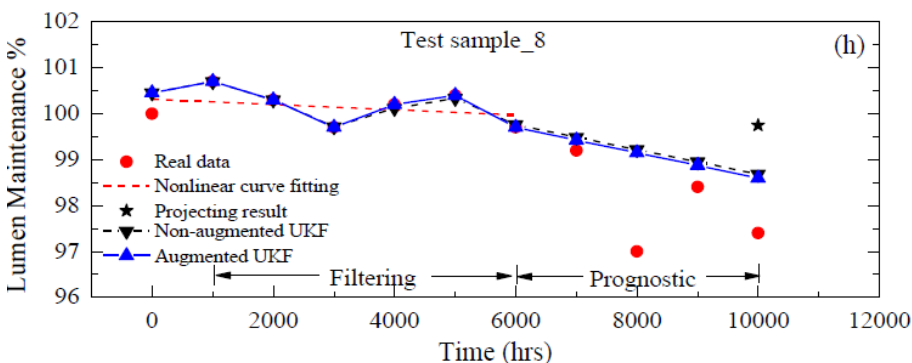
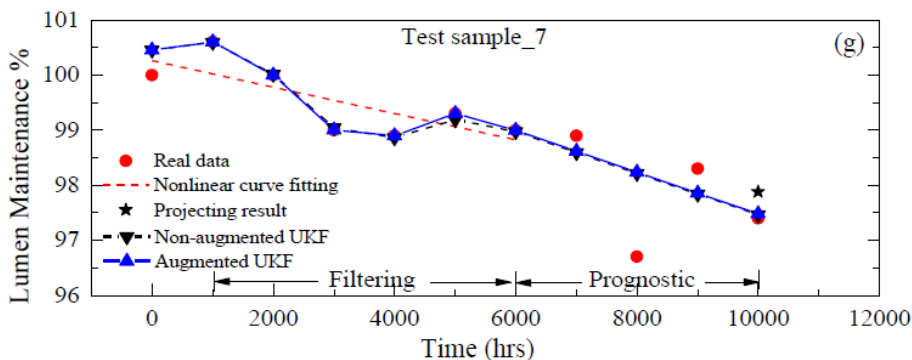
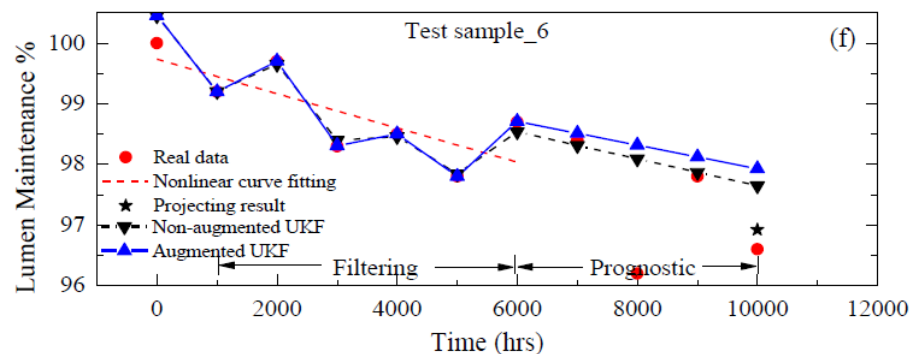
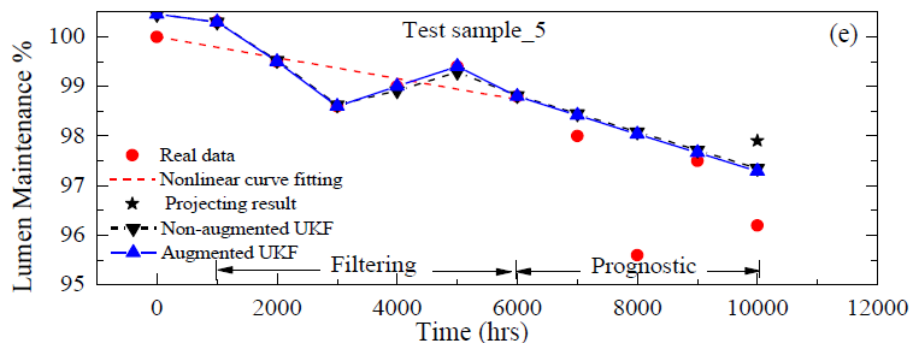
Table 6-1 Parameters of the measurement model obtained from training samples

<i>No.</i>	<i>A</i>	<i>A_errors</i>	<i>B</i>	<i>B_errors</i>	<i>Adjusted R-Square</i>	<i>RMSE</i>
1	99.904	0.312	4.63E-06	5.36E-07	0.881	0.005485
2	100.857	0.405	4.47E-06	6.87E-07	0.806	0.007106
3	99.674	0.433	3.89E-06	7.42E-07	0.725	0.007606
4	100.426	0.405	3.59E-06	6.89E-07	0.724	0.007129
5	100.422	0.447	3.99E-06	7.61E-07	0.727	0.007855
6	99.784	0.376	3.02E-06	6.42E-07	0.679	0.006622
7	100.388	0.355	2.96E-06	6.02E-07	0.698	0.006249
8	100.893	0.433	3.06E-06	7.32E-07	0.624	0.007629
9	101.055	0.434	3.70E-06	7.34E-07	0.710	0.007632
10	101.131	0.470	3.41E-06	7.94E-07	0.636	0.008277
Average	100.453	0.4070	3.67E-06	6.92E-07	0.721	0.007159
Covariance	0.2821	0.0023	3.428E-13	6.208E-15	0.0057	7.001E-07

6.3.3.3 Filtering

The next step in the UKF approach is the recursive filtering from 1,000 to 6,000 hrs, which was conducted to help updating the states with inputting new measurements. Fig. 6-8 shows the UKF prognostics for the ten test samples, which contains two steps: filtering (from 1,000 to 6,000 hrs) and prognosis (from 6,000 to 10,000 hrs).





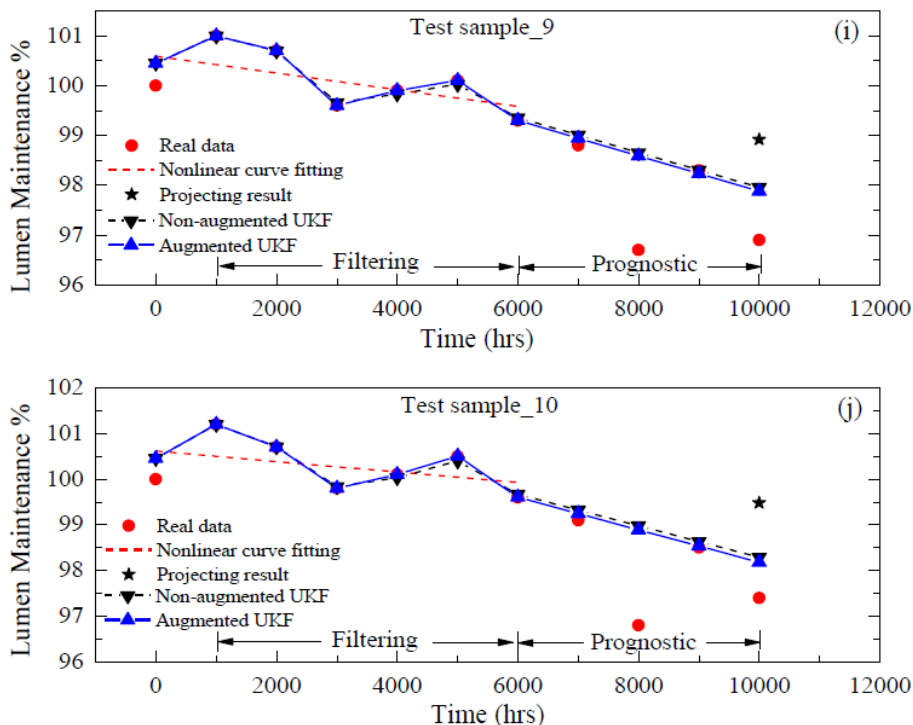


Fig. 6-8 Lumen maintenance prognostics with UKF approaches for test samples (Test sample_1 to Test sample_10 as shown from (a) to (j))

The filtering performances of the two proposed UKF approaches were compared using the mean square error (MSE), which is defined as:

$$MSE = \frac{1}{k} \sum_{i=1}^k (y_i - \bar{y}_i)^2 \quad (6-41)$$

where k is the measurement cycle ($= 6$ for the filtering step); and y_i and \bar{y}_i are the real measurements and the estimated values at each measurement cycle, respectively.

The calculated MSE values of the two UKF approaches of each test sample are shown in Fig. 6-9. The MSE values of the non-augmented UKF is nearly 400~1,500 times larger than that of the augmented UKF, which indicates that the augmented UKF has a better estimation performance than the non-augmented UKF. As discussed in

section 6.3.2, in order to maintain the accuracy of the state estimation, both UKF approaches consider the effect of process noise into the state model. However, the difference between these two approaches is that the augmented UKF supposes that the noises are non-additive and can be inserted into the sigma sampling step in recursion, while the non-augmented UKF just uses the re-sampling method with additive noises. The superiority of the augmented UKF approach can be attributed to its capacity in capturing and propagating the odd-order moment information through one filtering recursion. Mathematically, the augmented UKF approach can capture more statistical information by introducing the effect of process and measurement noises into both the state and measurement updating non-additively, which will reduce errors between the estimations and the actual measurements.

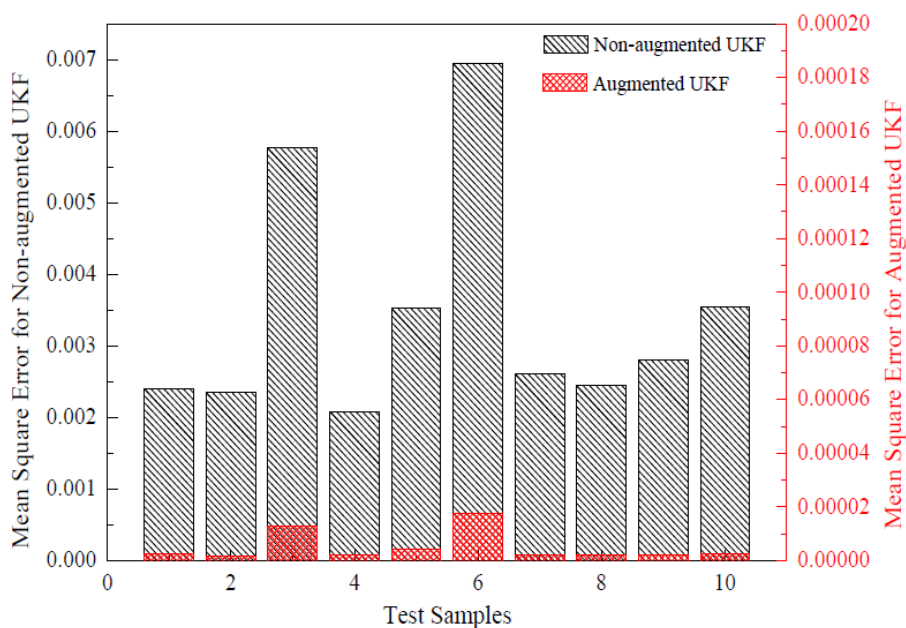


Fig. 6-9 Mean square errors of UKF filtering step

6.3.3.4 Prognostics

After the recursive filtering steps in both UKF approaches, the lumen maintenance of each test sample at 10,000 hrs was predicted, as shown in Fig. 6-9. At the same time, following the projection procedure shown in section 6.3.1, the lumen maintenance of test samples at 10,000 hrs were also extrapolated by the IES-TM-21-11 projection approach (marked by black stars in Fig. 6-9).

To evaluate the prognostic performance of the above mentioned approaches, both accuracy-based and precision-based metrics were used (Saxena et al., 2008). The accuracy-based metric is defined as the deviation between the prognostics results and the actual measurements, which can be expressed as the prognostics errors (Pe):

$$Pe_k = \frac{\bar{y}_k - y_k}{y_k} \times 100\% \quad (6-42)$$

where \bar{y}_k and y_k are the prognostics results and actual measurements of the lumen maintenance at the k^{th} cycle, respectively. The measurement cycle k is 10 for the prognostics step in this study.

Fig. 6-10 shows the lumen maintenance prognostics errors of the test samples. For the majority of the test samples (samples 2, 4, 5, 7, 8, 9, and 10), compared to the IES-TM-21-11 projecting approach, both UKF approaches had lower prognostics errors and increased prognostic accuracy. However, the UKF approach lost its superiority in samples 1, 3, and 6. In fact, the accuracy of the UKF-based prognostics

is determined by the last estimated state after recursive filtering (the state at 6,000 hrs for this chapter). The projecting results from using the IES-TM-21-11 approach, however, are affected by the least squares estimation, which depends on the minimization of the sum of the residuals between the actual measurements and the calculated values. The differences between the least squares method and the UKF approach are discussed by Sorenson (1970). Firstly, the UKF deals with dynamic stochastic systems, while the least squares method is used for deterministic systems. Secondly, the UKF updates system states recursively by absorbing new measurements, while the least squares implementation uses batch processing.

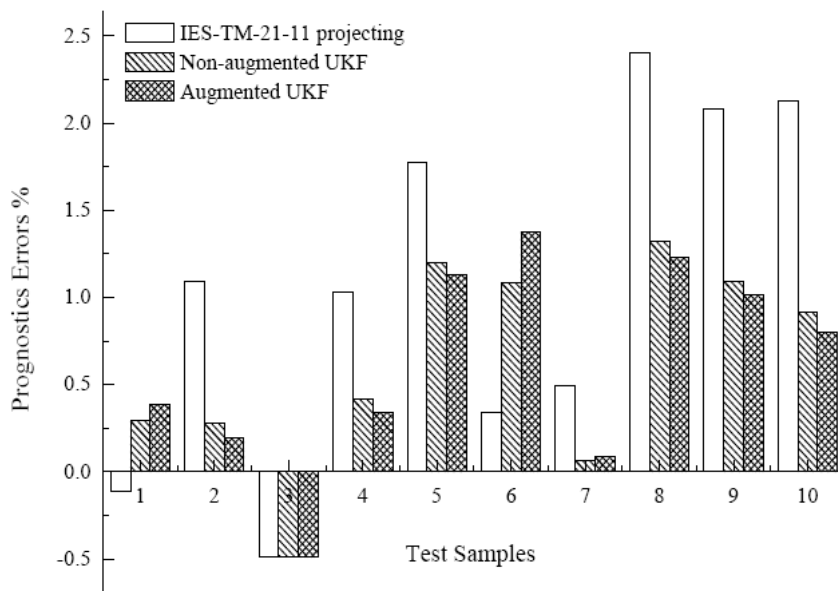


Fig. 6-10 Lumen maintenance prognostics errors at 10,000hrs

Besides accuracy-based metrics, we also chose a precision-based metric, which is

considered to be an evaluator of the stability of a prognostic model. The precision-based metric is derived from the mean ($E(Pe)$) and variance ($Var(Pe)$) of prognostic errors within a set of test samples.

$$E(Pe) = \frac{1}{N} \sum_{i=1}^N Pe_{10}^i \quad (6-43)$$

$$Var(Pe) = \frac{1}{N} \sum_{i=1}^N [Pe_{10}^i - E(Pe)]^2 \quad (6-44)$$

Table 6-2 lists the means and variances of prognostic errors from the above mentioned approaches, which indicates that the two proposed UKF approaches can lower both the mean and variance of the prognostic errors. This means that compared to the IES-TM-21-11 projecting approach, UKF is a more precise method for nonlinear prediction.

Table 6-2 Performances of prognostic approaches

Approaches	Prognostic errors mean $E(Pe)$	Prognostic errors variance $Var(Pe)$
IES-TM-21-11 projecting	1.07%	1.015E-4
Non-augmented UKF	0.62%	3.505E-5
Augmented UKF	0.61%	3.585E-5

6.4 Chromaticity State Estimation Using Filter Approaches

From the previous studies described in chapters three and four, it has been found that both lumen depreciation and chromatic state shift are considered to be the two dominating failures in white LEDs. Most attention has been paid to the lumen

depreciation of LED products (Tsaing & Peng, 2007, Liao & Elsayed, 2006), ignoring chromaticity state shift. In the LED industry, the Illuminating Engineering Society of North America (IESNA) (IES-LM-79-08 and IES-LM-80-08) has recommended test methods for measuring the chromaticity characteristics of LEDs. Additionally, the Next Generation Lighting Industry Alliance (NGLIA) with the U.S. Department of Energy (DoE), has recommended using chromaticity shift as an indicator of a white LED's "end of life". The American National Standard Lighting (ANSI) group has also developed specifications for the chromaticity of solid state lighting products, but they have not demonstrated a chromaticity state shift prediction method for white LED lighting.

6.4.1 Chromaticity State shift of High Power White LEDs

According to the approved electrical and photometric measurement method developed by IESNA (IES-LM-79-08), the chromaticity characteristics of white LEDs include the chromaticity coordinates, correlated color temperature, and color rendering index (CRI). Among them, the chromaticity coordinates are always chosen as the direct performance parameters to track the shift path.

The International Commission for Illumination (*Commission Internationale del' Eclairage*, CIE) has developed three types of chromaticity diagrams: CIE 1931 (x,y),

CIE 1960 uniform chromaticity scale (UCS) (u, v) , and CIE 1976 UCS (u', v') (Fig. 6-11). Among them, only the color difference in the CIE 1976 color space is proportional to the geometric difference, so the chromaticity coordinates in the CIE 1976 color space are widely used as a chromaticity performance characteristic by many LED manufacturers.

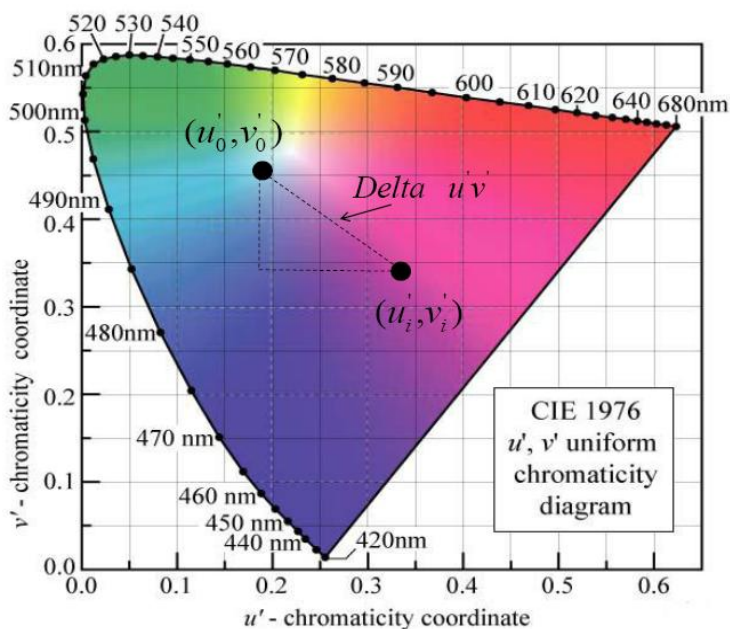


Fig. 6-11 CIE 1976 (u', v') uniform chromaticity diagram (REA, M. S. et al, 2000)

In this section, the collected chromaticity coordinates in the CIE 1976 color space from the LM-80 test report were selected to represent the chromaticity state of the white LUXEON Rebel LED. The Euclidean distance between the original chromaticity coordinates (u'_0, v'_0) and future coordinates (u'_i, v'_i) was used to

represent the chromaticity state shift of the LED after aging, and is denoted by $\Delta u'v'$ (Fig. 6-11).

$$\Delta u'v' = \sqrt{(u_i' - u_0')^2 + (v_i' - v_0')^2} \quad (6-45)$$

6.4.2 Results and Discussion

This section selected chromaticity coordinates data at the lowest stress aging conditions (a driven current I_F of 350mA and an aging temperature of 55 °C) from the LM-80 test report [DR04: LM-80 Test Report (Luxeon, 2011)] as shown in section 3.2.1. To begin with, this section developed a model for the chromaticity state shift of our test device. We chose three models (exponential, dual-exponential, and quadratic polynomial) to fit the chromaticity state shift data, $\Delta u'v'$, with the nonlinear least square techniques in the Matlab curve fitting toolbox. Ten samples were selected from a total of twenty-five samples to train the selected model and initialize the parameters of the model. The remaining fifteen samples were used to test the proposed prognostics model.

The averaged chromaticity state shift data of ten training samples at each test cycle were fitted by the three proposed models. The fitting results are shown in Fig. 6-12 and Table 6-3. The results indicate that the dual-exponential model was the best model to describe the process of chromaticity state shift because its averaged

R-square is nearest to 1 and it also has the smallest averaged RMSE.

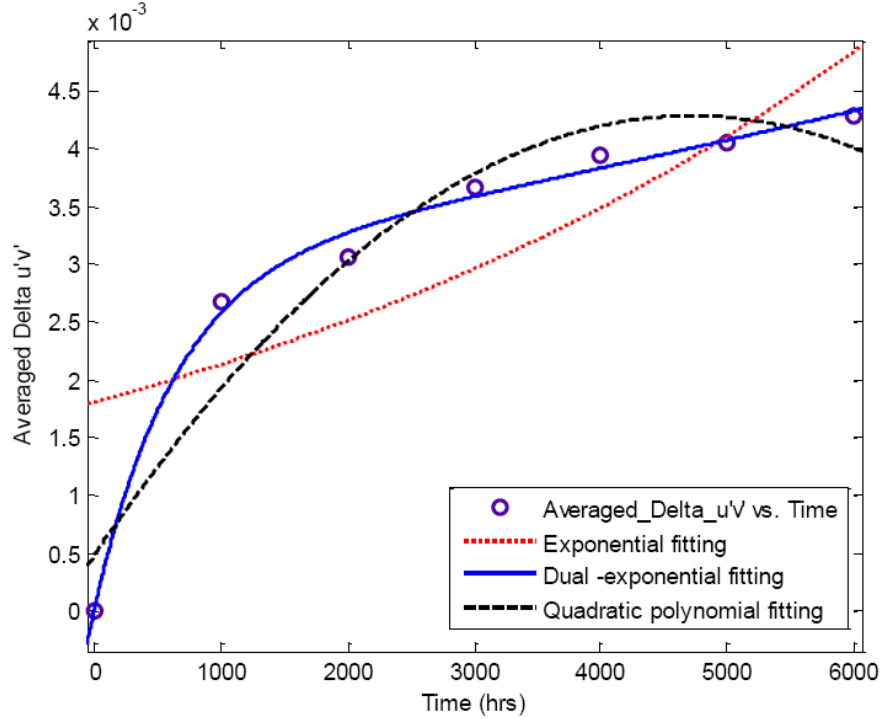


Fig. 6-12 Model selection for chromaticity state shift process

Table 6-3 Chromaticity state shift process model selection results

Models	Functions	Averaged R-square	Averaged RMSE
Exponential	$y=a \exp(b x)$	0.62403	0.0009927
Dual-exponential	$y= a \exp(b x)+ c \exp(d x)$	0.99337	0.0001681
Quadratic Polynomial	$y= a x^2+b x+c$	0.92191	0.000505

The state and measurement models in the UKF approach can be written as follows:

$$\text{State model: } x_k = [a_k; b_k; c_k; d_k] \tag{6-46}$$

$$a_k = a_{k-1} + v_{k-1}^a \quad v_{k-1}^a \sim N(0, Q_v^a); \quad b_k = b_{k-1} + v_{k-1}^b \quad v_{k-1}^b \sim N(0, Q_v^b);$$

$$c_k = c_{k-1} + v_{k-1}^c \quad v_{k-1}^c \sim N(0, Q_v^c); \quad d_k = d_{k-1} + v_{k-1}^d \quad v_{k-1}^d \sim N(0, Q_v^d).$$

$$\text{Measurement model: } y_k = a_k \cdot \exp(b_k \cdot 1000 \cdot k) + c_k \cdot \exp(d_k \cdot 1000 \cdot k) + n_k$$

$$n_k \sim N(0, R_k) \quad (6-47)$$

where $k=1, 2 \dots 7$ (from 0 to 6,000 hrs).

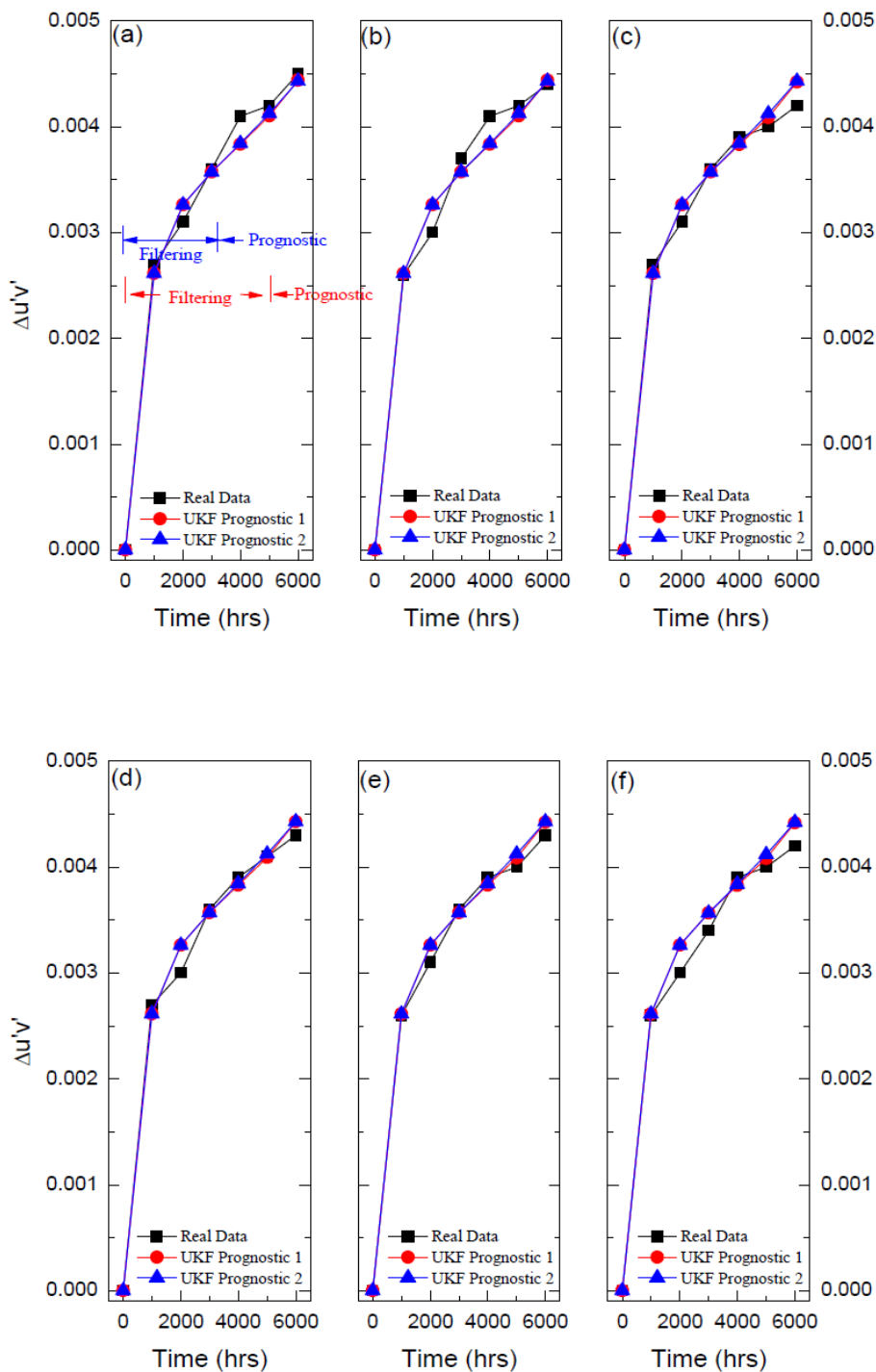
The parameters of the dual-exponential model of each training sample were estimated by the nonlinear least square method and averaged as the initial states of the test samples ($a_0=0.0029479$; $b_0=0.000065625$; $c_0=-0.002933$; $d_0=-0.0017$) (Table 6-4). Next, the test data from two filtering periods (Period I: 0–5,000 hrs and Period II: 0–3,000 hrs) were selected to update the states recursively, and then the chromaticity state shift at 6,000 hrs was predicted based on these two filtering periods.

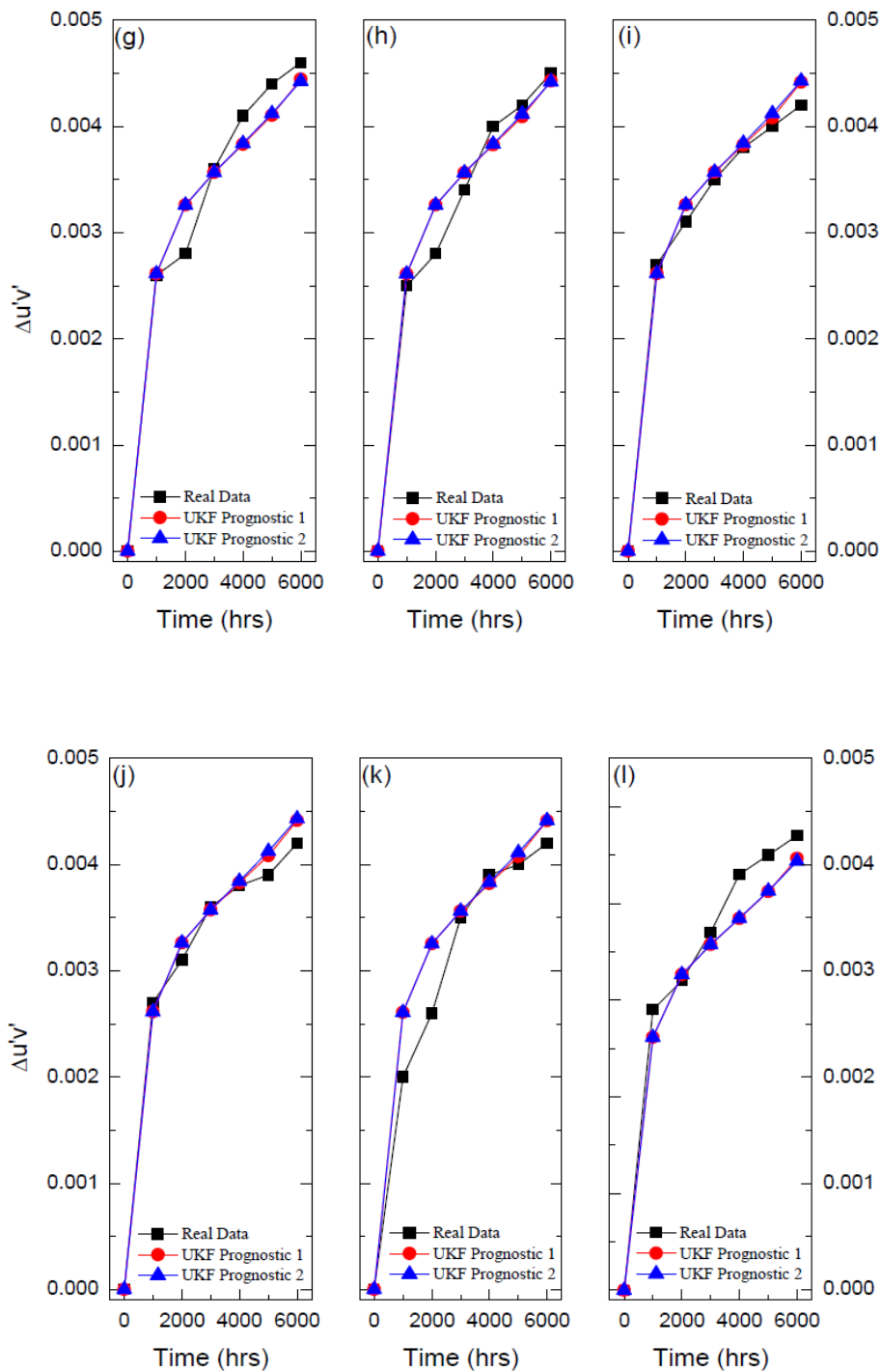
Table 6-4 Parameters of measurement model obtained from training samples

No.	<i>a</i>	<i>b</i>	<i>c</i>	<i>d</i>
1	0.003014	5.13E-05	-0.00301	-0.001766
2	0.00311	5.28E-05	-0.003078	-0.001414
3	0.002852	7.42E-05	-0.002844	-0.001649
4	0.002726	8.58E-05	-0.002722	-0.002156
5	0.00275	8.00E-05	-0.002746	-0.00214
6	0.002837	7.33E-05	-0.002833	-0.001931
7	0.00289	7.32E-05	-0.002883	-0.001773
8	0.00313	5.21E-05	-0.003099	-0.001427
9	0.00306	6.09E-05	-0.003034	-0.001331
10	0.00311	5.28E-05	-0.003078	-0.001414
Mean	0.0029479	0.000065625	-0.002933	-0.0017
STD	0.000154884	1.31008E-05	0.0001436	0.0003058
Variance	2.3989E-08	1.71632E-10	2.063E-08	9.35E-08

The Prognostic results of chromaticity state shift for the fifteen test samples

with UKF approach are shown in Fig. 6-13 (a) to Fig. 6-13 (o).





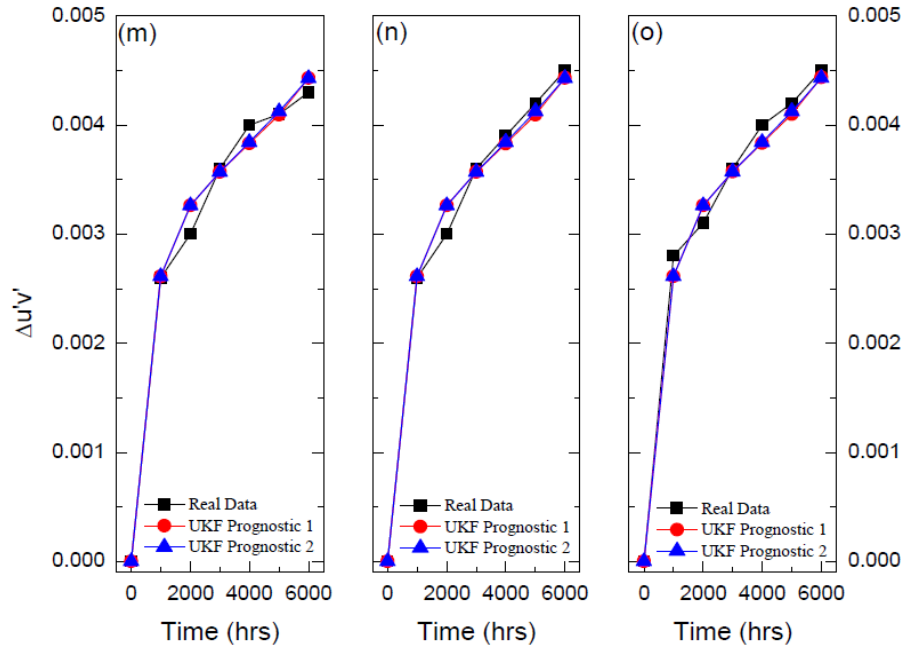


Fig. 6-13 Prognostic results of chromaticity state shift with UKF approach (from (a) to (o))

Fig. 6-14 indicates that the predicted results based on the period I data (UKF Prognostic 1) were slightly better than the results from the period II data (UKF Prognostic 2), because it utilized more observed measurements to update the state model. The prognostic RMSE from the two periods of data were 3.70% and 3.90%, respectively, and both predicted results were close to the actual state.

$$RMSE = \sqrt{\frac{1}{15} \sum_{i=1}^{15} (\bar{y}_i - y_i)^2} \quad (6-48)$$

where y_i is the i^{th} real $\Delta u'v'$ and \bar{y}_i is the predicted $\Delta u'v'$ at 6,000h.

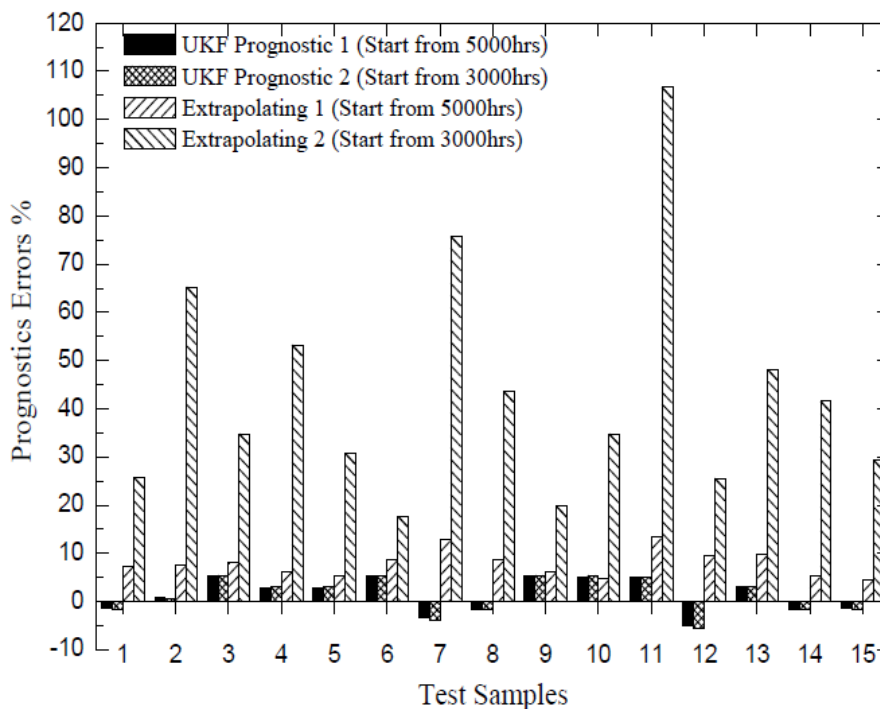


Fig. 6-14 Prognostics errors of chromaticity state shift at 6,000 hrs

This section also compared the prognostic performances between the UKF approach and an extrapolating approach. The extrapolating approach is widely used to project long term lumen maintenance of LED lighting sources. It relies on the nonlinear least squares method to fit the obtained data and extrapolates the fitting curve to get the future state. Although both are nonlinear estimation approaches, there are some differences between the least squares method and the UKF approach: Firstly, the UKF deals with dynamic stochastic systems while the least squares approach is used for deterministic systems; Secondly, the UKF approach updates the system states recursively by absorbing new measurements while the least squares implementation uses batch processing.

In this section, the two periods of data mentioned were also extrapolated to get the chromaticity state of samples at 6,000hrs, and are denoted as Extrapolating 1 (for Period I) and the Extrapolating 2 (for Period II) respectively. The predicted results are listed in Table 6-5, which shows that compared to the extrapolating approach, the UKF approach with lower prognostics errors (less than 4%) increased the prognostic accuracy more, even within a shorter data-collection time period.

Table 6-5 RMSE results for prognostic of chromaticity state shift

State Prognostic Method	RMSE
UKF Prognostic 1	3.70%
UKF Prognostic 2	3.90%
Extrapolating1	8.31%
Extrapolating2	49.32%

By comparison, the UKF approach utilized the whole information from the collected data for each test cycle and updated the state model from new measurement inputs step by step. It also had the ability to model the dynamic stochastic states of the chromaticity shift which were driven by the random process noise, while the extrapolation approach estimated the parameters of the measurement model with the batch measurement data to predict the future state. Therefore, with the proposed UKF based prognostic approach, the data collection time in the reliability test for LEDs can be shortened from the standard minimum required 6,000 hrs to 5,000 hrs, or even 3,000hrs.

6.5 Concluding Remarks

In this chapter, to increase the prediction accuracy, a nonlinear filter-based data-driven prognostic approach was presented (the recursive Unscented Kalman Filter) to predict the lumen maintenance and chromaticity state of HPWLEDs. The prognostic performance of the proposed approach and the IES projecting approach were also compared and evaluated with both accuracy- and precision-based metrics. The following conclusions can be drawn from these results.

- (i) The recursive UKF-based prognostic approach can be expressed in two steps: filtering and prognostics. With time and measurement updates, the states can be estimated and forwarded dynamically. This study defined the parameters of the lumen degradation model and the chromaticity state shift model as dynamic states, and they can be updated and optimized recursively within the UKF algorithm.
- (ii) Two types of UKF algorithm, the augmented UKF and the non-augmented UKF, were used in this study. The filtering results showed that the augmented UKF produced a better estimation than the non-augmented UKF, because it captured more statistical information by introducing the effect of process and measurement noises into both state and measurement updating non-additively. However, the non-augmented UKF is easier to implement with less calculation.

(iii) The prognostic results of the proposed approaches were evaluated based on both accuracy- and precision-based metrics, and indicated that both UKF approaches can increase the prediction accuracy for the majority of test samples and they both possess higher prediction precision compared to the IES-TM-21-11 projecting approach. The proposed prognostic approach and its application on lumen maintenance prediction have been published by author on the journal of Reliability Engineering and System Safety in 2014 (Fan et al., 2014b).

(iv) The chromaticity state was considered as another health indicator of pc-white LEDs in addition to lumen maintenance. The Euclidean distance between the original chromaticity coordinates and future coordinates in the CIE1976 color space (u',v') was used to represent the chromaticity state shift and modeled as a nonlinear dual-exponential model. A recursive augmented UKF prognostic approach was used to predict the chromaticity state of the pc-white LED. With the UKF approach, the prognostic root mean square error is lower (less than 4%) than the error found in the extrapolated results. These results have been published on the journal of IEEE Transactions on Device and Materials Reliability in 2014 (Fan et al., 2014a).

Chapter 7 Optimal Design of Reliability Testing for LEDs in a Six Sigma DMAIC Framework

7.1 Introductory Remarks

Reliability testing is an essential assessment procedure to qualify a new product or technology before being released to the market. However, owing to its long lifetime, few or no failures occur in high power white LEDs (HPWLEDs) within short-term testing. As a result, it is difficult to assess reliability with traditional approaches which record only failure time. Even though improved reliability testing methods, such as accelerated life testing and censoring technology, have been developed to estimate the rated lifetime distribution for highly reliable products, these approaches may not be feasible for products not having failures during life testing due to severe time and cost constraints (Meeker et al., 1998). Sometimes the duration of the reliability testing and assessment procedure is longer than the time between product updates, which may delay technological innovation and development.

Therefore, designing an optimal reliability testing method for HPWLEDs with consideration of time and cost savings is desirable for accelerating LED technology innovation and development. Six Sigma has been recognized as a well-structured problem-solving methodology for improving and managing product quality (Gijo et

al., 2011, Easton & Rosenzweig, 2012, Zu et al., 2008), reducing operation cycle time (Valles et al., 2009) and optimizing process management (Antony et al., 2012, Shafer & Moeller, 2012) in many companies, such as Motorola, General Electric, and Raytheon (Montgomery & Woodall, 2008), the benefits of the Six Sigma approach can be achieved through the utilization of its systematic step-wise DMAIC approach, which enables participants to find problems in an old product or process and improve them with solutions from Design of Experiment (DOE) (Jin et al., 2011, Schroeder et al., 2008). In this study, the step-by-step application of the Six Sigma DMAIC approach in an LED reliability testing case is applied.

The objectives of this study can be summarized as: (1) to establish an optimal reliability testing procedure for HPWLED, (2) to shorten the testing time, and reduce the testing operation cost, and (3) also to maintain the accuracy of the reliability assessment. In chapter 6, the recursive UKF based data-driven method has been proven to be a more effective approach to predict both the lumen maintenance and chromaticity state of HPWLEDs by comparing with the ordinary least squares (OLS) approach mentioned in the IES-TM-21-11 standard. Thus, in this chapter, a new reliability estimation method is proposed to deal with degradation data to predict the reliability of HPWLEDs by integrating both the statistical and filter data-driven methods mentioned in previous chapters.

7.2 Case Study

As shown in the experimental setup section (section 3.2.2), a high temperature reliability test for one type of high power white LED provided a LED manufacturer was carried out by author in the Center for Advanced Life Cycle Engineering (CALCE) of the University of Maryland. The experimental setup and data collection procedure are shown in Fig. 3-7. The objectives of this testing were: (1) to know the LED's reliability information (such as the failure time distribution, the 100th percentiles of failure time distribution t_p , and mean time to failure MTTF); (2) to estimate its rated lifetime for the LEDs in the given accelerated aging condition.

As introduced before, the traditional reliability testing and assessment methods (including the censoring technology) require collecting the failure data of testing units. In this experiment, after 1633 hrs of aging, only nine units failed and the remaining seven units still operated well. The operation cost was estimated as more than \$1,000.

7.3 Define Phase

The define phase of the DMAIC methodology aims to establish a cross-functional Six Sigma team to summarize the problems that occurred in the above case study, define the scope and goals of the improvement project in terms of

customer requirements, and develop a process that delivers these requirements.

To begin with, a cross-functional team of people associated with the process was firstly established to solve the problems in the Six Sigma methodology. The CALCE team selected for this project included the Center Director, Head of the LED research group, LED research assistants, the lab manager, and lab assistants. The Center Director was identified as the champion. The Head of the LED research group acted as the team leader and was responsible for the overall success of the project and was also the process owner. The primary responsibility of the team members was to support the team leader in executing the project-related actions. This helped the team members to clearly understand the project objectives, project duration, resources available, roles and responsibilities of team members, project scope and boundaries, expected results from the project, etc (Gijo et al., 2011).

After the cross-functional team was established, the project champion organized a meeting to discuss the problems within in the above LED reliability testing, which can be summarized as follows: Firstly, *Testing operation time is too long*. The customer is not satisfied with the operation time (1633 hrs aging time, more than 2 months operation) which is too long for the LED manufacturer to know the reliability of this device. Secondly, the *Cost of testing is too high*. The total operation cost of LED life testing every time is \$1142.60. For the manufacturers, they will run many

reliability tests for their products before released to the market, therefore, the accumulated testing cost will be huge if using the current testing plan. All necessary details of the project are shown in the project charter (see Table 7-1).

Table 7-1 Six Sigma Project Charter

Project Name	Optimal Design of Reliability Testing for High Power White LEDs				
Group Name	LED Research Group				
Department Name	The Center for Advanced Life Cycle Engineering (CALCE), University of Maryland, USA				
Project Champion	CALCE Director				
Project Leader	Head of LED Research Group				
Team Member	LED Research Assistants; Lab Assistants; Lab Manager				
Problem Statement	The operation time (1633 hrs) and cost (\$1142.6) of a cycle reliability testing for High Power White LEDs are too high for the customer (Avago Technology)				
Goal Statement	Project Y's		Baseline	Goal	Units
	Metric 1	Time	1633 hrs	50% reduced	hrs
	Metric 2	Cost	\$1142.6	50% reduced	\$
	Metric 3	Accuracy (estimated t_{10})	1452.98	Errors within 5%	%
Schedule		<i>Jan-2013</i>	<i>Feb-2013</i>	<i>Mar-2013</i>	<i>Apr-2013</i>
	Define				
	Measure				
	Analysis				
	Improve				
	Control				
	Project Review				
	Report Writing				
Required resources	Reliability statistical knowledge Minitab and Matlab statistical softwares				

To solve the above problems, the goals of the project were established as the following quantitative criteria: (1) reduce the life testing time by 50% from the

existing reliability testing process and give the customer quick and reliable feedback; (2) reduce the reliability testing cost by 50%; (3) keep the errors of the estimated 10th percentiles of the failure time distribution t_{10} within 5%. Our Six Sigma team used the critical-to-quality (CTQ) methodology to translate the voice of the customer to the engineering targets (Fig. 7-1).

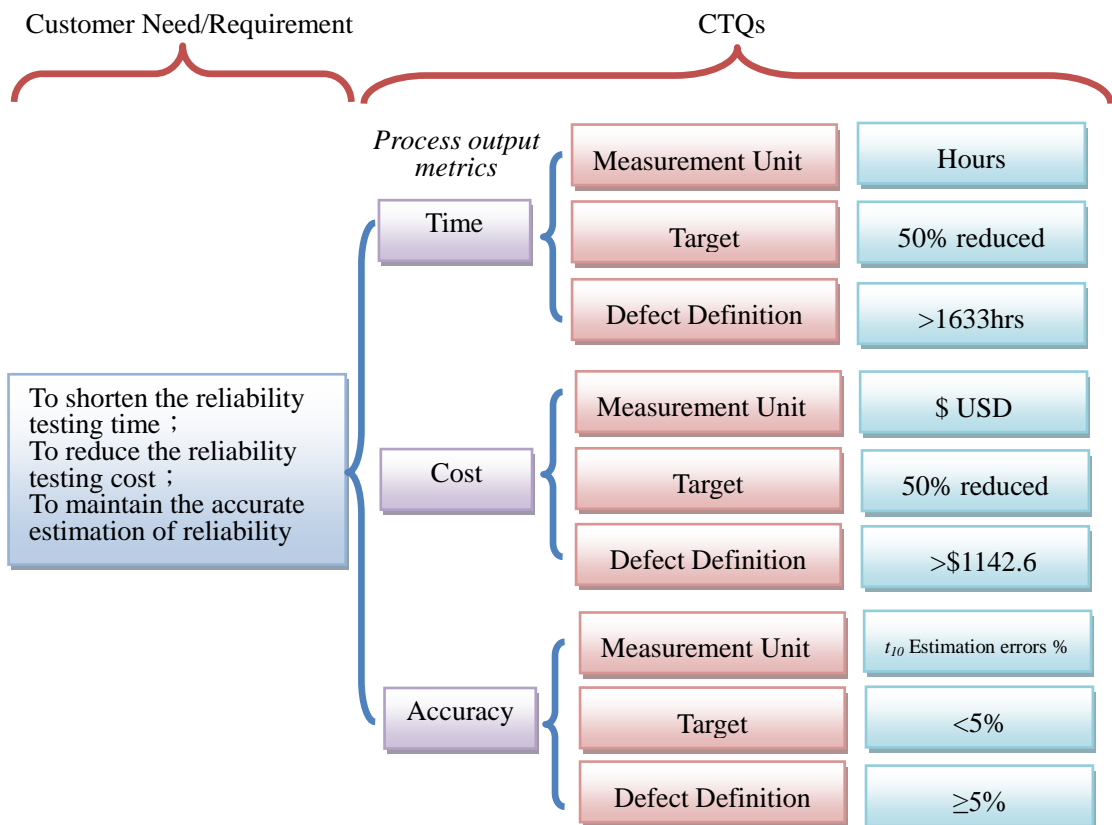


Fig. 7-1 Critical-to-quality (CTQ) methodology

The SIPOC approach (Supplier-Input-Process-Output-Customer) was implemented to help the team members understand the process (Table 7-2).

Table 7-2 Supplier-Input-Process-Output-Customer (SIPOC) diagram

Supplier	Inputs	Process	Outputs	Customer
LED manufacturer	LED test units	LED Reliability testing (See Fig. 6-3)	Standard LED reliability testing process and Reliability analysis report	LED manufacturer
Equipment suppliers	Aging chamber; Testing equipment; Data logger systems			
Planning and design team	DoE, statistical program design			
Facility department	Utility (power)			
CALCE reliability lab	Lab assistants			

As shown in the traditional LED reliability testing process and cycle operation profile in Fig. 7-2, after receiving the test units from the customer, they were first soldered onto an MCPCB aging test board. The traditional LED reliability testing was then conducted through the three sections: the aging section, the cooling section, and the testing section. For aging, sixteen high brightness white LEDs were thermally controlled in a chamber. After 23 hrs of aging, the aging test board was removed from the thermal chamber to be cooled to room temperature. For testing, the lighting performance data (such as light output, color coordinates, color temperature, color rendering index, and spectral power distribution) were measured manually by means of the BTS256-LED tester. After one hour of testing, the aging test board was returned to the thermal chamber to undergo the next aging cycle. When a test unit failed, the life testing was terminated and the LED's reliability was analyzed with

failure data or censored failure data based on traditional methods.

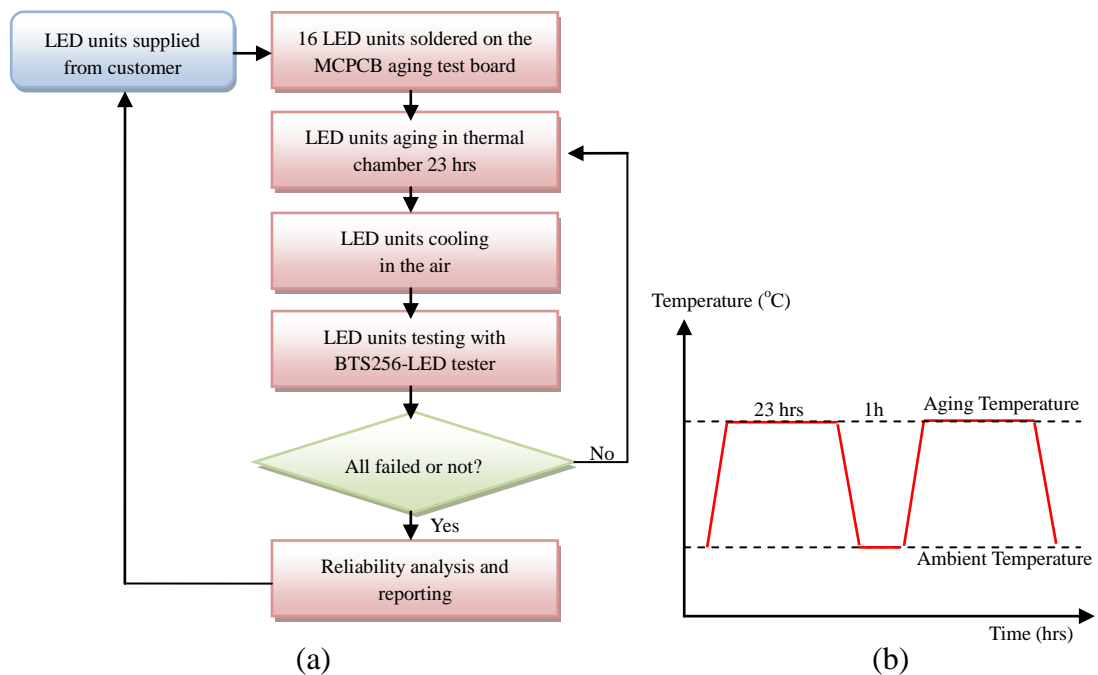


Fig. 7-2 (a) Traditional LED reliability testing process and (b) operation profile

7.4 Measure Phase

In the measure phase, the objective was to select appropriate product characteristics, map the respective processes, study the accuracy of the measurement system, record the data, and establish the baseline performance of the process (Wooles & Allardice, 2008).

In this experiment, the BTS256-LED tester was used to collect the light output data of sixteen test units over a 23 hrs per day collecting cycle. The BTS256-LED tester is a hand-held measurement system which allows qualification of luminous flux, spectral flux distribution, and color data of single LEDs (Fig. 7-3).

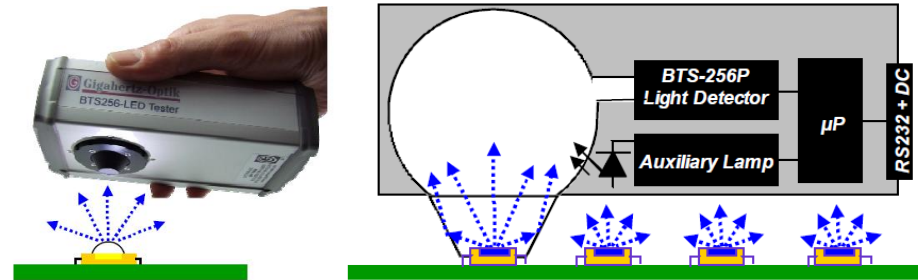


Fig. 7-3 BTS256-LED measurement system used for data collection
(BTS256-LED, 2009)

To validate the measurement system's accuracy and precision, a gauge repeatability and reproducibility (GR&R) study was conducted. Here, measurement on sixteen test units was repeatedly conducted five times by a lab assistant. After finishing collecting the data, GR&R analysis was performed with the help of Minitab statistical software. The result of the GR&R study is presented in Table 7-3.

Table 7-3 Results of gauge R&R study

Source	StdDev(SD)	Study variance	Study variance (%)
Total Gauge R&R	0.15594	0.93567	15.42
Repeatability	0.15594	0.93567	15.42
Part-to-Part	0.99938	5.99626	98.80
Total Variation	1.01147	6.06882	100.00

According to a previous study (Fang & Wang, 2005, Pan, 2006), the measurement system may be considered acceptable when the measurement system variability is between 10% and 30%; at above 30% variability, a measurement system is not considered acceptable. Since the total GR&R variance value in this

case was 15.42%, which was within the acceptable limit of 30%, it was concluded that the BTS256-LED measurement system was acceptable for further data collection.

In the LED industry, the light output data is usually used as one of the characteristics to determine the performance of LEDs. Normally, the LED lumen lifetime is measured from the lumen maintenance (LM), which can be defined as the maintained percentages of initial light output over time.

$$LM(t) = \frac{\Phi(t)}{\Phi(0)} \times 100\% \quad (7-1)$$

where $\Phi(0)$ is the initial light output, and $\Phi(t)$ is the lumen flux at time t .

Therefore, we transformed the light output data as the lumen maintenance data to determine LED failure. For LED general lighting, the lumen failure threshold is defined by the Alliance for Solid-State Illumination Systems and Technologies (ASSIST) as when the lumen maintenance decreases to 70%. The transformed time series lumen maintenance data of sixteen test units are shown in Fig. 7-4. As shown in Fig. 7-4, in our case, after 71 aging cycles (approximately 1633 hrs of aging time), there were only nine units failed and the remaining seven units were still operating. In this condition, the censoring approach was applied to these time-truncated failure data to estimate LED reliability as the baseline performance of the traditional life testing process. Censoring is a reliability estimation technology commonly used to

deal with cases where the extract lifetimes are known for only a portion of the products. With the censoring technology, the reliability information of the traditional life testing (e.g. failure time distribution, the 100pth percentiles of the failure time distribution t_p , and the mean time to failure MTTF) can be obtained.

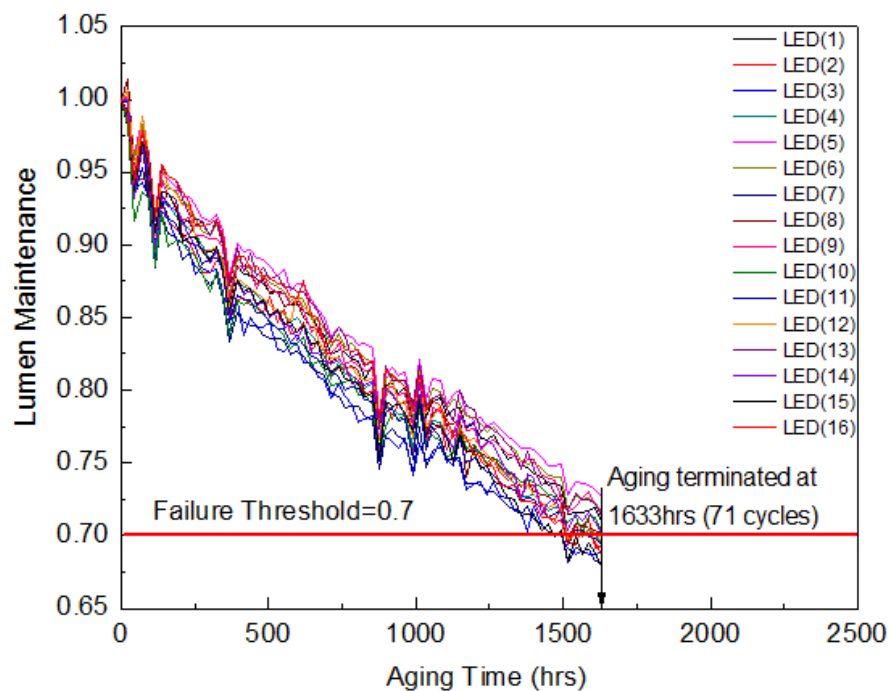


Fig. 7-4 Lumen degradation process of test units

In Fig. 7-5, the two-parameter *Weibull* distribution was used to fit the time-truncated data and estimate the shape and scale parameters of the *Weibull* distribution with the Maximum Likelihood (ML) method. The detailed results are shown in Table 7-4.

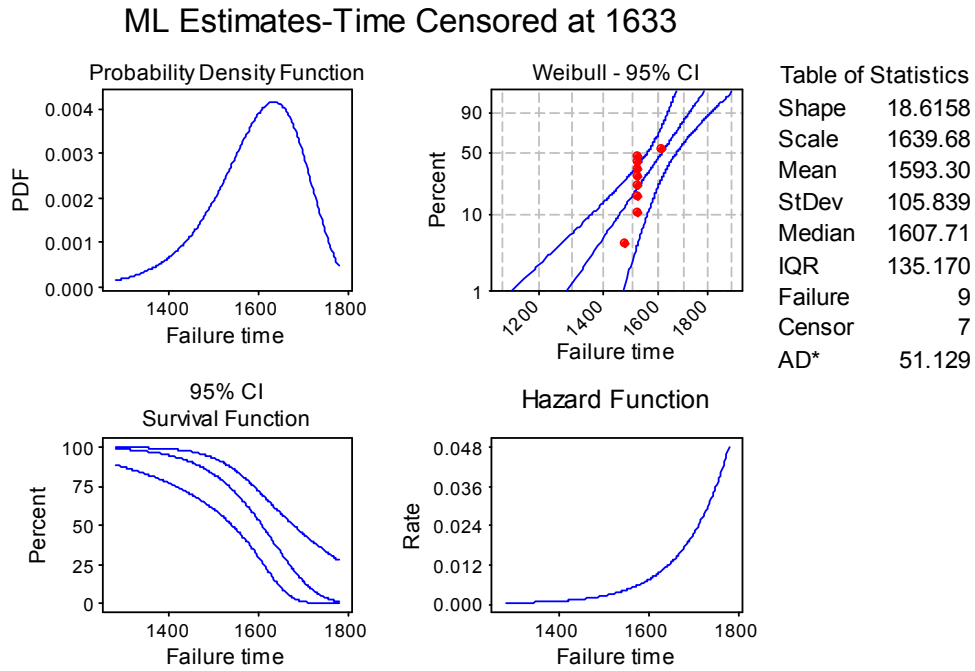


Fig. 7-5 Overview of failure time distribution of test units

Table 7-4 Reliability estimation with time-truncated failure data

No. of failures/Total No.	Weibull distribution parameters		MTTF	t_{10}
	shape	Scale		
9/16	18.6158	1639.68	1593.30	1452.98

7.5 Analyze Phase

The objective of the analyze phase is to identify the root cause that creates the problem in a process.

7.5.1 Cost Analysis

Operation time and cost are two major metrics for evaluating the efficiency of the reliability testing process. We established a financial function to analyze the life

testing operation cost. From the cost consideration in reliability testing, frequently asked questions from customers include, “How many units do I need to test?”, “How long do I need to run this life testing?”, and “How many times do I need to inspect the units in this testing?” (Wu & Chang, 2002, Marseguerra et al., 2003). As shown in the experimental procedure, the total cost of an experiment consists of the following three parts:

- (i) Sample cost nC_s : this can be defined as the cost of the total test units, where C_s represents the cost of a single test unit and n is the sample size.
- (ii) Inspection cost $n\tau C_m$: this includes the cost of using inspection equipment and materials and the operator’s labor cost. C_m denotes the cost of one inspection on one test unit, and τ is the inspection frequency.
- (iii) Operation cost $t_d(\tau-1)C_e$: this cost consists of the utility and depreciation of operation equipment (such as chambers, power suppliers, and data loggers). Let C_e be the operation cost in the time interval between two inspections, t_d .

Then the total operation cost, C_T , can be calculated as:

$$C_T = nC_s + n\tau C_m + t_d(\tau-1)C_e \quad (7-2)$$

Based on equation 7-2, the total operation cost of this LED reliability testing can be calculated as \$1142.60, which is out of the customer’s expectation. The relationship between total operation cost with inspection frequency and sample sizes

was also numerically simulated based on two assumptions: (1) the experimental termination time is 1633 hrs; (2) the operation cost between time intervals can be set as $\$0.2*n/16$, which means that the operation cost is mainly controlled by the sample sizes. A summary of the cost of traditional life testing is list in Table 7-5. In Fig. 7-6, the simulation results show that with the increase of inspection frequency and sample sizes, the total operation cost of the reliability testing is increased.

Table 7-5 Summary of the cost of traditional life testing

Items	Details
Sample size, n	16
Inspections frequency, τ	72 cycles
Time interval between two inspections, t_d	23 hrs per cycle
Termination time, T_d	71 cycles (1633 hrs)
Cost of a test unit, C_s	\$15
Cost of one inspection on one test unit, C_m	\$0.5
Operation cost in the time interval, C_e	\$0.2
Total cost, C_T	\$1142.6

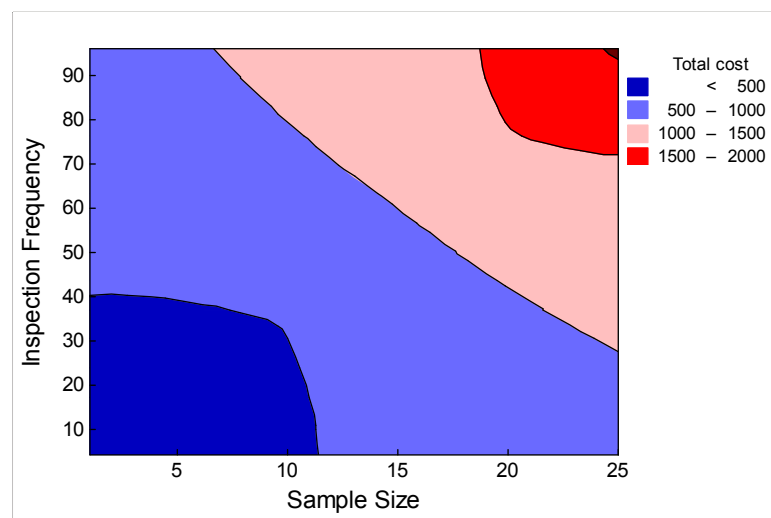


Fig. 7-6 Simulation contour plot of total operation cost vs. inspection numbers and sample size

7.5.2 Root Cause and Effect Analysis

From the previous analysis, there are several causes that affect the LED reliability testing time, cost, and final reliability estimation results. The cause and effect diagram shows the main root causes contributing to the project outputs from six factors (Materials, Machines, Measurements, Mans, Methods and Environment).

In this study, three major factors resulting in project defects are summarized as (see Fig. 7-7): (1) too large a sample size, which increases the life testing cost; (2) inspection frequency is too high, which also cost too much in terms of the depreciation of inspection equipment and materials and the operator's labor cost; (3) the traditional reliability test requires waiting for all test LEDs to fail (requires at least a portion of failures); therefore, this process requires a long operation time for highly reliable products.

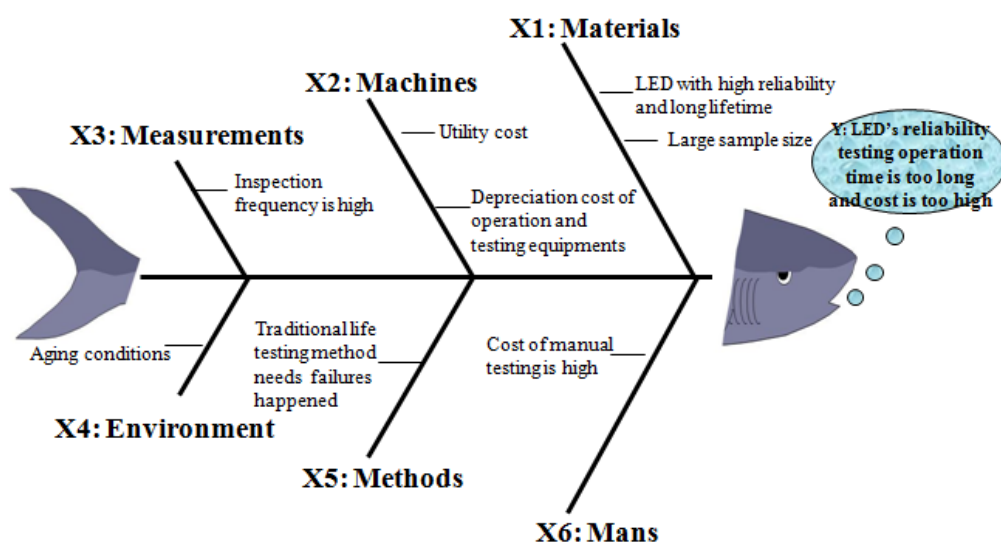


Fig. 7-7 Cause and effect diagram

7.6 Improve Phase

During this phase of the Six Sigma methodology, solutions were identified and implemented for all root causes selected during the analyze phase. To solve the major root causes resulting in the problems identified before, the LED reliability estimation methods were firstly improved by dealing with degradation data. Here, a general reliability estimation method based on degradation data was proposed and compared to the previous mixed-effect approach. Then, a DOE was planned for optimizing the LED reliability testing process parameters considering the reduction of both time and cost. Finally, an improved process flow for LED life testing was developed based on the DOE results.

7.6.1 Reliability Estimation Methods based on Degradation Data

7.6.1.1 Nonlinear mixed-effect model

For devices with long lifetimes, most of the traditional reliability testing techniques which require failure data are time-consuming and expensive. In this condition, using degradation data to do reliability assessment appears to be an attractive alternative for dealing with traditional failure time data, with benefits of identifying the degradation path and providing effective maintenance methods before failures occur. The nonlinear mixed-effect model first proposed by Lu and Meeker

(Lu & Meeker, 1993) is widely used to estimate reliability by modeling the degradation data with the general degradation path model.

The degradation path can be registered as time-performance measurement pairs $(t_{i1}, y_{i1}), (t_{i2}, y_{i2}), \dots, (t_{imi}, y_{imi})$, for $i = 1, 2, \dots, n$; and m_i represents the test time points for each unit:

$$y_{ij} = D(t_{ij}; \alpha; \beta_i) + \varepsilon_{ij} \quad (7-3)$$

where a random sample size is n , and the measurement times are $t_1, t_2, t_3, \dots, t_s$. The performance measurement for the i^{th} unit at the j^{th} test time is referred to as y_{ij} . $D(t_{ij}; \alpha; \beta_i)$ is the actual degradation path of unit i at the measurement time t_{ij} ; α is the vector of fixed effects which remains constant for each unit; β_i is a vector of random effects which varies according to the diverse material properties of the different units and their production processes or handling conditions; ε_{ij} represents the measurement errors for the unit i at the time t_{ij} , which is supposed to be a normal distribution with zero mean and constant variance.

Previous work on LEDs indicated that the degradation trajectory of lumen performance followed an exponential curve. Therefore, the exponential degradation path model with mixed effect parameter vector $\theta(\alpha, \beta_i)$ was used to represent the lumen maintenance degradation:

$$y_{ij} = D(t_{ij}; \theta) = \alpha \cdot \exp(-\beta_{ij} \cdot t_{ij}) + \varepsilon_{ij} \quad (7-4)$$

For the decreasing type of performance measurement (lumen degradation of LEDs), the failure definition for the general degradation path models is that the performance measurement, y_{ij} , is lower than the critical threshold, D_f , at time t . For LEDs, $D_f = 0.7$ is recommended by ASSIST. The cumulative probability of the failure function, $F(t)$, is given as follows:

$$F(t) = P(t \leq T) = P[D(t_{ij}, \alpha, \beta_i) \leq D_f] \quad (7-5)$$

And Time to Failure $T = \inf(t \geq 0; D(t_{ij}, \alpha, \beta_i) \leq D_f)$

Several statistical methods have been proposed by researchers to estimate reliability based on the degradation data. The estimation of the percentiles of the failure time distribution can be obtained with analytical methods by using the relation between the failure time distribution and the random effects parameter distribution. However, an assumption needs to be proposed first for the distribution of the random effects parameter, β_i . Wu and Shao (Wu & Shao, 1999) assumed that the random effects parameter, β_i , followed a normal distribution, whereas Wu and Chang (Wu & Chang, 2002) proposed an exponential distribution. Yu *et al* (Yu, 2006) designed it as a reciprocal *Weibull* distribution. The ordinary nonlinear least squares (ONLS) estimator was then used to estimate the model parameter vector $\theta(\alpha, \beta_i)$ by minimizing the residuals between the observed data and the curve-fitted data from models. The accuracy of estimation depends on which distribution of the random

effects parameter is chosen. Therefore, this analytical method has some limitations in dealing with small sample size problems without detailed statistical distributions. Meanwhile, there are some limiting requirements for the degradation path model. This method will not, however, solve estimation problems in some complicated expressions of degradation path models.

$$\min_{\theta} \left\{ \frac{1}{s} \sum_j^s [y_{ij} - D(t_{ij}; \theta)][y_{ij} - D(t_{ij}; \theta)]^T \right\} \quad (7-6)$$

7.6.1.2 New reliability estimation method with nonlinear degradation data

In this project, to establish a new reliability estimation method for LEDs with lumen maintenance degradation data, the following three basic steps are proposed: (1) Estimating the pair parameter set for the degradation path models of each test unit $\Theta(\alpha_i, \beta_i)$; (2) extrapolating the degradation path model of each unit to critical failure threshold, D_f , to estimate the “pseudo” failure time for each unit; (3) Fitting the probability distribution for these “pseudo” lifetime data and calculating the 100pth percentile of the failure time distribution, t_p . The operation procedure can be specified as follows:

Step 1: The estimation of parameters for the degradation path models is the first and most important step in the whole reliability estimation process. Here, one parameter is not required to be assumed as a fixed value. Both parameters in the pair

parameter set for the degradation path model are randomly distributed. Two estimation approaches were proposed to estimate the pair parameter set $\Theta(\alpha_i, \beta_i)$ (see Fig. 7-8): (1) nonlinear least squares (NLS); and (2) recursive unscented Kalman filter (Recursive UKF).

The NLS method adopts a similar approach to the above mentioned ONLS used in the analytical methods. It estimates parameters through minimizing the residuals between observed data and curve-fitted data from models. However, we did not assume any distribution for both parameters and we used the Matlab exponential curve-fitting tools with the trust region algorithm to estimate the pair parameter set $\Theta(\hat{\alpha}_i, \hat{\beta}_i)$ for each test unit.

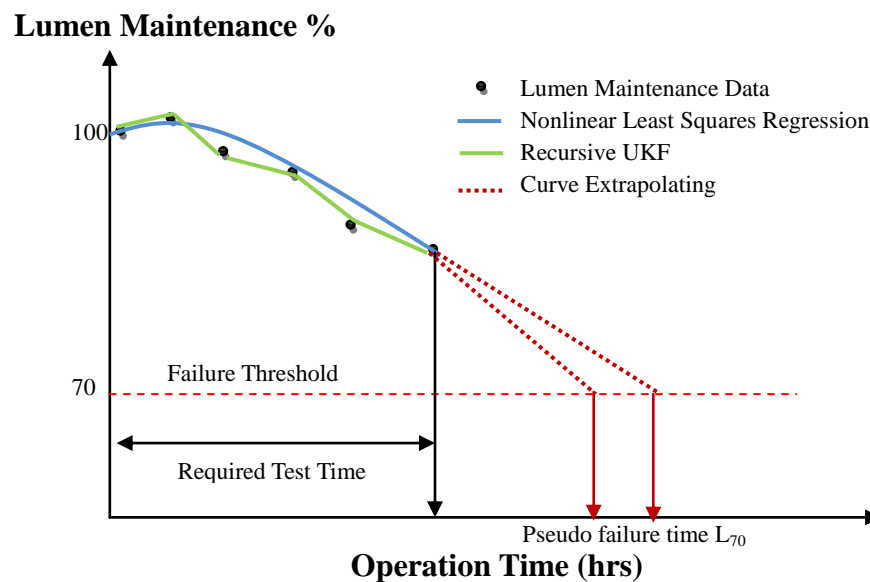


Fig. 7-8 General nonlinear estimation method with degradation data

Another approach proposed for estimating the pair parameter set of the degradation path model is the recursive UKF. The UKF approach was first proposed by Julier *et al.* and developed by Wan *et al.* (Julier & Uhlmann, 2004, Wan & van der Merwe, 2000) to estimate the state of nonlinear systems by using a deterministic sampling approach (sigma point sampling) to capture the mean and covariance estimates with a minimal set of sample points. The UKF algorithm always involves estimation of the state of a discrete-time nonlinear dynamic system, which can be represented by both a state model and a measurement model. Here, in order to estimate the pair parameter set $\Theta(\alpha_i, \beta_i)$, the lumen maintenance degradation model was used as the measurement model. The pair parameter set of the degradation model of each test unit is seen as the state.

$$\text{State model:} \quad x_{ij} = \Theta(\alpha_{ij}, \beta_{ij}) = [\alpha_{ij}; \beta_{ij}] \quad (7-7)$$

$$\alpha_{ij} = f(\alpha_{i,j-1}, v_{j-1}^\alpha) = \alpha_{i,j-1} + v_{j-1}^\alpha \quad v_{j-1}^\alpha \sim N(0, Q_v^\alpha);$$

$$\beta_{ij} = f(\beta_{i,j-1}, v_{j-1}^\beta) = \beta_{i,j-1} + v_{j-1}^\beta \quad v_{j-1}^\beta \sim N(0, Q_v^\beta);$$

$$\text{Measurement model:} \quad y_{ij} = h(\alpha_{ij}, \beta_{ij}, \varepsilon_{ij}) = \alpha_{ij} \exp(-\beta_{ij} t_d j) + \varepsilon_{ij} \quad (7-8)$$

where v_{j-1} is the state noise and is assumed to be the mean zero white Gaussian noise.

Then the recursive UKF was used to estimate the pair parameter set $\Theta(\alpha_i, \beta_i)$ for the i^{th} test unit. The main steps of the recursive UKF algorithm are summarized as follows:

1. $j=0$ Initialize states with mean and covariance:

$$\bar{x}_0 = E[x_0]; \quad P_0 = E[(x_0 - \bar{x}_0) \cdot (x_0 - \bar{x}_0)^T];$$

2. Express the initial state vector and covariance matrix as an augment vector:

$$\bar{x}_0^a = E[x_0^a] = [\bar{x}_0 \quad 0 \quad 0]^T; \quad P_0^a = \begin{bmatrix} P_0 & 0 & 0 \\ 0 & Q_0 & 0 \\ 0 & 0 & R_0 \end{bmatrix}$$

3. For $j \in [1, \infty)$

Calculate sigma points: $\chi_{j-1}^a = [\bar{x}_{j-1}^a \quad \bar{x}_{j-1}^a + \sqrt{n_a + \lambda} \cdot \sqrt{P_{j-1}^a} \quad \bar{x}_{j-1}^a - \sqrt{n_a + \lambda} \cdot \sqrt{P_{j-1}^a}]$;

Time update: $\chi_{j/j-1}^x = f(\chi_{j-1}^x, \chi_{j-1}^y)$; $\bar{x}_{j/j-1} = \sum_{\pi=0}^{2n_a} W_{\pi}^{(m)} \chi_{\pi, j/j-1}^x$;

$$P_{j/j-1} = \sum_{\pi=0}^{2n_a} W_{\pi}^{(c)} [(\chi_{\pi, j/j-1}^x - \bar{x}_{j/j-1}) \cdot (\chi_{\pi, j/j-1}^x - \bar{x}_{j/j-1})^T];$$

$$y_{j/j-1} = h(\chi_{j/j-1}^x, \chi_{j-1}^y); \quad \bar{y}_{j/j-1} = \sum_{\pi=0}^{2n_a} W_{\pi}^{(m)} y_{\pi, j/j-1};$$

Measurement update: $P_{j/j-1}^{yy} = \sum_{\pi=0}^{2n_a} W_{\pi}^{(c)} [(y_{\pi, j/j-1} - \bar{y}_{j/j-1}) \cdot (y_{\pi, j/j-1} - \bar{y}_{j/j-1})^T]$;

$$P_{j/j-1}^{xy} = \sum_{\pi=0}^{2n_a} W_{\pi}^{(c)} [(\chi_{\pi, j/j-1}^x - \bar{x}_{j/j-1}) \cdot (y_{\pi, j/j-1} - \bar{y}_{j/j-1})^T];$$

$$K_j = P_{j/j-1}^{xy} (P_{j/j-1}^{yy})^{-1};$$

$$\bar{x}_j = \bar{x}_{j/j-1} + K_j (y_j - \bar{y}_{j/j-1}); \quad P_j = P_{j/j-1} - K_j P_{j/j-1}^{yy} K_j^T$$

4. If $j < T_d/t_d$, $j = j+1$, repeat steps 2 to 3.

5. Otherwise, output the updated state x_j as the estimated pair parameter set

$$\Theta(\hat{\alpha}_i, \hat{\beta}_i) \text{ for the } i^{\text{th}} \text{ test unit.}$$

where λ is the composite scaling parameter, $\lambda = \alpha^2(n_a + k) - n_a$; W_{π} is the weight factor, $W_{\pi=0}^{(m)} = \lambda / (\lambda + n_a)$; $W_{\pi=0}^{(c)} = \lambda / (\lambda + n_a) + (1 - \alpha^2 + \beta)$; $W_{\pi}^{(m)} = W_{\pi}^{(m)} = 1/2(\lambda + n_a)$, $\pi = 1, 2, \dots, 2n_a$. Here, we set $\alpha = 0.01$, $\kappa = 3 - n_a$, and $\beta = 0$. K_j is the Kalman gain. T_d and t_d are the design termination time and the time interval between two inspections, respectively.

With the inputs of the updated measurement data, the parameter vector $\Theta(\alpha_i, \beta_i)$

can be estimated and then updated as the initial state of next step recursively.

Step 2: After receiving the estimated pair parameter set $\Theta(\hat{\alpha}_i, \hat{\beta}_i)$ of each test

unit, the degradation path model of each unit was extrapolated based on these

parameters to the critical failure threshold to estimate the “pseudo” failure time as L_{D_f} :

$$L_{D_f} = \ln\left(\frac{\hat{\alpha}}{D_f}\right) / \hat{\beta} \quad (7-9)$$

where D_f is the lumen maintenance degradation critical failure threshold (i.e. $D_f = 0.7$ recommended by ASSIST).

Step 3: Fitting these “pseudo” lifetime data with the two-parameter *Weibull* probability distribution, *Weibull*(η, γ) (Mazhar et al., 2007), and calculating the 100th percentile of the failure time distribution, t_p .

$$\text{Weibull p.d.f} \quad f(t; \eta, \gamma) = \frac{\gamma}{\eta} \left(\frac{t}{\eta}\right)^{\gamma-1} e^{-\left(\frac{t}{\eta}\right)^\gamma}, t > 0 \quad (7-10)$$

$$t_p = \eta \cdot [-(\ln(1-p))]^{1/\gamma} \quad (7-11)$$

7.6.2 Design of Experiment (DOE)

As shown in section 7.6.1, the degradation-data-driven reliability estimation method can also get reliability information (such as failure time distribution, the 100th percentiles of failure time distribution t_p , and mean time to failure MTTF) without waiting for failure to occur. Therefore, a new LED reliability testing process flow based on degradation data was planned by the Six Sigma team and a DOE was planned to optimize the LED reliability testing process parameters by considering the

reduction of both time and cost.

The team, along with the champion, conducted a series of brain storming sessions to identify the important parameters for experimentation (Gijo et al., 2011).

The parameters selected through these discussions are summarized as (see Fig. 7-9):

(1) sample size of test units; (2) termination time (hrs); (3) aging duration per cycle (hrs); and (4) reliability estimation methods. The factors and their levels for experimentation are presented in Table 7-6.

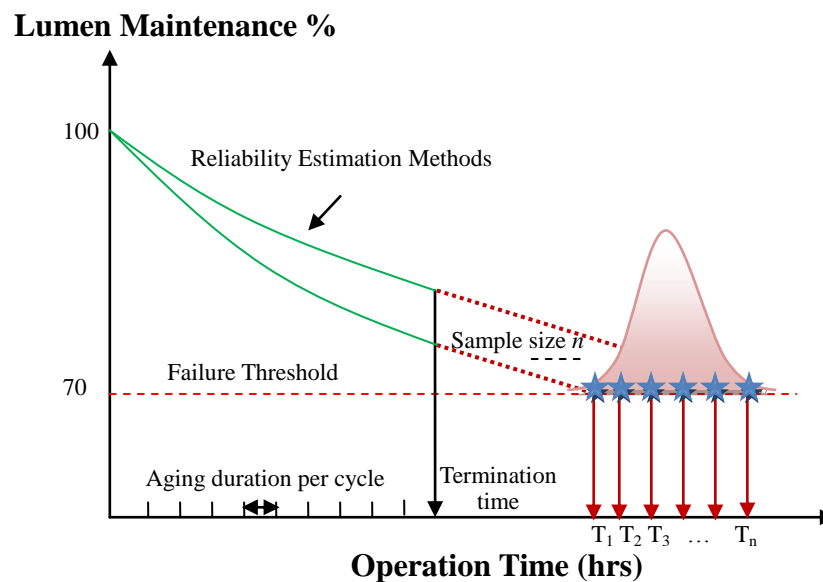


Fig. 7-9 The main parameters of LED reliability testing process

Table 7-6 The factors and their levels of DOE

Factors	Level 1	Level 2	Level 3
Reliability Estimation Methods	NLS	Recursive UKF	N.A.
Sample size of test units	12	10	8
Termination time (hrs)	1380	1035	690
Aging duration per cycle (hrs)	23	69	115

In this study, we designed eighteen experiments with four effects and one interaction between the termination time and the reliability estimation methods for the LED reliability testing process with the help of Taguchi Orthogonal Array (OA), $L_{18}(3^3 \cdot 1^2)$ (Table 7-7).

Table 7-7 Taguchi orthogonal array $L_{18}(3^3 \cdot 1^2)$ DOE

DOE No.	Methods	Sample size	Termination time (hrs)	Aging duration per cycle (hrs)
1	NLS	12	1380	23
2	NLS	10	1380	69
3	NLS	8	1380	115
4	NLS	12	1035	23
5	NLS	10	1035	69
6	NLS	8	1035	115
7	NLS	12	690	69
8	NLS	10	690	115
9	NLS	8	690	23
10	Recursive UKF	12	1380	115
11	Recursive UKF	10	1380	23
12	Recursive UKF	8	1380	69
13	Recursive UKF	12	1035	69
14	Recursive UKF	10	1035	115
15	Recursive UKF	8	1035	23
16	Recursive UKF	12	690	115
17	Recursive UKF	10	690	23
18	Recursive UKF	8	690	69

According to the DOE plan, the eighteen designed experiments were conducted and the data (operation time, cost, the 10th percentile of the failure time distribution

t_{10}) were calculated. Compared to the baseline data collected from the traditional reliability testing in the measure phase, the reduced operation time and cost and the estimated t_{10} absolute errors were calculated and are shown in Table 7-8.

Table 7-8 Summary of reliability testing performance from DOE

DOE No.	Project Y's metrics				
	Time reduced	Cost down	Accuracy (estimated t_{10} absolute errors)		
			Trial 1	Trial 2	Trial 3
1	15.49%	34.10%	3.79%	1.96%	3.46%
2	15.49%	62.59%	5.08%	5.24%	4.02%
3	15.49%	72.87%	4.11%	0.81%	1.84%
4	36.62%	46.50%	11.50%	8.77%	11.57%
5	36.62%	68.55%	12.87%	12.42%	12.10%
6	36.62%	76.94%	12.50%	8.46%	11.50%
7	57.75%	69.41%	22.23%	20.73%	23.25%
8	57.75%	76.26%	19.92%	20.29%	18.70%
9	57.75%	72.61%	17.34%	17.88%	18.49%
10	15.49%	59.30%	3.03%	4.04%	3.58%
11	15.49%	45.08%	2.29%	0.69%	4.09%
12	15.49%	70.07%	0.67%	1.43%	4.35%
13	36.62%	62.26%	8.08%	6.87%	8.93%
14	36.62%	71.17%	5.03%	3.26%	3.62%
15	36.62%	64.34%	7.29%	5.77%	8.45%
16	57.75%	71.51%	0.77%	0.38%	0.11%
17	57.75%	65.76%	8.63%	10.53%	8.46%
18	57.75%	79.61%	6.35%	10.06%	9.34%

To analyze the effects of the proposed factors on the accuracy of the reliability estimation, three trials were conducted for each experiment and then used the

Taguchi's signal-to-noise (S/N) ratio method then used to treat the response (output) of the experiment. This experimental output can be evaluated as the absolute estimation errors of the 10th percentiles of failure time distribution, t_{10} . The S/N ratio for the *nominal is best* type characteristic is defined as (Gijo et al., 2011):

$$S/N=10*\log (\bar{Y}^2 / s^2) \quad (7-12)$$

where \bar{Y}^2 is the average of the response and s is the standard deviation.

The main effect and interaction plots for the S/N ratios were made with the help of Minitab statistical software (Fig. 7-10 and 7-11). After ranking the responses in Table 7-9, it can be concluded that the termination time of reliability testing has the largest effect on the reliability estimation accuracy and the aging duration/cycle time has the smallest effect.

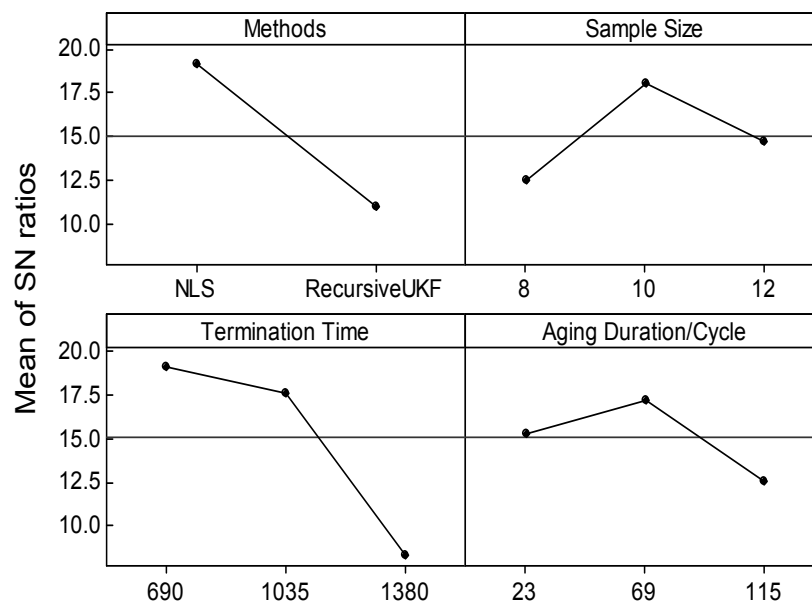


Fig. 7-10 Taguchi orthogonal array $L_{18}(3^3*1^2)$ DOE main effects plot for SN ratios

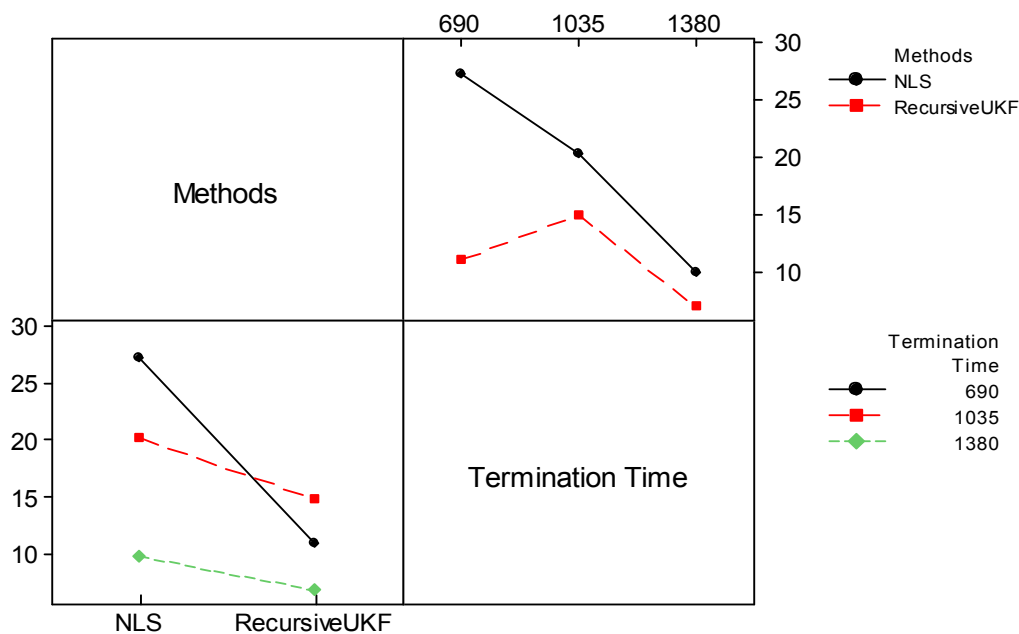


Fig. 7-11 Taguchi orthogonal array $L_{18}(3^3*1^2)$ DOE interaction plot for SN ratios

Table 7-9 Response for S/N ratios

Level	Main Effects for Accuracy of Reliability Estimation			
	Methods	Sample Size	Termination Time	Aging Duration/cycle
1	19.167	12.470	19.185	15.294
2	10.949	18.015	17.606	17.245
3	N.A.	14.688	8.382	12.634
Delta	8.217	5.545	10.803	4.611
Rank	2	3	1	4

Meanwhile, with the recursive UKF approach, the reliability estimation accuracy can be improved compared to the NLS approach. The reasons for this phenomenon can be concluded as: firstly, the UKF deals with dynamic stochastic systems, while least squares is used for deterministic systems; secondly, the UKF updates the system states recursively by absorbing new measurements while the least

squares implementation uses batch processing.

After comparing the output results from the three project metrics mentioned in the project charter (time, cost, and accuracy) (Table 7-8), we chose the DOE16 with the associated factor levels as the optimal LED reliability testing process (Table 7-10).

Table 7-10 Optimum factor level combination

No.	Factors	Optimum level
1	Sample size of test units	12
2	Termination time (hrs)	690
3	Aging duration per cycle (hrs)	115
4	Reliability estimation method	Recursive UKF

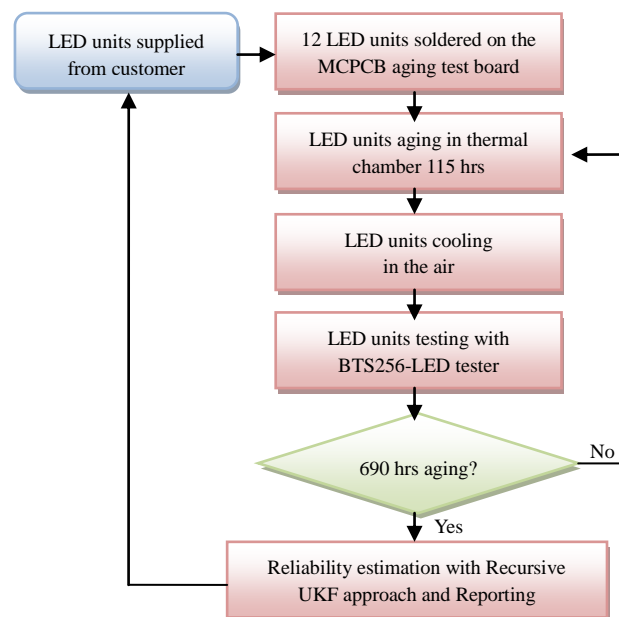


Fig. 7-12 The improved LED reliability testing process flow

The improved process flow is shown in Fig. 7-12. Compared to the traditional

testing shown in Fig. 7-2, with the help of recursive UKF approach applied in the reliability estimation, the new LED life testing process can be terminated at 690 hrs with 115 hrs aging duration per cycle. The operation cost is reduced from \$1142.60 to \$325.50 and the required sample size can be reduced from 16 to 12. Therefore, the total operation time and cost can be reduced by 57.75% and 71.51%, respectively, and the absolute errors of the estimated t_{10} can be controlled to under 5%.

7.7 Control Phase

Once optimal results are achieved, the challenge for any process owner is to sustain the improvement in the achieved results. Standardizing of the improved methods and continuous monitoring of the results can ensure the sustainability of the results. As discussed in the improve phase, once the optimal LED reliability testing process flow with the associated process parameters is selected (shown in Table 7-10), the experimental operation time and cost can be controlled to stable values (690 hrs of operation time and a cost of \$325.50).

Besides the time and cost metrics, accuracy is another requirement for reliability estimation in this study. To show the stability of the improved LED reliability testing process flow in terms of the accuracy metric, a control chart showing the absolute errors of the estimated t_{10} is presented in Fig. 7-13. The results show that the

improved reliability testing process is stable, having low estimation errors.

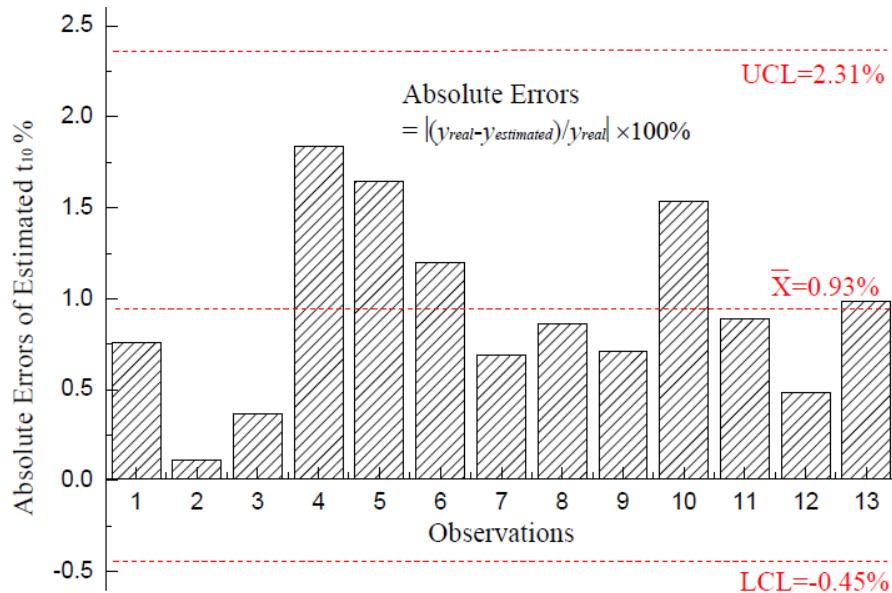


Fig. 7-13 Individual control chart for reliability estimation errors

7.8 Concluding Remarks

Traditional reliability testing methods for high power white light-emitting diodes are always time-consuming and expensive. The Six Sigma DMAIC method is a project-driven management approach to discover and solve problems for a specified process. This study presents the step-by-step application of the Six Sigma DMAIC methodology in reducing the LED reliability testing operation time and cost and in maintaining highly accurate reliability estimations. The outcomes of this study can be concluded as follows:

- (i) By implementing the proposed general reliability estimation method with both

the statistical and filter data-driven methods, the LED reliability (failure time distribution; percentiles of failure time distribution, t_p ; and MTTF) can be estimated with the lumen maintenance degradation data. There is no need to record failure data, such as the traditional reliability testing methods, with this proposed method.

(ii) Within dynamic stochastic systems, the recursive UKF approach can be used to predict the reliability and improve the accuracy of reliability estimation compared to the ordinary least squares approach recommended in the IES-TM-21-11 standard.

(iii) With the optimum process parameter setting obtained from DOE, the operation time and cost of LED reliability testing can be reduced by 57.75% and 71.51%, respectively, compared to traditional testing. The reliability estimation errors from the improved process can also be controlled to within customer's specification (within 5%);

(iv) Finally, as revealed in the control chart, the new LED reliability testing process is stable with low estimation errors.

The above work in this chapter has been documented as a journal paper submitted to the journal of Reliability Engineering and System Safety.

Chapter 8 Conclusions and Future Work

8.1 Conclusions Drawn from Research Work

This thesis developed failure diagnosis and reliability prediction methods for high power white LEDs lighting with Prognostics and Health Management (PHM) methodologies. The completed research work and contributions in this thesis are summarized in the following paragraphs:

Firstly, the Physics-of-Failure (PoF) based PHM approach was used to diagnosis the failure modes and failure mechanisms for high power white LED lighting from the chip level to the system level and assess the reliability. Three failure modes, (1) Catastrophic failure; (2) Lumen degradation; (3) Chromaticity state shift, were firstly categorized to the whole system and the potential failure mechanisms and their contributing loads were presented by the “bottom-up” method. Then, the physics-of-failure based damage models were built for the two failure mechanisms with highest priority in the degradations from the chip to the whole system. However, because the PoF based PHM method requires comprehensive knowledge of the materials and geometries of products and the thermal, mechanical, electrical and chemical life cycle environment as well as processes leading to failures in the field in advance, this always increases the time and cost in the actual applications.

Secondly, to solve the problems in the complexity of conducting a PoF modeling, the data-driven prognostic methods with both statistical and learning approaches were applied to predict the lumen lifetime, lumen maintenance and chromaticity state of high power white LED lightings. In detail, with the proposed statistical data-driven method, more reliability messages (e.g. Mean Time to Failure (MTTF), Confidence Interval (CI) and reliability function) could be predicted compared to the

IES TM-21-11 projecting method which only can estimate L_{70} . Three different approaches from this statistical data-driven method (the approximation method, analytical method and the two-stage method) were developed to estimate the failure time distribution and evaluate the product's reliability. Among these three methods, the two-stage method with the smallest widths of the 95% confidence intervals produced the highest degree of prediction accuracy. But the prediction errors and uncertainties of the ordinary least squares (OLS) regression used in both our proposed statistical data-driven method and IES TM-21-11 projecting method are still large.

Thirdly, both lumen maintenance and chromaticity state are considered as the health indicators of high power white LEDs in this thesis. To reduce the prediction errors and uncertainties introduced by the IES-TM-21-11 projecting approach, a filter-based data-driven method (recursive Unscented Kalman Filter (UKF)) was developed to predict both the lumen maintenance and chromaticity state of high power white LED lightings, replacing the ordinary least squares implementation recommended in the IES TM-21-11 projecting method. The results show that the proposed UKF filter-based data-driven method can improve the prediction accuracy in both applications, because it can utilize the whole information from the collected data for each test cycle and updated the state model from new measurement inputs step by step.

Finally, this study proposed a new reliability estimation method with degradation data to predict the reliability of HPWLEDs by means of integrating both statistical and filter data-driven methods. With the benefits of the Six Sigma DMAIC step-wise approach in identifying and solving problems, an optimal design of LED reliability testing was proposed with the proposed new reliability estimation method

in a Six Sigma DMAIC framework. The results from a case study show that with the optimum process parameter setting obtained from DOE, the operation time and cost of LED reliability testing can be reduced by 57.75% and 71.51%, respectively, compared to traditional testing. The reliability estimation errors from the improved process can also be controlled to within a customer's specification (within 5%).

8.2 Suggestions for Future Research Directions

The proposed PHM method described in this thesis is an off-line failure diagnosis and reliability prognostics approach which has been proven to be an effective solution to shorten the reliability testing time, to reduce the testing operation cost, and also to maintain the accuracy of reliability assessment. The consideration of applications of the proposed method, some future research directions can be suggested as:

Firstly, an LED lighting system is always composed of LED units or arrays, power driver, cooling module, optical house, thermal management module and so on. The lifetime of a LED component (package) is not the whole story of the reliability of LED lighting systems. Therefore, the prognostics and system health management (PHM) strategy applied for a LED lighting system, such as street lighting, emergency lighting, monitor backlights, can be a real application studies in the future, which must consider the reliability of both single modules and connections between modules.

Secondly, in the future, the work will be continued to develop online PHM methodologies for high power white LED lighting systems, which will integrate the proposed off-line PHM tools with online monitoring techniques. With the help of online monitoring techniques, the feature data will be collected, classified and

extracted with data mining tools and then real time failure diagnosis and reliability prognostics can be achieved with fusion PHM methods.

Thirdly, facing the lack of a unified and comprehensive standard system for reliability testing in the LED lighting industry, this research applied PHM methodologies in establishing reliability testing and prediction methods for LED lighting. Although the results show that the proposed models are superior to the IES TM-21-11 projecting standard, this study only covers the constant stress testing for LED lighting. As a systemic reliability testing method, other tests, such as step-stress tests, accelerated stress tests, cycle aging tests and so on, should be studied as future work.

References

- AKAIKE, H. 1974. A New Look at the statistical Model Identification, *IEEE Transactions on Automatic Control*, ac-19, 716-723.
- ANSI/ANSLG C78.377. 2008. *Specifications for the Chromaticity of Solid State Lighting Products: for electric lamps*. National Electrical Manufacturers Association, VA.
- ANSI/ANSLG C78.377. 2011. *Specifications for the Chromaticity of Solid State Lighting Products: for electric lamps*. National Electrical Manufacturers Association, VA.
- ANTONY, J., GIJO, E. V. & CHILDE, S. J. 2012. Case study in Six Sigma methodology: manufacturing quality improvement and guidance for managers. *Production Planning & Control*, 23, 624-640.
- ARIK, M., BECKER, C., WEAVER, S. & PETROSKI, J. 2004. Thermal management of LEDs: Package to system. *Third International Conference on Solid State Lighting*, 5187, 64-75.
- ASSIST RECOMMENDATION. 2005. *LED Life for General Lighting*, Lighting Research Center: Troy, NY, USA,.
- BENNETT, J. 2008. Telcordia Reliability Prediction Procedure: Upper Confidence Levels. *Annual Reliability and Maintainability Symposium, 2008 Proceedings*, 455-458.
- BLISCHKE, W. D. & MURTHY, N. P. 2000. *Reliability Modeling, Prediction, and Optimization*, John Wiley & Sons, Inc., New York.
- BTS256-LED. 2009. BTS256-LED Tester Data Sheet, Gigahertz-Optik. Germany. <http://www.led-measurement.com/>.
- CAI, Z. Q., SUN, S. D., SI, S. B. & WANG, N. 2009. Research of Failure Prediction Bayesian Network Model. *2009 IEEE 16th International Conference on Industrial Engineering and Engineering Management, Vols 1 and 2, Proceedings*, 2021-2025.
- CALCEPWA. 2004. *calcePWA Software: A Simulation Failure Assessment Solution of Printed Wiring Assemblies*, University of Maryland, College Park, USA. <http://www.calce.umd.edu/software/>
- CAO, X. A., SANDVIK, P. M., LEBOEUF, S. F. & ARTHUR, S. D. 2003. Defect generation in InGaN/GaN light-emitting diodes under forward and reverse electrical stresses. *Microelectronics Reliability*, 43, 1987-1991.
- CASSANELLI, G., MURA, G., CESARETTI, F., VANZI, M. & FANTINI, F. 2005. Reliability predictions in electronic industrial applications. *Microelectronics Reliability*, 45, 1321-1326.
- CASSANELLI, G., MURA, G., FANTINI, F. & VANZI, M. 2008. Failure analysis of

- high power white LEDs. *2008 26th International Conference on Microelectronics, Vols 1 and 2, Proceedings*, 255-257.
- CHANG, M. H., DAS, D., VARDE, P. V. & PECHT, M. 2012. Light emitting diodes reliability review. *Microelectronics Reliability*, 52, 762-782.
- CHARPENEL, P., DAVENEL, F., DIGOUT, R., GIRAUDEAU, M., GLADE, M., GUERVENO, J. P., GUILLET, N., LAURIAC, A., MALE, S., MANTEIGAS, D., MEISTER, R., MOREAU, E., PERIE, D., RELMY-MADINSKA, F. & RETAILLEAU, P. 2003. The right way to assess electronic system reliability: FIDES. *Microelectronics Reliability*, 43, 1401-1404.
- CHENG, S. F. & PECHT, M. 2009. A Fusion Prognostics Method for Remaining Useful Life Prediction of Electronic Products. *2009 IEEE International Conference on Automation Science and Engineering*, 102-107.
- CHIEN, C. L. C., HUANG, Y. C., HU, S. F., SUN, C. W., CHANG, C. M., HSU, C. P., YIP, M. C. & FANG, W. L. 2012. LED package with Dome/side-emitting-enhancement silicone lens achieved by dispensing and geometry transferring. *Twelfth International Conference on Solid State Lighting and Fourth International Conference on White Leds and Solid State Lighting*, 8484.
- CHOI, H. S., SEO, W. S. & CHOI, D. K. 2011. Prediction of Reliability on Thermoelectric Module through Accelerated Life Test and Physics-of-Failure. *Electronic Materials Letters*, 7, 271-275.
- CHRISTENSEN, A. & GRAHAM, S. 2009. Thermal effects in packaging high power light emitting diode arrays. *Applied Thermal Engineering*, 29, 364-371.
- CHUANG, S. L., ISHIBASHI, A., KIJIMA, S., NAKAYAMA, N., UKITA, M. & TANIGUCHI, S. 1997. Kinetic model for degradation of light-emitting diodes. *IEEE Journal of Quantum Electronics*, 33, 970-979.
- CONNOR, J. T., MARTIN, R. D. & ATLAS, L. E. 1994. Recurrent Neural Networks and Robust Time-Series Prediction. *IEEE Transactions on Neural Networks*, 5, 240-254.
- CREE. 2006. *CreeXLamp XR-E LED Data sheet*, CREE, USA.
- CREE. 2010. *Cree XLamp XR Family LED Reliability, Application Note: CLD-AP06 Rev 7*, CREE, USA.
- CREE. 2010. *LED Color Mixing: Basics and Background, (Technical Article)*, CREE, USA. www.cree.com/xlamp.
- CREE®. 2012. *LED Components IES LM-80-2008 Testing Results(Revision:12)*, CREE, USA.
- CREE. 2013. *Cree LED Components IES LM-80-2008 Testing Results*, CREE, USA.

- CUI, H. 2005. Accelerated temperature cycle test and Coffin-Manson model for electronic packaging. *Annual Reliability and Maintainability Symposium, 2005 Proceedings*, 556-560.
- CUSHING, M. J., MORTIN, D. E., STADTERMAN, T. J. & MALHOTRA, A. 1993. Comparison of Electronics-Reliability Assessment Approaches. *IEEE Transactions on Reliability*, 42, 542-546.
- DAIGLE, M., SAHA, B. & GOEBEL, K. 2012. A Comparison of Filter-based Approaches for Model-based Prognostics. *2012 IEEE Aerospace Conference*.
- DAL LAGO, M., MENEGHINI, M., TRIVELLIN, N., MENEGHESSO, G., ZANONI, E. 2011. Degradation mechanisms of high-power white LEDs actived by current and temperature. *Microelectronic Reliability*, 51, 1742-1746.
- DE MAESSCHALCK, R., JOUAN-RIMBAUD, D. & MASSART, D. L. 2000. The Mahalanobis distance. *Chemometrics and Intelligent Laboratory Systems*, 50, 1-18.
- DE OLIVEIRA, V. R. B. & COLOSIMO, E. A. 2004. Comparison of methods to estimate the time-to-failure distribution in degradation tests. *Quality and Reliability Engineering International*, 20, 363-373.
- DOE. 2008. *ENERGY STAR Program Requirements for SSL Luminaires, Version 1.1*, Department of Energy, USA. <http://www.energystar.gov/>.
- DOE. 2009. *LED Measurement Serious: LED Luminaire Reliability*, Department of Energy, USA.
- DOE. 2012. *Understanding LM-79 Reports*, Department of Energy, USA.
- EASTON, G. S. & ROSENZWEIG, E. D. 2012. The role of experience in six sigma project success: An empirical analysis of improvement projects. *Journal of Operations Management*, 30, 481-493.
- ELERATH, J. G. & PECHT, M. 2012. IEEE 1413: A Standard for Reliability Predictions. *IEEE Transactions on Reliability*, 61, 125-129.
- EPSMA. 2005. *Guidelines to Understanding Reliability Prediction*, European Power Supply Manufacturers Association, UK.
- ESCOBAR, L. A. & MEEKER, W. Q. 2006. A review of accelerated test models. *Statistical Science*, 21, 552-577.
- FAN, B. F., WU, H., ZHAO, Y., XIAN, Y. L. & WANG, G. 2007. Study of phosphor thermal-isolated packaging technologies for high-power white light-emitting diodes. *IEEE Photonics Technology Letters*, 19, 1121-1123.
- FAN, J. J., YUNG, K. C., PECHT, M. 2011. Physics-of-Failure-Based Prognostics and Health Management for High-Power White Light-Emitting Diode Lighting, *IEEE Transactions on Device and Materials Reliability*, 11,

- 407–416.
- FAN, J. J., YUNG, K. C., PECHT, M. 2012. Lifetime Estimation of High Power White LED using Degradation Data Driven Method, *IEEE Transactions on Device and Materials Reliability*, 12, 470–477.
- FAN, J. J., YUNG, K. C., PECHT, M. 2014a. Prognostics of Chromaticity State for Phosphor-converted White Light Emitting Diodes Using an Unscented Kalman Filter Approach, *IEEE Transactions on Device and Materials Reliability*, 14, 564–573.
- FAN, J. J., YUNG, K. C., PECHT, M. 2014b. Prognostics of Lumen Maintenance for High Power White Light Emitting Diodes Using a Nonlinear Filter-based Approach, *Reliability Engineering & System Safety*, 123, 63-72.
- FANG, J. J. & WANG, P. S. 2005. The analysis of gauge repeatability and reproducibility with interaction between operators and parts. *Proceedings of the 4th International Conference on Quality & Reliability*, 209-216.
- FATHI, M., CHIKOUCHE, A. & ABDERRAZAK, M. 2011. Design and realization of LED Driver for solar street lighting applications. *Impact of Integrated Clean Energy on the Future of the Mediterranean Environment*, 6, 160-165.
- FIDES Guide 2004, Issue A. 2004. *Reliability Methodology for Electronic Systems*, FIDES Group, France.
- FIDES Guide 2009, Edition A. 2010. *Reliability Methodology for Electronic Systems*, FIDES Group, France.
- FOUCHER, B., BOULLIE, J., MESLET, B. & DAS, D. 2002. A review of reliability prediction methods for electronic devices. *Microelectronics Reliability*, 42, 1155-1162.
- FREITAS, M. A. et al. 2010. Reliability Assessment Using Degradation Models: Bayesian and Classical Approaches, *Pesquisa Operacional*, 30, 195-219.
- GENTLE, J. E. 1998. *Random Number Generation and Monte Carlo Methods*, Springer, USA.
- GIBBS, B. 2011. *Advanced Kalman Filtering, Least-Squares and Modeling*, John Wiley & Sons, Inc., New Jersey.
- GIJO, E. V. et al. 2011. Application of Six Sigma Methodology to Reduce Defects of a Grinding Process, *Quality and Reliability Engineering International*, 27, 1221-1234.
- GOTTFRIED, P. 1997. Comparison of electronics-reliability assessment approaches. *IEEE Transactions on Reliability*, 46, 2-2.
- GRYLLIAS, K. C. & ANTONIADIS, I. A. 2012. A Support Vector Machine approach based on physical model training for rolling element bearing fault detection in industrial environments. *Engineering Applications of Artificial*

- Intelligence*, 25, 326-344.
- GU, J. & PECHT, M. 2008. Prognostics and Health Management Using Physics-of-Failure. *Annual Reliability and Maintainability Symposium, 2008 Proceedings*, 484-490.
- QU, J. 2011. *Support-Vector-Machine-Based Diagnostics and Prognostics for Rotating Systems (Thesis)*, University of Alberta, USA.
- HAITZ, R. & TSAO, J. Y. 2011. Solid-state lighting: 'The case' 10 years after and future prospects. *Physica Status Solidi a-Applications and Materials Science*, 208, 17-29.
- HANCOCK, J. P. & TRAN, L. P. 1989. A Data-Driven Approach to an Adaptive-Learning Diagnostic Assistant. *Aiaa Computers in Aerospace VII Conference, Pts 1 and 2*, 518-522.
- HELD, M. & FRITZ, K. 2009. Comparison and evaluation of newest failure rate prediction models: FIDES and RIAC 217Plus. *Microelectronics Reliability*, 49, 967-971.
- HOLONYAK, J. & BEVACQUA, S. 1962. Coherent (visible) light emission from Ga(As_{1-x}P_x) junction, *Applied Physics Letters*, 1(4), 82-83.
- HORNG, R. H., LIN, R. C., CHIANG, Y. C., CHUANG, B. H., HU, H. L., HUS, C. P. 2012. Failure modes and effects analysis for high-power GaN-based light-emitting diodes package technology, *Microelectronics Reliability*, 52, 818-821.
- HSU, Y. C., LIN, Y. K., CHEN, M. H., TSAI, C. C., KUANG, J. H., HUANG, S. B., HU, H. L., SU, Y. I. & CHENG, W. H. 2008. Failure mechanisms associated with lens shape of high-power LED modules in aging test. *IEEE Transactions on Electron Devices*, 55, 689-694.
- HU, J. Z., YANG, L. Q. & SHIN, M. W. 2007. Mechanism and thermal effect of delamination in light-emitting diode packages. *Microelectronics Journal*, 38, 157-163.
- HU, J. Z., YANG, L. Q. & SHIN, M. W. 2008a. Electrical, optical and thermal degradation of high power GaN/InGaN light-emitting diodes. *Journal of Physics D-Applied Physics*, 41.
- HU, J. Z., YANG, L. Q. & SHIN, M. W. 2008b. Thermal and mechanical analysis of high-power LEDs with ceramic packages. *IEEE Transactions on Device and Materials Reliability*, 8, 297-303.
- HUMPHREYS, C. J. 2008. Solid-state lighting. *Mrs Bulletin*, 33, 459-470.
- IEEE Std 1413. 1998. *IEEE Standard Methodology for Reliability Prediction and Assessment for Electronic Systems and Equipment*, The Institute of Electrical and Electronics Engineers, Inc., USA.

- IEEE 1413.1. 2002. *IEEE Guide for Selecting and Using Reliability Predictions Based on IEEE 1413*, The Institute of Electrical and Electronics Engineers, Inc., USA.
- IEEE Std 1413. 2010. *IEEE Standard Framework for Reliability Prediction of Hardware*, The Institute of Electrical and Electronics Engineers, Inc., USA.
- IES-LM-79-08. 2008. *Electrical and Photometric Measurements of Solid-State Lighting Products*, Illuminating Engineering Society, USA.
- IES-LM-80-08. 2008. *Approved Method for Lumen Maintenance Testing of LED Light Source*, Illuminating Engineering Society, USA.
- IES-TM-21-11. 2011. *Projecting Long Term Lumen Maintenance of LED Light Sources*, Illuminating Engineering Society, USA.
- ISHIZAKI, S. KIMURA, H. SUGIMOTO, M. 2007. Lifetime Estimation of High Power White LEDs. *J. Light & Vis. Env.* 31, 15.
- JAFARZADEH, S. et al. 2012. State Estimation of Induction Motor Drives Using the Unscented Kalman Filter, *IEEE Transactions on Industrial Electronics*, 59,4207-4216.
- JIANG, Q. C., YAN, X. F. & ZHAO, W. X. 2013. Fault Detection and Diagnosis in Chemical Processes Using Sensitive Principal Component Analysis. *Industrial & Engineering Chemistry Research*, 52, 1635-1644.
- JIN, T. D., JANAMANCHI, B. & FENG, Q. M. 2011. Reliability deployment in distributed manufacturing chains via closed-loop Six Sigma methodology. *International Journal of Production Economics*, 130, 96-103.
- JULIER, S. J. & UHLMANN, J. K. 2004. Unscented filtering and nonlinear estimation. *Proceedings of the Ieee*, 92, 401-422.
- JULIER, S. J., UHLMANN, J. K. & DURRANTWHYTE, H. F. 1995. A new approach for filtering nonlinear systems. *Proceedings of the 1995 American Control Conference, Vols 1-6*, 1628-1632.
- KRAMES, M. R., SHCHEKIN, O. B., MUELLER-MACH, R., MUELLER, G. O., ZHOU, L., HARBERS, G. & CRAFORD, M. G. 2007. Status and future of high-power light-emitting diodes for solid-state lighting. *Journal of Display Technology*, 3, 160-175.
- KUMAR, S., VICHARE, N. M., DOLEV, E. & PECHT, M. 2012. A health indicator method for degradation detection of electronic products. *Microelectronics Reliability*, 52, 439-445.
- LAFONT, U., VAN ZEIJL, H. & VAN DER ZWAAG, S. 2012. Increasing the reliability of solid state lighting systems via self-healing approaches: A review. *Microelectronics Reliability*, 52, 71-89.
- LALL, P. et al. 2012. Prognostics Health Management of Electronic Systems Under

- Mechanical Shock and Vibration Using Kalman Filter Models and Metrics, *IEEE Transactions on Industrial Electronics*, 59, 4301-4314.
- LAU, J.H. et al. 1998. *Electronic packaging: design, materials, process, and reliability*, McGraw-Hill, New York.
- LEE, S. N., PAEK, H. S., SON, J. K., KIM, H., KIM, K. K., HA, K. H., NAM, O. H. & PARK, Y. 2009. Effects of Mg dopant on the degradation of InGaN multiple quantum wells in AlInGaN-based light emitting devices. *Journal of Electroceramics*, 23, 406-409.
- LEE, W. W., NGUYEN, L. T. & SELVADURAY, G. S. 2000. Solder joint fatigue models: review and applicability to chip scale packages. *Microelectronics Reliability*, 40, 231-244.
- LENK, R. & LENK, C. 2011. *Practical Lighting Design with LEDs*, John Wiley & Sons. Inc., New Jersey.
- LIANG, J. & WANG, N. 2003. Faults diagnosis in industrial reheating furnace using principal component analysis. *Proceedings of 2003 International Conference on Neural Networks & Signal Processing, Proceedings, Vols 1 and 2*, 1615-1618.
- LIAO, H. & ELSAYED, E. A. 2006. Reliability inference for field conditions from accelerated degradation testing. *Naval Research Logistics*, 53, 576-587.
- LIN, C. C. & LIU, R. S. 2011. Advances in Phosphors for Light-emitting Diodes. *Journal of Physical Chemistry Letters*, 2, 1268-1277.
- LIU, S. & LUO, X. 2011. *LED Packaging for Lighting Applications*, John Wiley & Sons (Asia), Singapore.
- LU, C. J. & MEEKER, W. Q. 1993. Using Degradation Measures to Estimate a Time-to-Failure Distribution. *Technometrics*, 35, 161-174.
- LU, D. & WONG, C. P. 2009. *Materials for advanced packaging*, Springer, New York.
- LUMILEDS. 2012. *Optical Measurement Guidelines for High-Power LEDs and Solid State Lighting Products, (White Paper, WP17)*, PHILIPS, Netherlands.
- LUO, H., KIM, J. K., SCHUBERT, E. F., CHO, J., SONE, C. & PARK, Y. 2005. Analysis of high-power packages for phosphor-based white-light-emitting diodes. *Applied Physics Letters*, 86.
- LUO, X. B. & LIU, S. 2007. A microjet array cooling system for thermal management of high-brightness LEDs. *IEEE Transactions on Advanced Packaging*, 30, 475-484.
- LUTHRA, P. 1990. Mil-Hdbk-217 - What Is Wrong with It. *IEEE Transactions on Reliability*, 39, 518-518.
- LUXEON. 2007. *Luxeon K2 Reliability Data (RD06)*, PHILIPS, Netherlands.

- LUXEON. 2008. *Luxeon_K2 Technical Datasheet (DS51)*, PHILIPS, Netherlands.
- LUXEON. 2008a. *Technical Datasheet (DS56)*, PHILIPS, Netherlands.
- LUXEON. 2010. *LM-80 Test Report (DR03)*, PHILIPS, Netherlands.
- LUXEON. 2011. *LM-80 Test Report (DR04)*, PHILIPS, Netherlands.
- MARSEGUERRA, M., ZIO, E. & CIPOLLONE, M. 2003. Designing optimal degradation tests via multi-objective genetic algorithms. *Reliability Engineering & System Safety*, 79, 87-94.
- MAZHAR, M. I., KARA, S. & KAEBERNICK, H. 2007. Remaining life estimation of used components in consumer products: Life cycle data analysis by Weibull and artificial neural networks. *Journal of Operations Management*, 25, 1184-1193.
- MCCLUSKEY, F. P. & PECHT, M. 1999. Rapid reliability assessment using CADMP-II. *1999 International Conference on Modeling and Simulation of Microsystems*, 495-497.
- MEEKER, W. Q., ESCOBAR, L. A. & LU, J. C. 1998. Accelerated degradation tests: Modeling and analysis. *Technometrics*, 40, 89-99.
- MEEKER, W. Q. & ESCOBAR, L. A. 1998. *Statistical Methods for Reliability Data*, Wiley, New York.
- MENEGHESSO, G., LEVADA, S., ZANONI, E., SCAMARCIO, G., MURA, G., PODDA, S., VANZI, M., DU, S. & ELIASHEVICH, I. 2003. Reliability of visible GaN LEDs in plastic package. *Microelectronics Reliability*, 43, 1737-1742.
- MENEGHESSO, G., MENEGHINI, M. & ZANONI, E. 2010. Recent results on the degradation of white LEDs for lighting. *Journal of Physics D-Applied Physics*, 43.
- MENEGHINI, M., TAZZOLI, A., MURA, G., MENEGHESSO, G. & ZANONI, E. 2010. A Review on the Physical Mechanisms That Limit the Reliability of GaN-Based LEDs. *IEEE Transactions on Electron Devices*, 57, 108-118.
- MENEGHINI, M., TREVISANELLO, L. R., MENEGHESSO, G. & ZANONI, E. 2008. A review on the reliability of GaN-based LEDs. *IEEE Transactions on Device and Materials Reliability*, 8, 323-331.
- MIL-HDBK-217 F Notice 2, 1995. *Reliability Prediction of Electronic Equipment*, US Department of Defense, USA.
- MIAO, Q., XIE, L., CUI, H. J., LIANG, W. & PECHT, M. 2013. Remaining useful life prediction of lithium-ion battery with unscented particle filter technique. *Microelectronics Reliability*, 53, 805-810.
- MODARRES, M. 2010. *Reliability Engineering and Risk Analysis: A Practical Guide. Second Edition*, CRC Press, USA.

- MOMENTIVE PERFORMANCE MATERIALS. 2005. *Silicone Material Solutions for LED Packages and Assemblies*, <http://www.momentive.com/>
- MONTGOMERY, D. C. & WOODALL, W. H. 2008. An Overview of Six Sigma. *International Statistical Review*, 76, 329-346.
- MOTTIER, P. 2009. *LEDs for Lighting Applications*, John Wiley & Sons, Inc., USA.
- NARENDRAN, N. et al, 2004. *Developing Color Tolerance Criteria for White LEDs*, Lighting Research Center: Troy, NY, USA.
- NARENDRAN, N., DENG, L., PYSAR, R. M., GU, Y. & YU, H. 2004. Performance characteristics of high-power light-emitting diodes. *Third International Conference on Solid State Lighting*, 5187, 267-275.
- NARENDRAN, N. GU, Y. FREYSSINIER, J. P. et al. 2004. Solid-state lighting: Failure analysis of white LEDs, *J. Cryst. Growth*, 268, 449-456.
- NARENDRAN, N. & GU, Y. M. 2005. Life of LED-Based White Light Sources. *Journal of Display Technology*, 1, 167-171.
- NELSON, W. 1990. *Accelerated Testing: Statistical Methods, Test Plans, and Data Analysis*, Wiley, New York.
- NICHIA. 2009. *Specifications for White LED, NCSW119T-H3*, NICHIA, Japan.
- NICHIA. 2010. *LM-80 Test Report for Nichia Chip Type Warm White LED*, NICHIA, Japan.
- NICHOLLS, D. 2006. What is 217Plus (TM) and where did it come from? *Annual Reliability and Maintainability Symposium, 2007 Proceedings*, 22-27.
- NIKULIN, M. S. et al., 1998. *Advances in Degradation Modeling Applications to Reliability, Survival Analysis, and Finance*, Springer, Berlin.
- NIU, G., SINGH, S., HOLLAND, S. W. & PECHT, M. 2011. Health monitoring of electronic products based on Mahalanobis distance and Weibull decision metrics. *Microelectronics Reliability*, 51, 279-284.
- NOGUEIRA, E., VAZQUEZ, M. & NUNEZ, N. 2009. Evaluation of AlGaInP LEDs reliability based on accelerated tests. *Microelectronics Reliability*, 49, 1240-1243.
- O'CONNOR, P. D. T. 2002. *Practical Reliability Engineering, Fourth Edition*, John Wiley & Sons, Ltd, UK.
- O'LEARY, S. K., FOUTZ, B. E., SHUR, M. S. & EASTMAN, L. F. 2006. Steady-state and transient electron transport within the III-V nitride semiconductors, GaN, AlN, and InN: A review. *Journal of Materials Science-Materials in Electronics*, 17, 87-126.
- OHNO, Y. 2004. Color rendering and luminous efficacy of white LED spectra. *Fourth International Conference on Solid State Lighting*, 5530, 88-98.
- OSRAM. 2008. *Reliability and Lifetime of LEDs, Application Note*, OSRAM, USA.

- OSRAM. 2010. *Lumen and Chromaticity Maintenance Test Report for Golden Dragon Plus (IESNA LM-80)*, OSRAM, USA.
- PAGET, M. L. et al. 2007~2011. *Solid-State Lighting CALiPER Program*, The U.S. Department of Energy, USA.
- PAN, J. N. 2006. Evaluating the gauge repeatability and reproducibility for different industries. *Quality & Quantity*, 40, 499-518.
- PAN, R. & CRISPIN, T. 2011. A Hierarchical Modeling Approach to Accelerated Degradation Testing Data Analysis: A Case Study. *Quality and Reliability Engineering International*, 27, 229-237.
- PATCHA, A. & PARK, J. M. 2007. An overview of anomaly detection techniques: Existing solutions and latest technological trends. *Computer Networks*, 51, 3448-3470.
- PECHT, M. 1994. Physics-of-failure approach to design and reliability assessment of microelectronic packages. *Proceedings of the First International Symposium on Microelectronic Package and Pcb Technology*, 175-180.
- PECHT, M. 2008. *Prognostics and health management of electronics*, John Wiley & Sons, NJ.
- PECHT, M. 2009. *Product Reliability, Maintainability, and Supportability Handbook, second edition*, CRC Press/Taylor& Francis Group, USA.
- PECHT, M. & CU, J. 2009. Physics-of-failure-based prognostics for electronic products. *Transactions of the Institute of Measurement and Control*, 31, 309-322.
- PECHT, M., DAS, D. & RAMAKRISHNAN, A. 2002. The IEEE standards on reliability program and reliability prediction methods for electronic equipment. *Microelectronics Reliability*, 42, 1259-1266.
- PECHT, M. & JAAI, R. 2010. A prognostics and health management roadmap for information and electronics-rich systems. *Microelectronics Reliability*, 50, 317-323.
- PEEL, L. 2008. Data Driven Prognostics using a Kalman Filter Ensemble of Neural Network Models. *2008 International Conference on Prognostics and Health Management (Phm)*, 65-70.
- PENG, Y., DONG, M. & ZUO, M. J. 2010. Current status of machine prognostics in condition-based maintenance: a review. *International Journal of Advanced Manufacturing Technology*, 50, 297-313.
- PONCE, F. A. & BOUR, D. P. 1997. Nitride-based semiconductors for blue and green light-emitting devices. *Nature*, 386, 351-359.
- REA, M. S. et al. 2000. *The IESNA Lighting Handbook: Reference and Application, 9th Edition*, The Illuminating Engineering Society of North America, New

- York.
- RESTAINO, R. & ZAMBONI, W. 2012. Comparing Particle Filter and Extended Kalman Filter for Battery State-Of-Charge Estimation. *38th Annual Conference on Ieee Industrial Electronics Society (Iecon 2012)*, 4018-4023.
- RiAC-HDBK-217PLUS. 2006. *Handbook of 217Plus™ Reliability Prediction Models*, Reliability Information Analysis Center, USA.
- SANTHANAGOPALAN, S. & WHITE, R. E. 2010. State of charge estimation using an unscented filter for high power lithium ion cells, *International Journal of Energy Research*, 34, 152-163.
- SAXENA, A., CELAYA, J., BALABAN, E., GOEBEL, K., SAHA, B., SAHA, S. & SCHWABACHER, M. 2008. Metrics for Evaluating Performance of Prognostic Techniques. *2008 International Conference on Prognostics and Health Management (Phm)*, 174-190.
- SEESMART. 2010. *How To Choose The Right LED Lighting Product Color Temperature*, <http://www.seesmartled.com/>.
- SCHANDA, J. 2007. *Colorimetry: Understanding the CIE System*, John Wiley & Sons, Inc., New Jersey.
- SCHROEDER, R. G., LINDERMAN, K., LIEDTKE, C. & CHOO, A. S. 2008. Six Sigma: definition and underlying theory. *Journal of Operations Management*, 26, 536-554.
- SCHUBERT, E. F. 2006. *Light-emitting diodes, 2nd edition*, Cambridge University Press, UK.
- SCHUBERT, E. F. & KIM, J. K. 2005. Solid-state light sources getting smart. *Science*, 308, 1274-1278.
- SCHUBERT, E. F., KIM, J. K., LUO, H. & XI, J. Q. 2006. Solid-state lighting - a benevolent technology. *Reports on Progress in Physics*, 69, 3069-3099.
- SHAFER, S. M. & MOELLER, S. B. 2012. The effects of Six Sigma on corporate performance: An empirical investigation. *Journal of Operations Management*, 30, 521-532.
- SHEU, J. K., CHANG, S. J., KUO, C. H., SU, Y. K., WU, L. W., LIN, Y. C., LAI, W. C., TSAI, J. M., CHI, G. C. & WU, R. K. 2003. White-light emission from near UV InGaN-GaN LED chip precoated with blue/green/red phosphors. *IEEE Photonics Technology Letters*, 15, 18-20.
- SI, X. S., WANG, W. B., HU, C. H. & ZHOU, D. H. 2011. Remaining useful life estimation - A review on the statistical data driven approaches. *European Journal of Operational Research*, 213, 1-14.
- SIKORSKA, J. Z., HODKIEWICZ, M. & MA, L. 2011. Prognostic modelling options for remaining useful life estimation by industry. *Mechanical Systems*

- and Signal Processing*, 25, 1803-1836.
- SIMON, D. 2006. *Optimal state estimation : Kalman, H [infinity] and nonlinear approaches*, John Wiley & Sons, Inc., New Jersey.
- SMET, P. F., PARMENTIER, A. B. & POELMAN, D. 2011. Selecting Conversion Phosphors for White Light-Emitting Diodes. *Journal of the Electrochemical Society*, 158, R37-R54.
- SOLID-STATE LIGHTING PRODUCT QUALITY INITIATIVE. 2011. *LED Luminaire Lifetime Recommendations for Testing and Reporting, 2nd Edition*, Next Generation Light Industry Alliance with the U.S. Department of Energy, USA.
- SONG, B. M., HAN, B. T., BAR-COHEN, A., SHARMA, R. & ARIK, M. 2010. Hierarchical Life Prediction Model for Actively Cooled LED-Based Luminaire. *IEEE Transactions on Components and Packaging Technologies*, 33, 728-737.
- SORENSEN, H. W. 1970. Least-Squares Estimation - from Gauss to Kalman. *IEEE Spectrum*, 7, 63-&.
- SR-332, Issue 1. 2001. *Reliability Prediction Procedure for Electronic Equipment*, Telcordia, USA.
- SR-332, Issue 2. 2006. *Reliability Prediction Procedure for Electronic Equipment*, Telcordia, USA.
- STAMATIS, D.H. 2003. *Failure Mode and Effect Analysis: FMEA from Theory to Execution, Second Edition*, ASQ Quality Press, USA.
- STEEN, R. 2011. *The Color of White: Color Consistency with LEDs*, Global LEDs/OLEDs, 13-19. www.globalledoled.com
- SUTHARSSAN, T., BAILEY, C., STOYANOV, S. & ROSUNALLY, Y. 2011. Prognostics and Reliability Assessment of Light Emitting Diode Packaging. *2011 12th International Conference on Electronic Packaging Technology and High Density Packaging (Icept-Hdp)*, 938-944.
- SUTHARSSAN, T., STOYANOV, S., BAILEY, C. & ROSUNALLY, Y. 2012. Prognostics and Health Monitoring of High Power LED. *Micromachines*, 3(1), 78-100.
- TAGUCHI, G. CHOWDHURY, S. & WU, Y. 2001. *The Mahalanobis-Taguchi System*, McGraw-Hill, USA.
- TAGUCHI, G. & JUGULUM, R. 2002. *The Mahalanobis-Taguchi Strategy: A Pattern Technology System*, John Wiley & Sons, New York.
- TAN, C. M., CHEN, B. K. E., XU, G. & LIU, Y. J. 2009a. Analysis of humidity effects on the degradation of high-power white LEDs. *Microelectronics Reliability*, 49, 1226-1230.

- TAN, L. X., LI, J., WANG, K. & LIU, S. 2009b. Effects of Defects on the Thermal and Optical Performance of High-Brightness Light-Emitting Diodes. *IEEE Transactions on Electronics Packaging Manufacturing*, 32, 233-240.
- TARASHIOON, S., BAIANO, A., VAN ZEIJL, H., GUO, C., KOH, S. W., VAN DRIEL, W. D. & ZHANG, G. Q. 2012. An approach to "Design for Reliability" in solid state lighting systems at high temperatures. *Microelectronics Reliability*, 52, 783-793.
- TIAN, Z. G. & ZUO, M. J. 2009. Health Condition Prognostics of Gears Using a Recurrent Neural Network Approach. *Annual Reliability and Maintainability Symposium, 2009 Proceedings*, 461-466.
- TIPPING, M. E. 2001. Sparse Bayesian learning and the relevance vector machine. *Journal of Machine Learning Research*, 1, 211-244.
- TSAING, S. T. & PENG, C. Y. 2007. Stochastic Diffusion Modeling of Degradation Data", *Journal of Data Science*, 5, 315-333.
- UDDIN, A., WEI, A. C. & ANDERSSON, T. G. 2005. Study of degradation mechanism of blue light emitting diodes. *Thin Solid Films*, 483, 378-381.
- VACHTSEVANOS, G. & WANG, P. 2001. Fault prognosis using dynamic wavelet neural networks. *IEEE Systems Readiness Technology Conference*, 857-870.
- VALLES, A., SANCHEZ, J., NORIEGA, S. & NUNEZ, B. G. 2009. Implementation of Six Sigma in a Manufacturing Process: A Case Study. *International Journal of Industrial Engineering-Theory Applications and Practice*, 16, 171-181.
- VAN DRIEL, W. D. & FAN, X. J. 2012. *Solid State Lighting Reliability: Components to Systems*, Springer, New York.
- VASAN, S. & PECHT, M. 2011. Investigation of Stochastic Differential Models and a Recursive Nonlinear Filtering Approach for Fusion-Prognostics, *In Proceeding of Annual Conference of the Prognostics and Health Management Society*, 1-3.
- WAN, E. A. & VAN DER MERWE, R. 2000. The unscented Kalman Filter for nonlinear estimation. *IEEE 2000 Adaptive Systems for Signal Processing, Communications, and Control Symposium - Proceedings*, 153-158.
- WANG, W. & CARR, M. 2010. A Stochastic Filtering Based Data Driven Approach for Residual Life Prediction and Condition Based Maintenance Decision Making Support. *2010 Prognostics and System Health Management Conference*, 216-225.
- WELCH, G. & BISHOP, G. 2006. *An Introduction to the Kalman Filter*, UNC-Chapel Hill, USA.
- WHITE, M. & BERNSTEIN, J. B. 2008. *Microelectronics Reliability:*

- Physics-of-failure Based Modeling and Lifetime Evaluation*, JPL Publication, CA.
- WINDER, S. 2008. *Power supplies for LED lighting*, Elsevier Inc, UK.
- WONG, C. P. 1995. Thermal-Mechanical Enhanced High-Performance Silicone Gels and Elastomeric Encapsulants in Microelectronic Packaging. *Ieee Transactions on Components Packaging and Manufacturing Technology Part A*, 18, 270-273.
- WOOD, M. 2010. *MacAdam ellipses*. <http://www.mikewoodconsulting.com/>
- WOYLES, J. & ALLARDICE, B. 2008. An overview of six sigma methodology. *Australian and New Zealand Journal of Psychiatry*, 42, A38-A38.
- WU, S. J. & CHANG, C. T. 2002. Optimal design of degradation tests in presence of cost constraint. *Reliability Engineering & System Safety*, 76, 109-115.
- WU, S. J. & SHAO, J. 1999. Reliability analysis using the least squares method in nonlinear mixed-effect degradation models. *Statistica Sinica*, 9, 855-877.
- WU, Y. X., HU, D. W., WU, M. P. & HU, X. P. 2005. Unscented Kalman filtering for additive noise case: Augmented vs. non-augmented. *ACC: Proceedings of the 2005 American Control Conference, Vols 1-7*, 4051-4055.
- XIE, R. et al. 2011. *Nitride Phosphors and Solid-State Lighting*, CPC press/Taylor& Francis, USA.
- XIE, R. J., HIROSAKI, N., TAKEDA, T. & SUEHIRO, T. 2013. On the Performance Enhancement of Nitride Phosphors as Spectral Conversion Materials in Solid State Lighting. *Ecs Journal of Solid State Science and Technology*, 2, R3031-R3040.
- XU, J. P. & XU, L. 2011. Health management based on fusion prognostics for avionics systems. *Journal of Systems Engineering and Electronics*, 22, 428-436.
- YAN, J. H., GUO, C. Z., WANG, X. & ZHAO, D. B. 2011. A Data-Driven Neural Network Approach for Remaining Useful Life Prediction. *Advanced Design and Manufacture Iii*, 450, 544-547.
- YANG, S. C., LIN, P., WANG, C. P., HUANG, S. B., CHEN, C. L., CHIANG, P. F., LEE, A. T. & CHU, M. T. 2010. Failure and degradation mechanisms of high-power white light emitting diodes. *Microelectronics Reliability*, 50, 959-964.
- YANG, S. K. 2002. An experiment of state estimation for predictive maintenance using Kalman filter on a DC motor. *Reliability Engineering & System Safety*, 75, 103-111.
- YANG, S. K. & LIU, T. S. 1999. State estimation for predictive maintenance using Kalman filter. *Reliability Engineering & System Safety*, 66, 29-39.

- YE, S., XIAO, F., PAN, Y. X., MA, Y. Y. & ZHANG, Q. Y. 2010. Phosphors in phosphor-converted white light-emitting diodes Recent advances in materials, techniques and properties. *Materials Science & Engineering R-Reports*, 71, 1-34.
- YU, H. F. 2006. Designing an accelerated degradation experiment with a reciprocal Weibull degradation rate. *Journal of Statistical Planning and Inference*, 136, 282-297.
- ZHANG, S. & GANESAN, R. 1997. Multivariable trend analysis using neural networks for intelligent diagnostics of rotating machinery. *Journal of Engineering for Gas Turbines and Power-Transactions of the Asme*, 119, 378-384.
- ZIO, E. 2009. Reliability engineering: Old problems and new challenges. *Reliability Engineering & System Safety*, 94, 125-141.
- ZIO, E. & DI MAIO, F. 2010. A data-driven fuzzy approach for predicting the remaining useful life in dynamic failure scenarios of a nuclear system. *Reliability Engineering & System Safety*, 95, 49-57.
- ZIO, E. & PELONI, G. 2011. Particle filtering prognostic estimation of the remaining useful life of nonlinear components. *Reliability Engineering & System Safety*, 96, 403-409.
- ZU, X. X., FREDENDALL, L. D. & DOUGLAS, T. J. 2008. The evolving theory of quality management: The role of Six Sigma. *Journal of Operations Management*, 26, 630-650.
- ZUKAUSKAS, A., SHUR, M. S., GASKA, R. 2002. *Introduction to Solid State Lighting*, Jone Wiley & Sons, New York.

Appendix A

Ordinary Least Squares (OLS) Estimation Recommended by IES-TM-21-11

Supposing that a set of n data points $(t_1, y_1), (t_2, y_2), \dots, (t_n, y_n)$ follows an exponential model (A-1) and their transferred data set $(t_1, \zeta_1), (t_2, \zeta_2), \dots, (t_n, \zeta_n)$ can be fitted by a least square straight line defined as (A-2):

$$y = A \cdot \exp(-B \cdot t) \tag{A.1}$$

$$\zeta = \ln A - B \cdot t \tag{A.2}$$

where $\zeta = \ln(y)$.

Through minimizing the sum of the squares of the residuals between actual measurements and calculated values (A-3), the parameters of the exponential model (A-1) can be estimated as follows:

$$\min_{A:B} \left\{ \frac{1}{n} \sum_{i=1}^n [\zeta_i - (\ln A - B \cdot t_i)]^2 \right\} \tag{A.3}$$

$$B = \frac{\sum_{i=1}^n t_i \sum_{i=1}^n \zeta_i - n \sum_{i=1}^n t_i \zeta_i}{n \sum_{i=1}^n t_i^2 - (\sum_{i=1}^n t_i)^2} \tag{A.4}$$

$$A = \exp \left(\frac{\sum_{i=1}^n \zeta_i - B \sum_{i=1}^n t_i}{n} \right) \tag{A.5}$$